LA-UR-03-0047
Approved for public release;
distribution is unlimited.

January 9, 2003

Title: Notes on Elastic-Plastic Flow

Author(s): Ralph Menikoff

Submitted to: T14 web site
URL: `t14web.lanl.gov/Staff/rsm/preprints.html`
`#ElasticPlasticNotes`

Notes on Elastic-Plastic Flow

Notes on Elastic-Plastic Flow

Ralph Menikoff

A major complication of elastic-plastic flow, as compared to fluid flow, is that it is formulated in terms of tensors rather than scalars. Here the tensor notation is defined with attention to the spaces on which the various tensors act and the metrics for the different frames. Examples are shown illustrating the small strain limit and the case of uniaxial strain. The multiplicative decomposition formulation is used to split the deformation gradient into elastic and plastic components. Hyperbolic aspects of the elastic-plastic PDEs are emphasized.

1 Kinematic Variables

Elastic flow is formulated in terms of a time-dependent **mapping** $\boldsymbol{\phi}$ from the *body* reference frame to the *spatial* laboratory frame

$$\boxed{\boldsymbol{\phi}(\cdot,t) : \mathcal{B} \to \mathcal{S}}\ , \qquad x^i = \phi^i(\vec{X},t)\ ,$$

where $\vec{X} \in \mathcal{B}$ and $\vec{x} \in \mathcal{S}$. The **particle velocity** field in the reference frame is a map from the body frame to the tangent space of the spatial frame

$$\boxed{\vec{U}(\vec{X},t) = \frac{\partial}{\partial t}\boldsymbol{\phi} \in \mathbb{T}_{\boldsymbol{\phi}(\vec{X},t)}\,\mathcal{S}}\ . \tag{1.1}$$

Alternatively, the particle velocity can be expressed as a map from the spatial frame to the tangent space of the spatial frame

$$\vec{u}(\vec{x},t) = \left(\vec{U} \circ \boldsymbol{\phi}^{-1}\right) \in \mathbb{T}_{\vec{x}}\,\mathcal{S}\ .$$

It is important to note that the Lagrangian velocity $\vec{U}$ is a two-point rank-one tensor field, *i.e.*, the domain is $\mathcal{B}$ but the range is in $\mathbb{T}\,\mathcal{S}$.

The **deformation gradient** is the derivative of the mapping, and is a transformation from the tangent space of $\mathcal{B}$ to the tangent space of $\mathcal{S}$

$$\boxed{\mathbf{F} = \mathrm{D}\boldsymbol{\phi}}\,, \qquad \mathsf{F}^i{}_\alpha(\vec{X},t) = \frac{\partial \phi^i}{\partial X^\alpha} : \mathbb{T}_{\vec{X}}\,\mathcal{B} \to \mathbb{T}_{\vec{\phi}(\vec{X},t)}\,\mathcal{S}\,. \tag{1.2}$$

The deformation gradient is a two-point rank-two tensor field. This is in contrast to the rank-two stress and strain tensor fields defined later. For ordinary tensor fields, the domain and range are the tangent or cotangent spaces at the same point. Two-point tensors involve two different points, for example $\mathbf{F}$ goes between $\vec{X} \in \mathcal{B}$ and $\vec{x} = \vec{\phi}(\vec{X},t) \in \mathcal{S}$.

1.1 Multiplicative Decomposition

To motivate the decomposition of a flow into elastic and plastic components, we consider expressing the mapping $\boldsymbol{\phi}$ as the composition of maps, $\boldsymbol{\phi} = \boldsymbol{\phi}_e \circ \boldsymbol{\phi}_p$, from the reference frame to a *plastic* intermediate frame to the spatial frame (see [15], [22, chpt. 9] and references therein)

$$\begin{array}{ccccc} \mathcal{B}_\alpha & \xrightarrow{\phi_p} & \mathcal{P}_I & \xrightarrow{\phi_e} & \mathcal{S}_i \\ \uparrow & & & & \downarrow \\ \mathcal{B}_\alpha & & \xrightarrow{\qquad\qquad\phi\qquad\qquad} & & \mathcal{S}_i \end{array}$$

The chain rule for differentiation then leads to a **multiplicative decomposition** for the deformation gradient, in terms of elastic and plastic deformations, $\mathbf{F_e}$ and $\mathbf{F_p}$, respectively,

$$\boxed{\mathbf{F} = \mathbf{F_e}\mathbf{F_p}}\,, \qquad \mathsf{F}^i{}_\alpha = (\mathsf{F}_e)^i{}_A(\mathsf{F}_p)^A{}_\alpha\,.$$

The deformation gradients $\mathbf{F_e}$ and $\mathbf{F_p}$ are local quantities that we consider more fundamental than the mappings $\boldsymbol{\phi}_e$ and $\boldsymbol{\phi}_p$.

Physically, plasticity is due to processes that occur on a microscopic scale, such as the formation and movement of dislocations in a crystal. Dislocations prevents the microscopic mappings from being continuous functions. Consequently, the deformation gradients can be defined only as coarse-grain averages of the local lattice distortions. Mathematically, as a result of the averaging process the compatibility conditions needed to recover a mapping

from the deformation gradient are not satisfied. Nevertheless, we assume the multiplicative decomposition of the deformation gradients and consider the mappings only as a convenient heuristic.

There is still a question with non-uniqueness of the decomposition; *i.e.*, $\mathbf{F} = (\mathbf{F_e}\mathbf{Q}^{-1})(\mathbf{Q}\mathbf{F_p})$ for any invertible $\mathbf{Q} : \mathbb{T}\mathcal{P} \to \mathbb{T}\mathcal{P}$. The non-uniqueness is similar to the question of "frame indifference" discussed in a later section. The difficulty is resolved in part by formulating plasticity in terms of total strain and plastic strain rather than the deformation gradient alone. In addition, the choice of the plastic strain rate is needed to define the plasticity model.

1.2 Notation

The mathematical framework for elastic-plastic flow, or even elastic flow, is differential geometry [11]. To indicate the space for the domain and range of various transformations, superscripts (corresponding to **contravariant** vectors in the tangent space $\mathbb{T}$, called simply "vectors") and subscripts (corresponding to **covariant** vectors in the cotangent space $\mathbb{T}^*$, called simply "covectors") in lower case Greek letters are associated with $\mathcal{B}$, upper case roman letters with $\mathcal{P}$ and lower case roman letters with $\mathcal{S}$. Vectors with upper case letters are used to indicate points in the body frame ($\mathcal{B}$ or $\mathbb{T}\mathcal{B}$ or $\mathbb{T}^*\mathcal{B}$) while lower case letters indicate points in the spatial frame ($\mathcal{S}$ or $\mathbb{T}\mathcal{S}$ or $\mathbb{T}^*\mathcal{S}$), *e.g.*, $\vec{X} \in \mathcal{B}$ and $\vec{x} \in \mathcal{S}$.

To be more specific, we denote the basis elements of $\mathbb{T}_{\vec{X}}\mathcal{B}$ by

$$\vec{E}_\alpha = \frac{\partial}{\partial X^\alpha} \ .$$

Then a vector in $\mathbb{T}_{\vec{X}}\mathcal{B}$ may be written as

$$\vec{U} = U^\alpha \vec{E}_\alpha \ ,$$

where the summation over repeated indices, upper and lower, is assumed. Thus, it is the components of a vector relative to the basis $\vec{E}_\alpha$ that are denoted with superscripts.

Similarly, we denote the dual basis elements in $\mathbb{T}^*{}_{\vec{X}}\mathcal{B}$ by

$$\vec{E}^\alpha = dX^\alpha \ ,$$

with dual pairing

$$(\vec{E}^\alpha, \vec{E}_\beta) = \delta^\alpha{}_\beta \ ,$$

where the Kronecker-δ is 1 if the indices are the same and 0 otherwise. Alternatively, the duality can be expressed as $\vec{E}_\alpha \otimes \vec{E}^\alpha$ is the identity operator in $\mathbb{T}_{\vec{X}}\mathcal{B}$. An element of $\mathbb{T}^*{}_{\vec{X}}\mathcal{B}$ may be written

$$\vec{V}^* = V_\alpha \vec{E}^\alpha \ .$$

The components of a covector relative to the basis $\vec{E}^\alpha$ are denoted with subscripts. The dual pairing of a vector in $\mathbb{T}^*{}_{\vec{X}}\mathcal{B}$ with a vector in $\mathbb{T}_{\vec{X}}\mathcal{B}$ can be expressed in terms of their components as $(\vec{V}^*, \vec{U}) = V_\alpha U^\alpha$.

Under a change of basis $\vec{X} \mapsto \vec{X}' = \vec{\phi}(\vec{X})$, vectors and covectors transform in a complementary manner,

$$\begin{aligned} U^\alpha &\mapsto (U')^\alpha = (\mathbf{F})^\alpha{}_\beta U^\beta \\ V_\alpha &\mapsto (V')_\alpha = (\mathbf{F}^{-T})_\alpha{}^\beta V_\beta \ , \end{aligned}$$

where $\mathbf{F} = \mathsf{D}\vec{\phi}$, such that the dual pairing is invariant, *i.e.*, $V_\alpha U^\alpha = (V')_\alpha (U')^\alpha$. The purpose of subscripts and the superscripts is to provide a calculus for keeping track of the way the representation of physical quantities transform under change of basis. The number of upper and lower indices on the left and right hand sides of a tensorial equation must match. This provides a simple consistency check akin to dimensional analysis.

Inner products within $\mathbb{T}_{\vec{X}}\mathcal{B}$ and $\mathbb{T}_{\vec{x}}\mathcal{S}$ are defined by metrics

$$\begin{aligned} \langle \vec{W}, \vec{V} \rangle_{\vec{X}} = (\mathbf{G}\vec{W}, \vec{V})_{\vec{X}} &= \mathsf{G}_{\alpha\beta}(\vec{X}) W^\alpha V^\beta \\ \langle \vec{w}, \vec{v} \rangle_{\vec{x}} = (\boldsymbol{g}\vec{w}, \vec{v})_{\vec{x}} \quad &= g_{ab}(\vec{x}) w^a v^b \ , \end{aligned}$$

where $\mathbf{G}(\vec{X})$ and $\boldsymbol{g}(\vec{x})$ denote the **metric maps** between $\mathbb{T}$ and $\mathbb{T}^*$ in the body frame and the space frame, respectively,

$$\begin{aligned} \mathbf{G}(\vec{X}) : \mathbb{T}_{\vec{X}}\mathcal{B} \to \mathbb{T}^*{}_{\vec{X}}\mathcal{B} \qquad &\text{and} \qquad \mathbf{G}^{-1}(\vec{X}) : \mathbb{T}^*{}_{\vec{X}}\mathcal{B} \to \mathbb{T}_{\vec{X}}\mathcal{B} \ , \\ \boldsymbol{g}(\vec{x}) : \mathbb{T}_{\vec{x}}\mathcal{S} \ \to \mathbb{T}^*{}_{\vec{x}}\mathcal{S} \qquad &\text{and} \qquad \boldsymbol{g}^{-1}(\vec{x}) : \mathbb{T}^*{}_{\vec{x}}\mathcal{S} \to \mathbb{T}_{\vec{x}}\mathcal{S} \ . \end{aligned}$$

The metrics are independent of time but may vary from point to point in $\mathcal{B}$ or $\mathcal{S}$. The matrices $\mathsf{G}_{\alpha\beta}$ and g_{ij} are symmetric, consequently, $\langle \vec{W}, \vec{V} \rangle = \langle \vec{V}, \vec{W} \rangle$ and $\langle \vec{w}, \vec{v} \rangle = \langle \vec{v}, \vec{w} \rangle$.

The following identities hold

$$\begin{aligned}
\mathsf{G}^{-1}\mathsf{G} &= \mathbf{I}_{\mathbb{T}\ \mathcal{B}} = \text{identity in } \mathbb{T}\ \mathcal{B}, & (\mathsf{G}^{-1})^{\alpha\gamma}\ \mathsf{G}_{\gamma\beta} &= \delta^{\alpha}{}_{\beta}\\
\mathsf{G}\ \ \mathsf{G}^{-1} &= \mathbf{I}_{\mathbb{T}^*\mathcal{B}} = \text{identity in } \mathbb{T}^*\mathcal{B}, & \mathsf{G}_{\alpha\gamma}\ \ (\mathsf{G}^{-1})^{\gamma\beta} &= \delta_{\alpha}{}^{\beta}\\
\boldsymbol{g}^{-1}\boldsymbol{g} &= \mathbf{I}_{\mathbb{T}\ \mathcal{S}} = \text{identity in } \mathbb{T}\ \mathcal{S}, & (g^{-1})^{ik}\ \ g_{kj} &= \delta^{i}{}_{j}\\
\boldsymbol{g}\ \ \boldsymbol{g}^{-1} &= \mathbf{I}_{\mathbb{T}^*\mathcal{S}} = \text{identity in } \mathbb{T}^*\mathcal{S}, & g_{ik}\ \ (g^{-1})^{kj} &= \delta_{i}{}^{j}
\end{aligned}$$

By convention, we denote $(\mathsf{G}^{-1})^{\alpha\beta}$ by $\mathsf{G}^{\alpha\beta}$ and$(g^{-1})^{ij}$ by g^{ij}. Furthermore, raising or lowering the indices of a variable indicates the implicit use of the metric tensor to transform between $\mathbb{T}$ and $\mathbb{T}^*$, *e.g.*, $u_i v^i = u^i g_{ij} v^j = u_i g^{ij} v_j$. Finally, upper case bold letters denote tensors in $\mathcal{B}$ and lower case bold letters denote tensors in $\mathcal{S}$. A tilde over a letter is used to denote a tensor in the plastic frame.

1.3 Transpose, Inverse and Transpose-Inverse

In addition to the derivative of the mapping, $\mathsf{D}\boldsymbol{\phi}$, its transpose, inverse and transpose-inverse are important for transforming tensors between the domain and range of $\boldsymbol{\phi}$. In transforming tensors, it is helpful to keep track of the domain and range of these additional operators. In terms of indices, they can be written as follows:

$\mathbf{F}$	derivative,	$\mathsf{F}^{i}{}_{\alpha}(\vec{X},t) = \frac{\partial \phi^i}{\partial X^\alpha}$	$: \mathbb{T}\ _{\vec{X}}\mathcal{B} \to \mathbb{T}\ _{\vec{x}}\mathcal{S}$
$\mathbf{F}^T$	transpose,	$(\mathsf{F}^T)_{\alpha}{}^{i}(\vec{x},t) = \mathsf{F}^{i}{}_{\alpha} \circ \boldsymbol{\phi}^{-1}$	$: \mathbb{T}^*{}_{\vec{x}}\mathcal{S} \to \mathbb{T}^*{}_{\vec{X}}\mathcal{B}$
$\mathbf{F}^{-1}$	inverse,	$(\mathsf{F}^{-1})^{\alpha}{}_{i}(\vec{x},t) = (\mathsf{F}^{-1})^{\alpha}{}_{i} \circ \boldsymbol{\phi}^{-1}$	$: \mathbb{T}\ _{\vec{x}}\mathcal{S} \to \mathbb{T}\ _{\vec{X}}\mathcal{B}$
$\mathbf{F}^{-T}$	transpose-inverse,	$(\mathsf{F}^{-T})_{i}{}^{\alpha}(\vec{X},t) = (\mathsf{F}^{-1})^{\alpha}{}_{i}$	$: \mathbb{T}^*{}_{\vec{X}}\mathcal{B} \to \mathbb{T}^*{}_{\vec{x}}\mathcal{S}$

where $\vec{x} = \boldsymbol{\phi}(\vec{X},t)$ or $\vec{X} = \boldsymbol{\phi}^{-1}(\vec{x},t)$. Moreover, these operators satisfy the following identities

$$\begin{aligned}
\mathbf{F}^{-1}\mathbf{F} &= \mathbf{I}_{\mathbb{T}\ _{\vec{X}}\mathcal{B}} \quad \text{and} \quad \mathbf{F}\ \ \mathbf{F}^{-1} = \mathbf{I}_{\mathbb{T}\ _{\vec{x}}\mathcal{S}}\\
\mathbf{F}^T\ \mathbf{F}^{-T} &= \mathbf{I}_{\mathbb{T}^*{}_{\vec{X}}\mathcal{B}} \quad \text{and} \quad \mathbf{F}^{-T}\mathbf{F}^T = \mathbf{I}_{\mathbb{T}^*{}_{\vec{x}}\mathcal{S}}
\end{aligned}$$

Remark 1.1 In the language of differential geometry, the induced mapping of tensors on $\mathcal{B}$ to tensors on $\mathcal{S}$ is referred to as the push-forward of the map

$\boldsymbol{\phi} : \mathcal{B} \to \mathcal{S}$ and denoted $\boldsymbol{\phi}_*$. For a vector and covector

$$(\boldsymbol{\phi}_* \vec{U})(\vec{x}) = (\mathbf{F}\vec{U}) \circ \boldsymbol{\phi}^{-1} \ ,$$
$$(\boldsymbol{\phi}_* \vec{V}^*)(\vec{x}) = (\mathbf{F}^{-T}\vec{V}^*) \circ \boldsymbol{\phi}^{-1} \ .$$

The induced mapping in the other direction, from tensors on $\mathcal{S}$ to tensors on $\mathcal{B}$ is referred to as the pull-back and denoted $\boldsymbol{\phi}^*$. For a vector and covector

$$(\boldsymbol{\phi}^* \vec{u})(\vec{X}) = (\mathbf{F}^{-1}\vec{u}) \circ \boldsymbol{\phi} \ ,$$
$$(\boldsymbol{\phi}^* \vec{v}^*)(\vec{X}) = (\mathbf{F}^{T}\vec{v}^*) \circ \boldsymbol{\phi} \ .$$

The inverse of the derivative map is simply the derivative of the inverse map, $\mathbf{F}^{-1} = \mathsf{D}(\phi^{-1})$. The **transpose** can be defined in a co-coordinate free manner by the relation

$$(\vec{v}^*, \mathbf{F}\vec{W})_{\vec{x}} = (\mathbf{F}^T\vec{v}^*, \vec{W})_{\vec{X}} = v^*_i \mathsf{F}^i{}_\alpha W^\alpha \ ,$$

where $\vec{v}^* \in \mathbb{T}^*{}_{\vec{x}}\mathcal{S}$ and $\vec{W} \in \mathbb{T}_{\vec{X}}\mathcal{B}$. Instead of the transpose, ref. [11] uses the **adjoint** $\mathbf{F}^\dagger$, defined by the relation

$$\langle \mathbf{F}\vec{W}, \vec{v} \rangle_{\vec{x}} = \langle \vec{W}, \mathbf{F}^\dagger \vec{v} \rangle_{\vec{X}} \ ,$$

and represented in coordinates by

$$(\mathsf{F}^\dagger)^\alpha{}_a(\vec{x}, t) = (\mathsf{G}^{\alpha\beta} \circ \boldsymbol{\phi}^{-1})(\mathsf{F}^b{}_\beta \circ \boldsymbol{\phi}^{-1})\, g_{ba} : \mathbb{T}_{\vec{x}}\mathcal{S} \to \mathbb{T}_{\vec{X}}\mathcal{B} \ .$$

The transpose and adjoint operators are related by

$$\mathbf{F}^T \boldsymbol{g} = \mathbf{G} \circ \boldsymbol{\phi}^{-1}\, \mathbf{F}^\dagger \ .$$

We note that the domain and range of $\mathbf{F}^\dagger$ are the same as those for $\mathbf{F}^{-1}$.

1.4 Strain Tensors

In order to define a strain tensor, it is convenient to introduce several additional tensors. The right and left **Cauchy-Green tensors** are

$$\boxed{\mathbf{C} = (\mathbf{F}^T\boldsymbol{g}) \circ \boldsymbol{\phi}\, \mathbf{F}} \qquad \mathsf{C}_{\alpha\beta}(\vec{X}, t) = (g_{ij} \circ \boldsymbol{\phi})\, \mathsf{F}^i{}_\alpha \mathsf{F}^j{}_\beta \qquad : \mathbb{T}_{\vec{X}}\mathcal{B} \to \mathbb{T}^*{}_{\vec{X}}\mathcal{B}$$

$$\boxed{\mathbf{b} = (\mathbf{F}\mathbf{G}^{-1}) \circ \boldsymbol{\phi}^{-1}\, \mathbf{F}^T} \qquad \mathsf{b}^{ij}(\vec{x}, t) = (\mathsf{G}^{\alpha\beta}\, \mathsf{F}^i{}_\alpha \mathsf{F}^j{}_\beta) \circ \boldsymbol{\phi}^{-1} : \mathbb{T}^*{}_{\vec{x}}\mathcal{S} \to \mathbb{T}_{\vec{x}}\mathcal{S}$$

The **Lagrangian strain tensor** is defined by

$$\boxed{\mathbf{E} = \tfrac{1}{2}(\mathbf{C} - \mathbf{G})} \quad \mathsf{E}_{\alpha\beta}(\vec{X}, t) = \tfrac{1}{2}(\mathsf{C}_{\alpha\beta} - \mathsf{G}_{\alpha\beta}) : \mathbb{T}_{\vec{X}}\mathcal{B} \to \mathbb{T}^*{}_{\vec{X}}\mathcal{B} \ . \tag{1.3}$$

Transforming the strain tensor from the Lagrangian frame to the spatial frame, $\mathbf{E} \mapsto \mathbf{F}^{-T}\mathbf{E}\mathbf{F}^{-1}$, results in the **Eulerian** or **Almansi strain tensor**

$$\boxed{\mathbf{e} = \tfrac{1}{2}(\boldsymbol{g} - \mathbf{b}^{-1})} \quad \mathsf{e}_{ij}(\vec{x}, t) = \tfrac{1}{2}[g_{ij} - (\mathsf{b}^{-1})_{ij}] : \mathbb{T}_{\vec{x}}\mathcal{S} \to \mathbb{T}^*{}_{\vec{x}}\mathcal{S} \ . \tag{1.4}$$

The inverse of the left Cauchy-Green tensor $\mathbf{b}^{-1}$ is known as the **Finger tensor**.

The tensors $\mathbf{E}$ and $\mathbf{e}$ represent the total strain. In analogy with Eq. (1.3), the Lagrangian **plastic strain tensor** is defined by

$$\mathbf{E_p} = \tfrac{1}{2}(\mathbf{C_p} - \mathbf{G}) \ , \quad (\mathsf{E}_p)_{\alpha\beta}(\vec{X}, t) : \mathbb{T}_{\vec{X}}\mathcal{B} \to \mathbb{T}^*{}_{\vec{X}}\mathcal{B} \ , \tag{1.5}$$

where heuristically

$$\mathbf{C_p} = (\mathbf{F_p}^T\widetilde{\mathcal{G}}) \circ \boldsymbol{\phi}_p\, \mathbf{F_p} \ , \quad (\mathsf{C}_p)_{\alpha\beta}(\vec{X}, t) : \mathbb{T}_{\vec{X}}\mathcal{B} \to \mathbb{T}^*{}_{\vec{X}}\mathcal{B}$$

is the right Cauchy-Green plastic tensor, and $\widetilde{\mathcal{G}}$ is the metric in the plastic frame.

Similarly, in analogy with Eq. (1.4), the Eulerian **elastic strain tensor** is defined by

$$\mathbf{e_e} = \tfrac{1}{2}(\boldsymbol{g} - \mathbf{b_e}^{-1}) \ , \quad (\mathsf{e}_e)_{ij}(\vec{x}, t) : \mathbb{T}_{\vec{x}}\mathcal{S} \to \mathbb{T}^*{}_{\vec{x}}\mathcal{S} \ , \tag{1.6}$$

where heuristically

$$\begin{aligned} \mathbf{b_e} &= (\mathbf{F_e}\widetilde{\mathcal{G}}^{-1}) \circ \boldsymbol{\phi}_e^{-1}\, \mathbf{F_e}^T \ , \quad (\mathsf{b}_e)^{ij}(\vec{x}, t) : \mathbb{T}^*{}_{\vec{x}}\mathcal{S} \to \mathbb{T}_{\vec{x}}\mathcal{S} \\ &= \mathbf{F}\mathbf{C_p}^{-1}\mathbf{F}^T \end{aligned}$$

is the left Cauchy-Green elastic tensor.

The plastic strain tensor can be transformed to the spatial frame

$$\begin{aligned} \mathbf{e_p} &= \mathbf{F}^{-T}\mathbf{E_p}\mathbf{F}^{-1} \ , \quad \mathbf{e_p}(\vec{x}, t) : \mathbb{T}_{\vec{x}}\mathcal{S} \to \mathbb{T}^*{}_{\vec{x}}\mathcal{S} \\ &= \tfrac{1}{2}(\mathbf{b_e}^{-1} - \mathbf{b}^{-1}) \\ &= \tfrac{1}{2}(\boldsymbol{g} - \mathbf{b}^{-1}) - \tfrac{1}{2}(\boldsymbol{g} - \mathbf{b_e}^{-1}) \end{aligned} \tag{1.7}$$

Consequently, the total strain can be expressed as the **super-position** or sum of elastic and plastic strains

$$\mathbf{e} = \mathbf{e_e} + \mathbf{e_p} \ .$$

Similarly, the elastic strain tensor can be transformed to the body frame

$$\begin{aligned} \mathbf{E_e} &= \mathbf{F}^T \mathbf{e_e} \mathbf{F} \ , \quad \mathbf{E_e}(\vec{X}, t) : \mathbb{T}_{\vec{X}} \mathcal{B} \to \mathbb{T}^*{}_{\vec{X}} \mathcal{B} \\ &= \tfrac{1}{2}(\mathbf{C} - \mathbf{C_p}) \\ &= \tfrac{1}{2}(\mathbf{C} - \mathbf{G}) - \tfrac{1}{2}(\mathbf{C_p} - \mathbf{G}) \end{aligned} \tag{1.8}$$

Again the super-position of strains is satisfied

$$\mathbf{E} = \mathbf{E_e} + \mathbf{E_p} \ .$$

Many theories of plasticity start out with the super-position assumption independent of the multiplicative decomposition. All theories are constructed to have the same small strain limit. However, theories can differ greatly in the large strain or non-linear regime.

Remarks:

1.2 One could also define elastic and plastic strains in the intermediate plastic frame as

$$\begin{aligned} \widetilde{\mathbf{e}}_{\boldsymbol{e}} &= \tfrac{1}{2}[(\mathbf{F_e}^T \boldsymbol{g}) \circ \boldsymbol{\phi}_e \, \mathbf{F_e} - \widetilde{\mathcal{G}}] \ , & \widetilde{\mathbf{e}}_{\boldsymbol{e}}(\vec{X}, t) &: \mathbb{T}_{\vec{X}} \mathcal{P} \to \mathbb{T}^*{}_{\vec{X}} \mathcal{P} \\ \widetilde{\mathbf{E}}_{\boldsymbol{p}} &= \tfrac{1}{2}[\widetilde{\mathcal{G}} - (\mathbf{F_p}^{-T} \mathbf{G}) \circ \boldsymbol{\phi}_p^{-1} \, \mathbf{F_p}^{-1}] \ , & \widetilde{\mathbf{E}}_{\boldsymbol{p}}(\vec{X}, t) &: \mathbb{T}_{\vec{X}} \mathcal{P} \to \mathbb{T}^*{}_{\vec{X}} \mathcal{P} \end{aligned}$$

Provided that the total strain is transformed to the plastic frame

$$\widetilde{\mathbf{E}} = \mathbf{F_p}^{-T} \mathbf{E} \mathbf{F_p}^{-1}$$

the super-position assumption $\widetilde{\mathbf{E}} = \widetilde{\mathbf{e}}_{\boldsymbol{e}} + \widetilde{\mathbf{E}}_{\boldsymbol{p}}$ again holds. Super-position only makes sense when the total, elastic and plastic strains are transformed to the same frame.

1.3 The strain tensor defines a bilinear map from $\mathbb{T}\mathcal{B} \otimes \mathbb{T}\mathcal{B} \to \mathbb{R}$ by

$$\mathbf{E}(\vec{U}_1, \vec{U}_2) = (\mathbf{E}\vec{U}_1, \vec{U}_2) \ ,$$

where $\vec{U}_1, \vec{U}_2 \in \mathbb{T}\mathcal{B}$. The bilinear form is symmetric $\mathbf{E}(\vec{U}_1, \vec{U}_2) = \mathbf{E}(\vec{U}_2, \vec{U}_1)$. This is the coordinate free expression of the symmetry $\mathsf{E}_{\alpha\beta} = \mathsf{E}_{\beta\alpha}$.

1.5 Volumetric and Deviatoric Components

The ratio $\boxed{\mathsf{J} = \frac{V}{V_0}}$ of the specific volume in the spatial frame to the specific volume in the reference frame is determined from the deformation gradient by the relation

$$\begin{aligned}\mathsf{J}^2(\vec{X},t) &\equiv \mathsf{det}\Big(\mathbf{F}^\dagger \circ \boldsymbol{\phi}\,\mathbf{F}\Big) = \mathsf{det}\Big(\mathbf{G}^{-1}\mathbf{C}\Big)\\ &= \mathsf{det}\Big([\mathbf{G}+2\mathbf{E}]\mathbf{G}^{-1}\Big)\\ &= \mathsf{det}\Big(\mathbf{I}_{\mathbb{T}^*_{\vec{X}}\mathcal{B}} + 2\mathbf{E}\mathbf{G}^{-1}\Big)\end{aligned}$$

For small strain, $\epsilon \equiv \|\mathbf{E}\|_{\mathbf{G}^{-1}} \ll 1$, (see Remark 1.5 for definition of norm and Remark 1.4 for definition of trace) we can write

$$\mathsf{J}^2 = 1 + 2\,\mathsf{Tr}\left(\mathbf{E}\,\mathbf{G}^{-1}\right) + \mathcal{O}\left(\epsilon^2\right). \tag{1.9}$$

Consequently, the change in the specific volume can be expressed as

$$\frac{V-V_0}{V_0} = \mathsf{Tr}\left(\mathbf{E}\,\mathbf{G}^{-1}\right) + \mathcal{O}\left(\epsilon^2\right).$$

We note that the relative change in specific volume or volumetric strain is positive in expansion and negative in compression. In addition, similar arguments can be used to yield

$$\mathsf{J}^2 \circ \boldsymbol{\phi} = \mathsf{det}\Big[(\mathbf{I}_{\mathbb{T}^*_{\vec{X}}\mathcal{S}} - 2\mathbf{e}\boldsymbol{g}^{-1})^{-1}\Big],$$

and for small strain to leading order $(V-V_0)/V_0 = \mathsf{Tr}\,(\mathbf{e}\,\boldsymbol{g}^{-1})$.

From the identity $\mathsf{det}(AB) = \mathsf{det}(A)\,\mathsf{det}(B)$ it follows that the specific volume ratio can be expressed as

$$\boxed{\mathsf{J} = \Big[\mathsf{det}(\boldsymbol{g}\circ\boldsymbol{\phi})/\,\mathsf{det}(\mathbf{G})\Big]^{1/2}\mathsf{det}(\mathbf{F})}.$$

The determinant factors enter because $(\mathsf{det}\,\mathbf{G})^{1/2}d^3X$ is the volume element in $\mathcal{B}$, and $(\mathsf{det}\,\boldsymbol{g})^{1/2}d^3x$ is the volume element in $\mathcal{S}$. When the metrics are normalized, $\mathsf{det}(\boldsymbol{g}) = \mathsf{det}(\mathbf{G}) = 1$, the specific volume ratio can be expressed simply as $\mathsf{J} = \mathsf{det}(\mathbf{F})$. However, the metric still is needed in Eq. (1.9) to relate J directly to the strain tensor.

The strain tensor can be split into the sum of a volumetric component and a deviatoric component, (see Remark 1.6 for definition of deviator)

$$\mathbf{E} = \tfrac{1}{3}\,\mathsf{Tr}\left(\mathbf{E}\,\mathbf{G}^{-1}\right)\,\mathbf{G} + \mathsf{dev}_{\mathbf{G}}\left(\mathbf{E}\right)\ .$$

Transforming to the Eulerian strain, leads to a decomposition identical in form

$$\mathbf{e} = \mathbf{F}^{-T}\mathbf{E}\mathbf{F}^{-1} = \tfrac{1}{3}\,\mathsf{Tr}\left(\mathbf{e}\,\mathbf{b}\right)\,\mathbf{b}^{-1} + \mathsf{dev}_{\mathbf{b}^{-1}}\left(\mathbf{e}\right)$$

when the transformation of the metric

$$\mathbf{b}^{-1} = \mathbf{F}^{-T}\mathbf{G}\mathbf{F}^{-1} : \mathbb{T}\,\mathcal{S} \to \mathbb{T}^*\,\mathcal{S}$$

is taken into account. Thus, $\mathbf{b}^{-1}$ can be interpreted as the reference frame metric transformed to the spatial frame.

Alternatively, the decomposition can be based on the metric $\boldsymbol{g}$, *i.e.*,

$$\mathbf{e} = \tfrac{1}{3}\,\mathsf{Tr}\left(\mathbf{e}\,\boldsymbol{g}^{-1}\right)\,\boldsymbol{g} + \mathsf{dev}_{\boldsymbol{g}}\left(\mathbf{e}\right)\ .$$

Transforming the Eulerian strain to the Lagrangian frame gives the decomposition

$$\mathbf{E} = \tfrac{1}{3}\,\mathsf{Tr}\left(\mathbf{E}\,\mathbf{C}^{-1}\right)\,\mathbf{C} + \mathsf{dev}_{\mathbf{C}}\left(\mathbf{E}\right)\ .$$

Thus, $\mathbf{C} = \mathbf{F}^T\boldsymbol{g}\mathbf{F}$ can be interpreted as the spatial frame metric transformed to the reference frame. Since the decomposition of a tensor is not unique, it is important to specify the metric in the definition of the deviator.

Remarks:

1.4 The **trace** is defined by

$$\mathsf{Tr}\left(\mathbf{G}^{-1}\mathbf{E}\right) = \mathsf{Tr}\left(\mathbf{E}\mathbf{G}^{-1}\right) \equiv \mathsf{E}_{ij}\mathsf{G}^{ji}\ .$$

The contraction of upper and lower indices is invariant under any transformation. Hence the trace of an operator on $\mathbb{T}\,\mathcal{B}$ or $\mathbb{T}^*\,\mathcal{B}$, such as the tensor $\mathbf{G}^{-1}\mathbf{E} : \mathbb{T}\,\mathcal{B} \to \mathbb{T}\,\mathcal{B}$ or the tensor $\mathbf{E}\mathbf{G}^{-1} : \mathbb{T}^*\,\mathcal{B} \to \mathbb{T}^*\,\mathcal{B}$, is invariant under a change of basis.

1.5 The **norm with respect to a metric** is defined as

$$\|\mathbf{E}\|^2_{\mathbf{G}^{-1}} \equiv \mathsf{G}^{\alpha\alpha'}\mathsf{G}^{\beta\beta'}\mathsf{E}_{\alpha\beta}\mathsf{E}_{\alpha'\beta'}\ .$$

The metric is needed in order for the norm to be independent of the choice of basis. The norm also can be express in terms of the trace,

$$\|\mathbf{E}\|^2_{\mathbf{G}^{-1}} = \mathsf{Tr}\Big[(\mathbf{G}^{-1}\,\mathbf{E})^T\,\mathbf{G}^{-1}\,\mathbf{E}\Big] \ .$$

1.6 The **deviator** is defined by

$$\mathsf{dev}_{\mathbf{Q}}\,(\mathbf{E}) \equiv \mathbf{E} - \tfrac{1}{3}\,\mathsf{Tr}\left(\mathbf{E}\mathbf{Q}^{-1}\right)\mathbf{Q} \ .$$

Since physical space is three dimensional, $\mathsf{Tr}\,(\mathbf{I}_{\mathbb{T}\mathcal{B}}) = \mathsf{Tr}\,(\mathbf{I}_{\mathbb{T}^*\mathcal{B}}) = 3$. Consequently, the deviator is a projection operator, *i.e.*,

$$\mathsf{dev}_{\mathbf{Q}}\,(\mathsf{dev}_{\mathbf{Q}}\,(\mathbf{E})) = \mathsf{dev}_{\mathbf{Q}}\,(\mathbf{E}) \ .$$

Another important formula is for the transform of a deviator

$$\mathbf{F}^{-T}\,\mathsf{dev}_{\mathbf{Q}}\,(\mathbf{E})\,\mathbf{F}^{-1} = \mathsf{dev}_{\mathbf{F}^{-T}\mathbf{Q}\mathbf{F}^{-1}}\left(\mathbf{F}^{-T}\mathbf{E}\,\mathbf{F}^{-1}\right) \ .$$

2 Hyper-Elasticity

A material model is called **elastic** if the stress is a function of the strain. Some engineering models are defined in terms of the stress rate as a function of stress, strain and strain rate. These models have the property that the stress depends on the strain path. Material models for which the stress can not be expressed in terms of only the current strain state are called **hypo-elastic**. In order to have a thermodynamic description an energy function is needed such that the stress is the derivative of the energy with respect to the strain. Materials models with such an energy function are called **hyper-elastic**.

Frame indifference requires that the energy function is invariant for all isometries on $\mathbb{T}\,\mathcal{S}$, *i.e.*, under the transformation $\mathbf{F} \mapsto \mathbf{Q}\,\mathbf{F}$ for all $\mathbf{Q} : \mathbb{T}\,\mathcal{S} \to \mathbb{T}\,\mathcal{S}$ such that

$$\mathbf{Q}^T\,\boldsymbol{g}\,\mathbf{Q} = \boldsymbol{g} \ .$$

As a consequence the energy can depend on the material deformation only through the strain tensor $\mathbf{E}$ and not on the deformation gradient by itself.

A similar requirement, that the energy is invariant for all isometries on $\mathbb{T}\mathcal{P}$, *i.e.*, under the transformation $\mathbf{F_p} \mapsto \mathbf{Q}\,\mathbf{F_p}$ for all $\mathbf{Q} : \mathbb{T}\mathcal{P} \to \mathbb{T}\mathcal{P}$ such that $\mathbf{Q}^T\,\widetilde{\mathcal{G}}\,\mathbf{Q} = \widetilde{\mathcal{G}}$, leads to the conclusion that the energy can depend on the plastic deformation only through the plastic strain tensor $\mathbf{E_p}$. Consequently, for an elastic-plastic material we are led to assume that there is a function for the **specific energy** depending on total strain, plastic strain and entropy

$$\boxed{\mathcal{E} = \mathcal{E}(\mathbf{E}, \mathbf{E_p}, \eta)}\,,$$

where η is the **specific entropy**. Furthermore, we assume the **thermodynamic relation**

$$\boxed{d\mathcal{E} = V_0\,\mathbf{S} : d\mathbf{E} - V_0\,\mathbf{S_p} : d\mathbf{E_p} + T\,d\eta}\,, \tag{2.1}$$

where T is the temperature, and $\mathbf{S}$ and $\mathbf{S}_p$ are the elastic and plastic stress tensors in the Lagrangian frame. The ':' denotes **contraction** over a pair of tensor indices, *e.g.*, $\mathbf{S} : d\mathbf{E} = \mathsf{Tr}(\mathbf{S}^T \cdot d\mathbf{E}) = \mathsf{S}^{\alpha\beta} d\mathsf{E}_{\alpha\beta}$.

The **second Piola-Kirchhoff stress tensor** and the corresponding plastic stress tensor are given by

$$\boxed{\mathbf{S} \;=\; \rho_0 \frac{\partial \mathcal{E}}{\partial \mathbf{E}}}\,, \qquad \mathsf{S}^{\alpha\beta}(\vec{X}, t) = \;\rho_0 \frac{\partial \mathcal{E}}{\partial \mathsf{E}_{\alpha\beta}} \quad : \mathbb{T}^*{}_{\vec{X}}\,\mathcal{B} \to \mathbb{T}_{\vec{X}}\,\mathcal{B}$$

$$\boxed{\mathbf{S_p} = -\rho_0 \frac{\partial \mathcal{E}}{\partial \mathbf{E_p}}}\,, \quad (\mathsf{S_p})^{\alpha\beta}(\vec{X}, t) = -\rho_0 \frac{\partial \mathcal{E}}{\partial (\mathsf{E}_p)_{\alpha\beta}} : \mathbb{T}^*{}_{\vec{X}}\,\mathcal{B} \to \mathbb{T}_{\vec{X}}\,\mathcal{B}$$

The Eulerian or **Cauchy stress tensor** is given by

$$\boxed{\boldsymbol{\sigma} = \mathsf{J}^{-1}\mathbf{F}\mathbf{S}\mathbf{F}^T}\,, \qquad \sigma^{ij}(\vec{x}, t) = (\mathsf{J}^{-1}\mathsf{F}^i{}_\alpha \mathsf{F}^j{}_\beta \mathsf{S}^{\alpha\beta}) \circ \boldsymbol{\phi}^{-1} : \mathbb{T}^*{}_{\vec{x}}\,\mathcal{S} \to \mathbb{T}_{\vec{x}}\,\mathcal{S}$$

or alternatively as [2]

$$\boldsymbol{\sigma} = 2\rho \frac{\partial \mathcal{E}}{\partial \boldsymbol{g}}\,.$$

Since the strain $\mathsf{E}_{\alpha\beta}$ is a symmetric matrix, it follows that both the second Piola-Kirchhoff stress $\mathsf{S}^{\alpha\beta}$ and the Cauchy stress σ^{ij} are symmetric matrices.

Remark 2.1 The symmetry of the stress tensor is required to ensure local angular momentum conservation. This condition assumes that individual atoms or molecules within a material have no angular momentum.

In analogy to the strain decomposition, the stress can be split into a hydrostatic and deviatoric part

$$\boldsymbol{\sigma} = -P\,\boldsymbol{g}^{-1} + \mathsf{dev}_{\boldsymbol{g}^{-1}}(\boldsymbol{\sigma}) \ ,$$

where $P = -\frac{1}{3}\,\mathsf{Tr}\,(\boldsymbol{\sigma}\,\boldsymbol{g})$ is the **pressure**. When strain is positive in expansion, the stress is positive in tension, hence, the negative sign in the definition of the pressure. In the Lagrangian frame, the pressure can be expressed as $P = -\frac{1}{3}\mathsf{J}^{-1}\,\mathsf{Tr}\,(\mathbf{S}\,\mathbf{C})$. In addition,

$$\mathsf{J}\,\mathbf{F}^{-1}\,\mathsf{dev}_{\boldsymbol{g}^{-1}}(\boldsymbol{\sigma})\,\mathbf{F}^{-T} = \mathsf{dev}_{\mathbf{C}^{-1}}(\mathbf{S}) \ . \tag{2.2}$$

This formula enables us to transform the stress deviator between the Eulerian and Lagrangian frames.

2.1 Isotropic Material

A material is isotropic if its energy function is invariant for all isometries on $\mathbb{T}\,\mathcal{B}$, *i.e.*, under the transformation $\mathbf{F} \mapsto \mathbf{F}\,\mathbf{Q}$ for all $\mathbf{Q} : \mathbb{T}\,\mathcal{B} \to \mathbb{T}\,\mathcal{B}$ such that

$$\mathbf{Q}^T\,\mathbf{G}\,\mathbf{Q} = \mathbf{G} \ .$$

The energy can then be expressed as function of the invariants of

$$\mathbf{G}^{-1}\mathbf{C} : \mathbb{T}\,\mathcal{B} \to \mathbb{T}\,\mathcal{B} \ , \qquad (\mathsf{F}^\dagger\mathsf{F})^\alpha{}_\beta = \mathsf{G}^{\alpha\gamma}\mathsf{C}_{\gamma\beta} \ .$$

The **invariants** of a 3×3 matrix are the coefficients of its characteristic polynomial

$$P(\lambda) = \lambda^3 - I_1\lambda^2 + I_2\lambda - I_3$$

whose roots are the eigenvalues of the matrix. For $\mathbf{G}^{-1}\mathbf{C}$, the invariants can be expressed as

$$\boxed{\begin{aligned} I_1 &= \mathsf{Tr}(\mathbf{G}^{-1}\mathbf{C}) \\ I_2 &= \tfrac{1}{2}\Big(I_1^2 - \mathsf{Tr}\big[(\mathbf{G}^{-1}\mathbf{C})^2\big]\Big) \\ I_3 &\equiv \det(\mathbf{G}^{-1}\mathbf{C}) = \mathsf{J}^2 \end{aligned}}$$

Remark 2.2 Under a transformation the tensor $\mathbf{G}^{-1}\mathbf{C} \mapsto \mathbf{Q}^{-1}(\mathbf{G}^{-1}\mathbf{C})\mathbf{Q}$. By Lemma A.5 the eigenvalues of the matrix $\mathbf{G}^{-1}\mathbf{C}$ and hence the invariants

of $\mathbf{G}^{-1}\mathbf{C}$ are unchanged by the transformation. From the definition of $\mathbf{C}$ it follows that the eigenvalues of $\mathbf{G}^{-1}\mathbf{C}$ are real and positive. Consequently, there are constraints on the invariants of $\mathbf{G}^{-1}\mathbf{C}$.

Applying the chain rule

$$\frac{\partial \mathcal{E}}{\partial \mathbf{C}} = \frac{\partial \mathcal{E}}{\partial I_1}\frac{\partial I_1}{\partial \mathbf{C}} + \frac{\partial \mathcal{E}}{\partial I_2}\frac{\partial I_2}{\partial \mathbf{C}} + \frac{\partial \mathcal{E}}{\partial I_3}\frac{\partial I_3}{\partial \mathbf{C}}$$

and using Lemma A.1, the stress can be expressed as [22, p. 261, Eq. (7.1.108)]

$$\begin{aligned}
\tfrac{1}{2}V_0\mathbf{S} &= \left(\frac{\partial \mathcal{E}}{\partial I_1} + I_1\frac{\partial \mathcal{E}}{\partial I_2}\right)\mathbf{G}^{-1} - \left(\frac{\partial \mathcal{E}}{\partial I_2}\right)\mathbf{G}^{-1}\mathbf{C}\,\mathbf{G}^{-1} + \left(I_3\frac{\partial \mathcal{E}}{\partial I_3}\right)\mathbf{C}^{-1} \\
\tfrac{1}{2}V\boldsymbol{\sigma} &= \left(I_3\frac{\partial \mathcal{E}}{\partial I_3}\right)\boldsymbol{g}^{-1} + \left(\frac{\partial \mathcal{E}}{\partial I_1} + I_1\frac{\partial \mathcal{E}}{\partial I_2}\right)\mathbf{b} - \left(\frac{\partial \mathcal{E}}{\partial I_2}\right)\mathbf{b}\,\boldsymbol{g}\,\mathbf{b}
\end{aligned}$$

2.2 Illustrative Elastic Models

Two example models for an isotropic elastic material are described. The first model is known as linear elasticity. The second model is for a non-linear isotropic material. For each model, the specific energy and the corresponding stress tensors are presented.

2.2.1 Linear Elasticity

Linear elasticity represents the leading order expansion of the energy function about the ambient state of an isotropic material,

$$\mathcal{E} = \tfrac{1}{2}V_0\lambda\left[\mathsf{Tr}\left(\mathbf{G}^{-1}\mathbf{E}\right)\right]^2 + V_0 G\,\mathsf{Tr}\left[(\mathbf{G}^{-1}\mathbf{E})^2\right] ,$$

where λ and G are the **Lamé coefficients**. The second Piola-Kirchhoff stress is then given by

$$\begin{aligned}
\mathbf{S} &= \rho_0\frac{\partial \mathcal{E}}{\partial \mathbf{E}} \\
&= K\,\mathsf{Tr}\left(\mathbf{G}^{-1}\mathbf{E}\right)\mathbf{G}^{-1} + 2\,G\,\mathsf{dev}_{\mathbf{G}^{-1}}\left(\mathbf{G}^{-1}\,\mathbf{E}\,\mathbf{G}^{-1}\right) ,
\end{aligned}$$

and the Cauchy stress is given by

$$\begin{aligned}\boldsymbol{\sigma} &= \mathsf{J}^{-1}\,\mathbf{F}\,\mathbf{S}\,\mathbf{F}^{T} \\ &= \frac{V_0}{V}\,K\,\mathsf{Tr}\,(\mathbf{b}\cdot\mathbf{e})\;\mathbf{b} + 2\,\frac{V_0}{V}\,G\;\mathsf{dev}_{\mathbf{b}}\,(\mathbf{b}\,\mathbf{e}\,\mathbf{b})\;\;,\end{aligned}$$

where $K = \lambda + \frac{2}{3}G$, is the **bulk modulus**, and G is the **shear modulus**.

In the small strain limit $\mathbf{b} = \boldsymbol{g}^{-1} + \mathcal{O}\left(\|\mathbf{e}\|_{\boldsymbol{g}^{-1}}\right)$, and the Cauchy stress reduces to

$$\boldsymbol{\sigma} = K\,\mathsf{Tr}\left(\boldsymbol{g}^{-1}\,\mathbf{e}\right)\,\boldsymbol{g}^{-1} + 2\,G\;\mathsf{dev}_{\boldsymbol{g}^{-1}}\left(\boldsymbol{g}^{-1}\,\mathbf{e}\,\boldsymbol{g}^{-1}\right) + \mathcal{O}\left(\|\mathbf{e}\|^2_{\boldsymbol{g}^{-1}}\right).$$

With the identity matrix for the spatial metric, $g_{ij} = \delta_{ij}$, this equation corresponds to the standard form for the stress of a linearly elastic isotropic material.

Remark 2.3 Linear elasticity is a reasonable description of many metals at a stress low compared to the yield strength. It is frequently used in engineering applications.

2.2.2 Non-linear Isotropic Model

As an illustrative example of a non-linear isotropic material, suppose the energy has the form

$$\mathcal{E} = \tfrac{1}{8}V_0\,K\,(I_3 - 1)^2 + \tfrac{1}{2}V_0\,G\Big(I_1\,I_3^{-1/3} - 3\Big) \tag{2.3}$$

Then the stress is given by

$$\begin{aligned}\mathbf{S} &= \tfrac{1}{2}K I_3(I_3-1)\,\mathbf{C}^{-1} + 2\,G\,{I_3}^{-1/3}\,\mathsf{dev}_{\mathbf{C}^{-1}}\Big(\mathbf{G}^{-1}\mathbf{E}\mathbf{C}^{-1}\Big) \\ \mathsf{J}\,\boldsymbol{\sigma} &= \tfrac{1}{2}K I_3(I_3-1)\,\boldsymbol{g}^{-1} + 2\,G\,{I_3}^{-1/3}\,\mathsf{dev}_{\boldsymbol{g}^{-1}}\Big(\mathbf{b}\mathbf{e}\boldsymbol{g}^{-1}\Big)\end{aligned} \tag{2.4}$$

Despite its appearance, we note that the deviator term is a symmetric matrix, due to the identity

$$\mathbf{G}^{-1}\mathbf{E}\mathbf{C}^{-1} = \tfrac{1}{2}\mathbf{G}^{-1}(\mathbf{C}-\mathbf{G})\mathbf{C}^{-1} = \tfrac{1}{2}\Big(\mathbf{G}^{-1} - \mathbf{C}^{-1}\Big)\;.$$

We also note that

$$\begin{aligned}\mathbf{G}^{-1} - \mathbf{C}^{-1} &= \mathbf{G}^{-1} - (\mathbf{G} + 2\,\mathbf{E})^{-1} \\ &= 2\,\mathbf{G}^{-1}\mathbf{E}\mathbf{G}^{-1} - 4\,\mathbf{G}^{-1}\mathbf{E}\mathbf{G}^{-1}\mathbf{E}\mathbf{G}^{-1} + \cdots\end{aligned}$$

which converges for $\left\|\mathbf{G}^{-1}\mathbf{E}\right\| < \frac{1}{2}$. Thus, in this example the stress is really a non-linear function of the strain.

In the limit of small strain, $\|\mathbf{E}\|_{\mathbf{G}^{-1}} \ll 1$,

$$\begin{aligned}I_1 &= 3 + 2\epsilon + \mathcal{O}\left(\|\mathbf{E}\|^2_{\mathbf{G}^{-1}}\right) \\ I_3 &= 1 + 2\epsilon + \mathcal{O}\left(\|\mathbf{E}\|^2_{\mathbf{G}^{-1}}\right) \\ \mathbf{C} &= \mathbf{G} + \mathcal{O}\left(\|\mathbf{E}\|_{\mathbf{G}^{-1}}\right) \\ \mathbf{b} &= \boldsymbol{g}^{-1} + \mathcal{O}\left(\|\mathbf{E}\|_{\mathbf{G}^{-1}}\right)\end{aligned}$$

where $\epsilon = \mathsf{Tr}\left(\mathbf{G}^{-1}\mathbf{E}\right)$. Moreover, the Cauchy stress can be expressed as

$$\boldsymbol{\sigma} = K\,\frac{V - V_0}{V_0}\,\boldsymbol{g}^{-1} + 2\,G\,\mathsf{dev}_{\boldsymbol{g}^{-1}}\left(\boldsymbol{g}^{-1}\mathbf{e}\boldsymbol{g}^{-1}\right) + \mathcal{O}\left(\|\mathbf{E}\|^2_{\mathbf{G}^{-1}}\right)\,.$$

This is the standard form for linear elasticity, in which the bulk and shear moduli are taken to be constants. In general, for arbitrary strain, it is not consistent with hyper-elasticity for the moduli to be constant [1, 23]. In other words, linear elasticity is **only** valid for small strain. The illustrative example is a simple model that is equivalent to linear elasticity for small strain, yet consistent with hyper-elasticity for large strain.

Remarks:

2.4 Though isotropy is a convenient modeling assumption, in reality most materials are not isotropic. Metals, for example, are polycrystalline and crystals by their very nature are anisotropic. But at the cell size typically used in an engineering simulation, metals behave as if they are isotropic when their grains are randomly oriented. In other words, isotropy can be a reasonable approximation on a coarse grain scale. However, there are circumstances when a material, even on a coarse scale, has a preferred direction. This occurs, for example, due to the rolling of sheets or the drawing of wire. In these cases the isotropic approximation breaks down. The non-uniform distribution of grain orientations is referred to as 'texture' in the materials community.

2.5 Even if a material is initially isotropic, the material does not remain isotropic for non-hydrostatic deformations. The stress is still determined by the isotropic specific energy for the reference state. However, the elastic tensor for a particular strain state need not be isotropic. This is important outside the domain of linear elasticity, *i.e.*, large elastic strains, though plastic deformation may mitigate the anisotropy of the deformed state by limiting the non-hydrostatic component of the elastic strain tensor.

2.3 Conservation Equations

2.3.1 Eulerian Form

The conservation laws of mass, momentum and energy in the Eulerian frame are expressed as

$$\boxed{\begin{aligned} \frac{\partial}{\partial t}\Big(\rho\Big) + \Big(\rho u^j\Big)_{;j} &= 0 \\ \frac{\partial}{\partial t}\Big(\rho u^i\Big) + \Big(\rho u^i u^j - \sigma^{ij}\Big)_{;j} &= 0 \\ \frac{\partial}{\partial t}\Big(\rho\Big[\tfrac{1}{2}u_i u^i + \mathcal{E}\Big]\Big) + \Big(\rho\Big[\tfrac{1}{2}u_i u^i + \mathcal{E}\Big]u^j - u_i\sigma^{ij}\Big)_{;j} &= 0 \end{aligned}} \tag{2.5}$$

where $\rho = 1/V$ is the density, the subscript ';j' denotes **covariant differentiation**,

$$\begin{aligned} u^i{}_{;j} &= \frac{\partial}{\partial x^j}u^i + \gamma^i_{jk}u^k \\ u_{i;j} &= \frac{\partial}{\partial x^j}u_i - \gamma^k_{ij}u_k \end{aligned}$$

and

$$\gamma^a_{dc} = \tfrac{1}{2}\, g^{ab'}\left(\frac{\partial g_{cb'}}{\partial x^d} + \frac{\partial g_{db'}}{\partial x^c} - \frac{\partial g_{dc}}{\partial x^{b'}}\right) \tag{2.6}$$

is the **Christoffel symbol** corresponding to the metric $\boldsymbol{g}$. The covariant derivative obeys the usual product rule for differentiation, *e.g.*, $(u_i\sigma^{ij})_{;j} = u_{i;j}\sigma^{ij} + u_i(\sigma^{ij}{}_{;j})$. In addition, from Eq. (2.6) it follows that $g_{ik;j} = 0$, hence $g_{ik}\,(u^k)_{;j} = u_{i;j}$.

The covariant derivative accounts for the curvature of the coordinate system, *i.e.*, if $\vec{e}_i$ are basis vectors in $\mathbb{T}\,\mathcal{S}$ then $\frac{\partial \vec{e}_i}{\partial x^j} = \gamma^k_{ij}\vec{e}_k$. This is illustrated in the directional derivative $\vec{w}\cdot\vec{\nabla}$ and the divergence of the vector $\vec{u} = u^i\vec{e}_i$,

$$(\vec{w}\cdot\vec{\nabla})(u^i\vec{e}_i) = w^j\Big(\frac{\partial}{\partial x^j}u^i + \gamma^i_{jk}u^k\Big)\vec{e}_i = w^j u^i{}_{;j}\vec{e}_i$$
$$\vec{\nabla}\cdot(u^i\vec{e}_i) = \quad \frac{\partial}{\partial x^i}u^i + \gamma^i_{ik}u^k \quad = \quad u^i{}_{;i}$$

In addition, the covariant derivative of a tensor with contravariant indices is

$$\sigma^{ij}{}_{;k} = \frac{\partial}{\partial x^k}\sigma^{ij} + \gamma^i_{kp}\sigma^{pj} + \gamma^j_{kp}\sigma^{ip}\ ,$$

and a tensor with covariant indices

$$\mathbf{e}_{ij;k} = \frac{\partial}{\partial x^k}\mathbf{e}_{ij} - \gamma^p_{ik}\mathbf{e}_{pj} - \gamma^p_{jk}\mathbf{e}_{ip}\ .$$

In particular, the divergence of the Cauchy stress is

$$\sigma^{ij}{}_{;j} = \frac{\partial}{\partial x^j}\sigma^{ij} + \gamma^i_{kj}\sigma^{kj} + \gamma^j_{kj}\sigma^{ik}\ .$$

The Christoffel symbol is symmetric in the lower indices, *i.e.*, $\gamma^a_{bc} = \gamma^a_{cb}$. The **curvature tensor** is defined in terms of the Christoffel symbol by

$$r^a{}_{bcd} = \frac{\partial\gamma^a_{db}}{\partial x^c} - \frac{\partial\gamma^a_{cb}}{\partial x^d} + \gamma^a_{ce}\gamma^e_{db} - \gamma^a_{de}\gamma^e_{cb}\ .$$

The non-commutivity of the covariant derivative,

$$u^a{}_{;bc} - u^a{}_{;cb} = r^a{}_{bcd}u^d\ ,$$

is characterized by the curvature tensor.

Remark 2.6 The Christoffel symbol is *not* a tensor, *i.e.*, for the transformed metric $\mathbf{C} = \mathbf{F}^T\boldsymbol{g}\mathbf{F}$, the transformed Christoffel symbol $\Gamma^\alpha_{\beta\Xi} \neq (\mathsf{F}^{-1})^\alpha{}_i\gamma^i_{jk}\mathsf{F}^j{}_\beta\mathsf{F}^k{}_\Xi$.

2.3.2 Lagrangian Form

The flow equations can be transformed from the Eulerian frame to the Lagrangian frame by applying the Piola identity. Define the **Piola transform** of $\vec{y}\in\mathbb{T}\,\mathcal{S}\mapsto\vec{Y}\in\mathbb{T}\,\mathcal{B}$ by

$$Y^\alpha = \mathsf{J}\,(\mathsf{F}^{-1})^\alpha{}_i y^i\ . \tag{2.7}$$

Then the **Piola identity** is expressed as

$$Y^{\alpha}{}_{;\alpha} = \mathsf{J}\, y^{i}{}_{;i} \ , \tag{2.8}$$

where the covariant derivatives in $\mathbb{T}\,\mathcal{S}$ and $\mathbb{T}\,\mathcal{B}$ are based on Christoffel symbol for the metrics $\boldsymbol{g}$ and G, respectively.

The conservation laws can be expressed in integral form. In fact, this is how they are derived physically. For example, momentum conservation is expressed as

$$\frac{\partial}{\partial t}\int_{\boldsymbol{\phi}(\Omega,t)} d^3x\, \rho u^i + \oint_{\partial\boldsymbol{\phi}(\Omega,t)} da\, \hat{n}_j \sigma^{ji} = 0 \ , \quad \text{for any } \Omega \subset \mathcal{B},$$

where $\boldsymbol{\phi}(\Omega,t) = \{\vec{x} = \boldsymbol{\phi}(\vec{X},t) \mid \vec{X} \in \Omega\}$. As a consequence of Piola identity and Gauss' law

$$\oint_{\partial\Omega} dA\, \hat{N}\cdot\vec{Y} = \int_{\Omega} d^3X\, Y^{\alpha}{}_{;\alpha} = \int_{\boldsymbol{\phi}(\Omega)} d^3x\, y^{i}{}_{;i} = \oint_{\partial\boldsymbol{\phi}(\Omega)} da\, \hat{n}\cdot\vec{y}\ .$$

This enables the surface terms in the integral form of the conservation laws to be transformed readily between frames. Then re-expressing the conservation laws as differential equations leads to the Lagrangian form of the flow equations

$$\boxed{\begin{aligned} \frac{d}{dt}\Big(\mathsf{J}\Big) - \Big(\mathsf{J}\,(\mathsf{F}^{-1})^{\alpha}{}_{i} U^i\Big)_{;\alpha} &= 0 \\ \rho_0 \frac{d}{dt}\Big(U^i\Big) - \mathsf{P}^{i\alpha}{}_{;\alpha} &= 0 \\ \rho_0 \frac{d}{dt}\Big(\tfrac{1}{2}U_i U^i + \mathcal{E}\Big) - \Big(U_i \mathsf{P}^{i\alpha}\Big)_{;\alpha} &= 0 \end{aligned}} \tag{2.9}$$

where $\frac{d}{dt} = \frac{\partial}{\partial t}\big|_{\vec{X}} = \frac{\partial}{\partial t}\big|_{\vec{x}} + \vec{u}\cdot\vec{\nabla}$ is the **convective derivative**, and

$$\boxed{\mathsf{P} = \boldsymbol{g}^{-1}\frac{\partial \mathcal{E}}{\partial \mathsf{F}} = \mathsf{FS}} \ , \quad \mathsf{P}^{i\alpha}(\vec{X},t) = \mathsf{F}^{i}{}_{\beta}\mathsf{S}^{\beta\alpha} : \mathbb{T}^{*}{}_{\vec{X}}\,\mathcal{B} \to \mathbb{T}_{\vec{X}}\,\mathcal{S}$$

is the **first Piola-Kirchhoff stress tensor**. In addition, mass conservation is trivial, $\frac{d}{dt}\rho_0 = 0$, and has been replaced by volume conservation. Equation (2.9·a) is derived by applying the Piola Identity to Lemma A.4. We note that the first Piola-Kirchhoff stress is a two-point tensor and is not represented by a symmetric matrix.

2.4 Kinematic Equations

The conservations laws alone give a system of partial differential equations (PDEs), either in Eulerian form Eq. (2.5) or in Lagrangian form Eq. (2.9), that is not closed. In contrast to fluid flow, the stress depends on the strain deviator in addition to the specific volume. Consequently, a kinematic equation for the evolution of the strain tensor is needed to complete the flow equations.

Remark 2.7 Continuum mechanics can be formulated directly in terms of the mapping $\boldsymbol{\phi}$ by writing the momentum equation in the form of Newton's second law ($F = ma$),

$$\rho_0 \frac{\partial^2}{\partial t^2}\phi^i = \frac{\partial}{\partial X^\alpha}\tilde{\mathsf{P}}^{i\alpha}\big(\mathsf{D}\vec{\phi}\big) \ .$$

This is well defined for smooth flows but not for discontinuous flows, because the right hand side is a nonlinear function of $\frac{\partial}{\partial X^\alpha}\phi^i$. Discontinuities, known as shock waves, commonly arise in the solution of nonlinear wave equations even when the initial data is smooth. The strain tensor is introduced as an independent variable in order to obtain a system of quasi-linear PDEs (*i.e.*, first order and linear in all derivatives) and use the theory of hyperbolic PDEs to regularize the continuum model.

In Lagrangian form, the evolution of the deformation gradient

$$\frac{d}{dt}\mathbf{F} = \mathsf{D}\vec{U} \ , \qquad \boxed{\frac{d}{dt}\mathsf{F}^i{}_\alpha = \frac{\partial}{\partial X^\alpha}U^i} \ , \tag{2.10}$$

is conveniently in conservation form. However, to recover the mapping $\boldsymbol{\phi}$ from the deformation gradient requires the **compatibility conditions**

$$\boxed{\frac{\partial}{\partial X^\alpha}\mathsf{F}^i{}_\beta = \frac{\partial}{\partial X^\beta}\mathsf{F}^i{}_\alpha} = \frac{\partial^2}{\partial X^\alpha \partial X^\beta}\phi^i \ . \tag{2.11}$$

From Eq. (2.10) it follows that if the compatibility conditions are satisfied at some initial time then the compatibility conditions will be satisfied for all time. Consequently, Eq. (2.10) is equivalent to 3 independent equations and subsume the volume conservation equation (2.9·a). The effective system of PDEs has 7 independent equations. Hence, physically there are 7 wave

families. With Eq. (2.11) the full system has 6 additional physically irrelevant waves. Later we show that the full system is indeed hyperbolic and that the physical waves can be identified with 3 acoustic wave families (one quasi-longitudinal and two quasi-transverse) in both the forward and backward directions and a linearly degenerate mode for the advection of entropy.

Remark 2.8 When the continuum equations are discretized for numerical simulations, the compatibility conditions may not be satisfied exactly. The problem is analogous for incompressible fluid flow to enforcing the condition that the divergence of the velocity vanishes. If the error in the compatibility conditions increases with time of run then the simulations can be seriously inaccurate or numerical instabilities may develop. Part of the problem is that vorticity in the flow can lead to stirring on a fine scale and when resolution of $\boldsymbol{\phi}$ is lost, the discretization errors can become large.

The Eulerian form for the evolution of the deformation gradient is obtained by applying the chain rule to Eq. (2.10)

$$\frac{d}{dt}\mathsf{f} = (\vec{\nabla}\vec{u})\cdot\mathsf{f}\ , \qquad \frac{d}{dt}\mathsf{f}^i{}_\alpha = u^i{}_{;j}\mathsf{f}^j{}_\alpha\ , \tag{2.12}$$

where $\mathsf{f}(\vec{x},t) = \mathsf{F}\circ\phi^{-1} : \mathbb{T}_{\vec{\phi}^{-1}(\vec{x},t)}\mathcal{B} \to \mathbb{T}_{\vec{x}}\mathcal{S}$. Plohr and Sharp [16] have shown that this evolution equation may be recast in conservation form.

Lemma 2.1. The evolution of the deformation gradient can be expressed as

$$\boxed{\frac{\partial}{\partial t}\left(\mathsf{J}^{-1}\mathsf{f}^i{}_\alpha\right) + \left(\mathsf{J}^{-1}\mathsf{f}^i{}_\alpha u^j\right)_{;j} = \left(\mathsf{J}^{-1}\mathsf{f}^j{}_\alpha u^i\right)_{;j}}\ . \tag{2.13}$$

Proof. From the mass conservation Eq. (2.5·a) and Eq. (2.12), the left hand side of Eq. (2.13) can be expressed as

$$\begin{aligned}\frac{\partial}{\partial t}\left(\mathsf{J}^{-1}\mathsf{f}^i{}_\alpha\right) + \left(\mathsf{J}^{-1}\mathsf{f}^i{}_\alpha u^j\right)_{;j} &= \mathsf{J}^{-1}\frac{d}{dt}\mathsf{f}^i{}_\alpha \\ &= \mathsf{J}^{-1}\mathsf{f}^j{}_\alpha u^i{}_{;j}\end{aligned}$$

The right hand side of Eq. (2.13) can be expressed as

$$\left(\mathsf{J}^{-1}\mathsf{f}^j{}_\alpha u^i\right)_{;j} = \mathsf{J}^{-1}\mathsf{f}^j{}_\alpha u^i{}_{;j} + \left(\mathsf{J}^{-1}\mathsf{f}^j{}_\alpha\right)_{;j} u^i\ .$$

Apply the Piola identity Eq. (2.8) to the second term on the right hand side, we find

$$\left(\mathsf{J}^{-1}\mathsf{f}^{j}{}_{\alpha}\right)_{;j} = \mathsf{J}^{-1}\,\delta^{\beta}{}_{\alpha;\beta} = 0\ .$$

Combining the above three equations yields Eq. (2.13). ⊠

Alternatively, the analog of Eq. (2.10) for the inverse map leads to the evolution equation for f^{-1} [27]

$$\frac{\partial}{\partial t}\left((\mathsf{f}^{-1})^{\alpha}{}_{i}\right) + \left((\mathsf{f}^{-1})^{\alpha}{}_{j}u^{j}\right)_{;i} = 0\ , \tag{2.13′}$$

which can be used in place of Eq. (2.13).

Remark 2.9 The time derivative in Eq. (2.13) does not enter in the combination $\partial_t + \vec{u}\cdot\nabla$. Consequently, the Eulerian form of the evolution equation for the deformation gradient is not Galilean invariant ($\vec{x} \mapsto \vec{x} + \vec{u}_0 t$ and $\vec{u} \mapsto \vec{u} + \vec{u}_0$). However, solutions for initial data that satisfy the kinematic compatibility condition Eq. (2.11) are Galilean invariant. This emphasises the importance of the compatibility condition in the Eulerian formulation.

2.5 Dissipation

The external rate of working is given by $V_0\,\mathbf{S} : \frac{d\mathbf{E}}{dt}$. Using Eq. (2.12) the strain rate can be written as

$$\boxed{\frac{d\mathbf{E}}{dt} = \mathbf{F}^T\mathbf{d}\mathbf{F}}\ , \tag{2.14}$$

where the **rate of deformation tensor** is

$$\boxed{\mathbf{d} = \tfrac{1}{2}\Big(\vec{\nabla}(\boldsymbol{g}\vec{u}) + [\vec{\nabla}(\boldsymbol{g}\vec{u})]^T\Big)}\ , \qquad \mathsf{d}_{ij} = \tfrac{1}{2}(u_{i;j} + u_{j;i})\ . \tag{2.15}$$

Therefore, the external rate of working can be expressed as

$$\begin{aligned} V_0\,\mathsf{Tr}\left(\mathbf{S}\,\frac{d\mathbf{E}}{dt}\right) &= V_0\,\mathsf{Tr}\left(\mathbf{S}\,\mathbf{F}^T\mathbf{d}\,\mathbf{F}\right) \\ &= V\,\boldsymbol{\sigma}\big] \ .:\mathbf{d} \\ &= -P\frac{dV}{dt} + V\ \mathsf{dev}_{\boldsymbol{g}^{-1}}(\boldsymbol{\sigma}) : \mathsf{dev}_{\boldsymbol{g}}(\mathbf{d}) \end{aligned} \tag{2.16}$$

where in the last equation we substituted mass conservation equation expressed as

$$\vec{\nabla} \cdot \vec{u} = \tfrac{1}{V} \tfrac{d}{dt} V \ .$$

The conservation form of the energy equation (2.5·c) is expressed in terms of the total energy, $\frac{1}{2} |\vec{u}|^2 + \mathcal{E}$. Substituting the mass and momentum equations yields an evolution equation for the specific internal energy

$$\boxed{\frac{d}{dt}\mathcal{E} = V\, \boldsymbol{\sigma} : \mathbf{d}} \ . \tag{2.17}$$

Substituting the relation for the external work Eq. (2.16) and the rate of change of internal energy Eq. (2.17) into the thermodynamic identity Eq. (2.1) gives a constraint on the plastic strain rate

$$\boxed{T \tfrac{d}{dt}\eta = V_0\, \mathbf{S_p} : \tfrac{d}{dt}\mathbf{E_p} \geq 0} \ . \tag{2.18}$$

A constraint of this kind, obtained by requiring the local dissipation to be positive, is known as the **Clausius-Duhem inequality**. Since we are neglecting source terms, such as arise from heat conduction, in the absence of plastic strain the flow is isentropic.

Even with plasticity, as discussed later, the plastic strain rate is a source function. Hence, Eq. (2.18) is in characteristic form. Advection of entropy corresponds to a degenerate wave family. This is analogous to the what occurs for the Euler equations describing fluid flow.

Remarks:

2.10 It is instructive to transform the strain rate from the Lagrangian frame to the Eulerian frame.

$$\begin{aligned} \frac{d\mathbf{e}}{dt} &= \mathbf{F}^{-T} \frac{d\mathbf{E}}{dt} \mathbf{F}^{-1} - (\vec{\nabla}\vec{u})^T \mathbf{e} - \mathbf{e}\,(\vec{\nabla}\vec{u}) \\ &= \mathbf{d} - (\vec{\nabla}\vec{u})^T \mathbf{e} - \mathbf{e}\,(\vec{\nabla}\vec{u}) \end{aligned}$$

Consequently, the external rate of working is not equal to $V\, \boldsymbol{\sigma} : \frac{d\mathbf{e}}{dt}$.

2.11 The time derivative of the Eulerian strain can be expressed as a **Lie derivative**, $\frac{d\mathbf{e}}{dt} = L_{\vec{u}}(\mathbf{e})$. In effect, the time derivative is defined as the

transform of the derivative of the transformed quantity in the reference frame. This is necessary for the theory to be frame invariant. The concept of a Lie derivative is described in more detail in Appendix E.

2.6 Wave Analysis

The wave speeds for a hyperbolic system of PDEs are determined from the eigenvalues of the flux matrix. Because of the complications that arise from the compatibility relations, we shall use the Lagrangian equations and then transform to the spatial frame.

A few preliminary definitions are needed. The fourth rank **stiffness tensor** is defined by

$$\overline{\overline{\mathbf{C}}} \equiv \frac{\partial \mathbf{S}}{\partial \mathbf{E}} = \rho_0 \frac{\partial^2 \mathcal{E}}{\partial \mathbf{E}\, \partial \mathbf{E}} \ .$$

It follows from the definition that the stiffness tensor has the following symmetry properties

$$\overline{\overline{\mathsf{C}}}^{\beta\alpha\alpha'\beta'} = \overline{\overline{\mathsf{C}}}^{\alpha\beta\alpha'\beta'} = \overline{\overline{\mathsf{C}}}^{\alpha'\beta'\alpha\beta} = \overline{\overline{\mathsf{C}}}^{\alpha\beta\beta'\alpha'} \ .$$

The stiffness tensor allows small changes in the stress to be related to small changes in the strain

$$\Delta\mathbf{S} = \overline{\overline{\mathbf{C}}} : \Delta\mathbf{E} \ , \qquad (\Delta\mathsf{S})^{\alpha\beta} = \overline{\overline{\mathsf{C}}}^{\alpha\beta\alpha'\beta'} (\Delta\mathsf{E})_{\alpha'\beta'} \ .$$

Hence,

$$\begin{aligned} \frac{d}{dt}\mathbf{S} &= \overline{\overline{\mathbf{C}}} : \frac{d}{dt}\mathbf{E} \\ &= \overline{\overline{\mathbf{C}}} : (\mathbf{F}^T \mathbf{d} \mathbf{F}) \ . \end{aligned}$$

The transformed stiffness tensor

$$\overline{\overline{\mathsf{c}}}^{ipjq} = \mathsf{J}^{-1}\, \mathsf{F}^i{}_{\alpha'} \mathsf{F}^p{}_{\alpha} \mathsf{F}^j{}_{\beta'} \mathsf{F}^q{}_{\beta} \overline{\overline{\mathsf{C}}}^{\alpha'\alpha\beta'\beta} \ ,$$

relates changes in the Cauchy stress to changes in the Eulerian strain

$$\overset{\bullet}{\boldsymbol{\sigma}} = \overline{\overline{\mathbf{c}}} : \overset{\circ}{\mathbf{e}} \ ,$$

where

$$\begin{aligned}\overset{\bullet}{\boldsymbol{\sigma}} &= \frac{1}{\mathsf{J}}\mathbf{F}\frac{d\mathbf{S}}{dt}\mathbf{F}^T \\ &= \frac{d}{dt}\boldsymbol{\sigma} - (\vec{\nabla}\vec{u})\boldsymbol{\sigma} - \boldsymbol{\sigma}(\vec{\nabla}\vec{u})^T + \mathsf{Tr}\left(\boldsymbol{g}^{-1}\mathbf{d}\right)\boldsymbol{\sigma}\ , \\ \overset{\circ}{\mathbf{e}} &= \mathbf{F}^{-T}\frac{d\mathbf{E}}{dt}\mathbf{F}^{-1} \\ &= \frac{d}{dt}\mathbf{e} + (\vec{\nabla}\vec{u})^T\mathbf{e} + \mathbf{e}(\vec{\nabla}\vec{u})\ .\end{aligned}$$

Consequently, the time derivative of the Cauchy stress can be expressed as

$$\frac{d}{dt}\boldsymbol{\sigma} - \boldsymbol{\omega}\boldsymbol{\sigma} + \boldsymbol{\sigma}\boldsymbol{\omega} = \tilde{\tilde{\mathbf{c}}} : \mathbf{d}\ , \tag{2.19}$$

where

$$\tilde{\tilde{\mathsf{c}}}^{ijpq} = \overline{\overline{\mathsf{c}}}^{ijpq} + \tfrac{1}{2}\Big(g^{ip}\sigma^{jq} + \sigma^{ip}g^{jq} + g^{jp}\sigma^{iq} + \sigma^{jp}g^{iq}\Big) - \sigma^{ij}g^{pq},$$

and

$$\boldsymbol{\omega} = \tfrac{1}{2}\Big[(\vec{\nabla}\vec{u}) - (\vec{\nabla}\vec{u})^T\Big]\ .$$

Remark 2.12 The form of the time derivative of the Cauchy stress given by Eq. (2.19) is frame indifferent. The form of $\overset{\bullet}{\boldsymbol{\sigma}}$ is known as Truesdell's objective derivative. There are other forms for objective time derivatives of tensors, see for example [5] and [11, §1.6]. They are related to the choice of frame in which the stiffness tensor is specified. The form of objective derivative is important for numerical simulations based on hypo-elastic constitutive models, especially when the shear component of the stiffness tensor is assumed constant. A constant stiffness tensor is a useful approximation for small strain but in general is not consistent with hyper-elasticity [1, 23].

The inverse of the stiffness tensor is called the **compliance tensor** and allows small changes in the strain to be related to small changes in the stress

$$\Delta\mathbf{E} = \overline{\overline{\mathbf{S}}} : \Delta\mathbf{S}\ , \qquad (\Delta\mathsf{E})_{\alpha\beta} = \overline{\overline{\mathsf{S}}}_{\alpha\beta\alpha'\beta'}(\Delta\mathsf{S})^{\alpha'\beta'}\ ,$$

where

$$\overline{\overline{\mathsf{C}}}^{\alpha\beta\alpha'\beta'}\ \overline{\overline{\mathsf{S}}}_{\alpha'\beta'\iota\kappa} = \tfrac{1}{2}\Big(\delta^{\alpha}{}_{\iota}\delta^{\beta}{}_{\kappa} + \delta^{\alpha}{}_{\kappa}\delta^{\beta}{}_{\iota}\Big)\ .$$

The symmetry requirement, *i.e.*, the symmetric identity operator on the right hand side, complicates the computation of $\overline{\overline{\mathbf{S}}}$ from $\overline{\overline{\mathbf{C}}}$. Details are given in Appendix B.

An additional tensor, closely related to the stiffness tensor, is the **acoustic tensor**

$$\overline{\overline{\mathbf{A}}} = \boldsymbol{g}^{-1}\frac{\partial \mathbf{P}}{\partial \mathbf{F}} , \qquad \overline{\overline{\mathsf{A}}}^{i\alpha j\beta} = \mathsf{F}^{i}{}_{\alpha'}\mathsf{F}^{j}{}_{\beta'}\overline{\overline{\mathsf{C}}}^{\alpha'\alpha\beta'\beta} + g^{ij}\,\mathsf{S}^{\alpha\beta}$$

The acoustic tensor is a two-point rank-four tensor. However, in the spatial frame, the acoustic tensor,

$$\overline{\overline{\mathsf{a}}}^{ipjq} = \mathsf{J}^{-1}\,\mathsf{F}^{p}{}_{\alpha}\mathsf{F}^{q}{}_{\beta}\overline{\overline{\mathsf{A}}}^{i\alpha j\beta} = \overline{\overline{\mathsf{c}}}^{ipjq} + g^{ij}\,\sigma^{pq} ,$$

is a one-point rank-four tensor.

In the previous subsection we found that one characteristic is associated with the advection of entropy. To find the other wave families, we take the entropy to be constant and drop the energy equation. We analyze the system of 12 PDEs consisting of the three momentum equation (2.9·b) and the nine kinematic equations (2.10)

$$\begin{aligned} \rho_0\frac{d}{dt}U^i - \overline{\overline{\mathsf{A}}}^{i\alpha\ \ \beta}_{\ j}\frac{\partial}{\partial X^\alpha}\mathsf{F}^{j}{}_{\beta} &= 0 \\ \frac{d}{dt}\mathsf{F}^{i}{}_{\alpha} - \frac{\partial}{\partial X^\alpha}U^i &= 0 \end{aligned}$$

Here, the metric is assumed constant and the covariant derivative reduces to the ordinary derivative in flat space.

We look for traveling wave solutions of the form $\vec{W} = \vec{W}(\Xi)$ where $\Xi = \langle \hat{N}, \vec{X}\rangle - Ct$, C is the wave speed, the direction of propagation $\hat{N}$ is normalized to satisfy $\langle \hat{N}, \hat{N}\rangle = 1$, and the vector of unknowns is

$$\vec{W} = (\mathsf{F}^{j}{}_{\beta=1}, \mathsf{F}^{j}_{\beta=2}, \mathsf{F}^{j}_{\beta=3}, U^i)^T , \quad \text{with } i,j = 1,2,3 .$$

Then the system of equations can be written as $\mathcal{L}\vec{W} = 0$ with $\mathcal{L}$ in block matrix form

$$\mathcal{L} = \begin{pmatrix} C\mathbf{I} & 0 & 0 & N_1\mathbf{I} \\ 0 & C\mathbf{I} & 0 & N_2\mathbf{I} \\ 0 & 0 & C\mathbf{I} & N_3\mathbf{I} \\ N_\alpha\overline{\overline{\mathsf{A}}}^{i\alpha\ \ \beta=1}_{\ j} & N_\alpha\overline{\overline{\mathsf{A}}}^{i\alpha\ \ \beta=2}_{\ j} & N_\alpha\overline{\overline{\mathsf{A}}}^{i\alpha\ \ \beta=3}_{\ j} & \rho_0 C\mathbf{I} \end{pmatrix} \frac{d}{d\Xi}\vec{W} = \vec{0} .$$

The wave speeds are the solution to the equation obtained by setting the determinant of $\mathcal{L}$ to zero. By adding multiples of the first three columns to the fourth column the determinant equation reduces to

$$
\begin{aligned}
0 &= \mathsf{det}(\mathcal{L}) \\
&= \mathsf{det}\begin{pmatrix} C\mathbf{I} & 0 & 0 & 0 \\ 0 & C\mathbf{I} & 0 & 0 \\ 0 & 0 & C\mathbf{I} & 0 \\ N_\alpha \overline{\overline{\mathsf{A}}}^{i\alpha}{}_{j}{}^{\beta=1} & N_\alpha \overline{\overline{\mathsf{A}}}^{i\alpha}{}_{j}{}^{\beta=2} & N_\alpha \overline{\overline{\mathsf{A}}}^{i\alpha}{}_{j}{}^{\beta=3} & \rho_0 C\mathbf{I} - C^{-1}\overline{\mathbf{A}}(\hat{N}) \end{pmatrix} \\
&= C^6\, \mathsf{det}\left(\overline{\mathbf{A}}(\hat{N}) - \rho_0 C^2 \mathbf{I}\right)
\end{aligned}
$$

where $\overline{\mathsf{A}}(\hat{N})^{i}{}_{j} = N_\alpha \overline{\overline{\mathsf{A}}}^{i\alpha}{}_{j}{}^{\beta} N_\beta$. Thus, there are six trivial wave speeds, $C = 0$, and three pairs of non-trivial waves, $\pm C$, determined by the equation

$$
\mathsf{det}\left(\overline{\mathsf{A}}(\hat{N})^{i}{}_{j} - \rho_0 C^2 \delta^{i}{}_{j}\right) = 0 \ . \tag{2.20}
$$

We show that the trivial waves are ruled out by the compatibility condition Eq. (2.11), and that each pair of non-trivial waves corresponds to an acoustic wave family.

First we examine the non-trivial waves. Let $\vec{\mathsf{U}}$ be an eigenvalue of $\overline{\mathbf{A}}(\hat{N})$ with eigenvalue $\rho_0 C^2$. Then a solution to the linearized equations is given by

$$
\begin{aligned}
\vec{U} &= \vec{U}_0 + \vec{\mathsf{U}}\, W(\Xi) \\
\mathsf{F}^{i}{}_{\alpha} &= (\mathsf{F}_0)^{i}{}_{\alpha} - N_\alpha(\mathsf{U}^i/C) W(\Xi)
\end{aligned}
$$

for any smooth function $W(\Xi)$. We note that the deformation gradient caused by the wave $\Delta\mathsf{F}^{i}{}_{\alpha} = -N_\alpha(\mathsf{U}^i/C)W(\Xi)$ satisfies the compatibility condition Eq. (2.11) and is physically admissible.

The eigenvector corresponding to the eigenvalue $C = 0$ have $\Delta\vec{U} = 0$ and the change in the deformation gradient satisfying

$$
N_\alpha \overline{\overline{\mathsf{A}}}^{i\alpha}{}_{j}{}^{\beta} \Delta\mathsf{F}^{j}{}_{\beta} = 0 \ , \quad \text{for } i = 1, 2, 3. \tag{2.21}
$$

Since there are three linear equations for nine unknowns, $\Delta\mathsf{F}^{j}{}_{\beta}$, there are six families of solutions corresponding to the six fold degeneracy of the zero

eigenvalue. Moreover, if $\Delta \mathsf{F}^j{}_\beta$ satisfies the compatibility condition Eq. (2.11) then it has the form $\mathsf{U}^j N_\beta$ and Eq. (2.21) implies that U^j is an eigenvector of $\overline{\mathbf{A}}(\hat{N})$ with 0 eigenvalue. Conversely, if zero is not an eigenvalue of $\overline{\mathbf{A}}(\hat{N})$ then the solutions to Eq. (2.21) do not satisfy the compatibility condition and are physically inadmissible.

The results of the wave analysis can be summarized as follows. Provided that $\overline{\mathbf{A}}(\hat{N})$ is a positive matrix for all $\hat{N}$, the Lagrangian flow equations (2.9) and (2.10) are a hyperbolic system of PDEs. The system has one degenerate wave family corresponding to the advection of entropy and three pair of non-degenerate acoustic waves. The remaining six degenerate waves are physically irrelevant for solutions to initial value problems in which the initial data satisfies the compatibility condition Eq. (2.11).

Physical experiments measure waves speeds in the spatial frame. Therefore, it is important to transform the wave speeds we derived in the body frame into the spatial frame. The form of a traveling wave variable in the spatial frame is

$$\xi = \langle \hat{n}, \vec{x} \rangle - ct = \hat{n}_k (\mathsf{F}_0)^k{}_\alpha X^\alpha - ct$$

where the propagation direction $\hat{n}$ is normalized to satisfy $\langle \hat{n}, \hat{n} \rangle = 1$. Replacing $\Xi \mapsto \xi$, the equation for the sound speed Eq. (2.20) becomes

$$\det\Big(\overline{\mathsf{a}}(\hat{n})^{ij} g_{jk} - \rho c^2 \delta^i{}_k\Big) = 0 \ , \tag{2.22}$$

where $\overline{\mathsf{a}}(\hat{n})^{ij} = n_p \overline{\overline{\mathsf{a}}}^{ipjq} n_q = \overline{\mathsf{c}}(\hat{n})^{ij} + \sigma_{nn}\, g^{ij}$, $\overline{\mathsf{c}}(\hat{n})^{ij} = n_p \overline{\overline{\mathsf{c}}}^{ipjq} n_q$ and $\sigma_{nn} = \hat{n} \cdot \boldsymbol{\sigma} \cdot \hat{n}$. Or in terms of the stiffness tensor

$$\det\Big(\overline{\mathsf{c}}(\hat{n})^{ij} g_{jk} - (\rho c^2 - \sigma_{nn}) \delta^i{}_k\Big) = 0 \ .$$

Hence the eigenvalues of $\overline{\mathbf{c}}(\hat{n})$ must be greater than $-\sigma_{nn}$. We note that in compression $-\sigma_{nn}$ is positive.

Remark 2.13 The direction of propagations in the body frame and the spatial frame are related by $\vec{n}^* = \mathbf{F}^{-T} \vec{N}^*$. However, the spatial normalization is equivalent to $N^\alpha \mathsf{C}_{\alpha\beta} N^\beta = 1$. The normalization of the propagation direction affects the magnitude of the eigenvalues.

Let $\vec{\mathfrak{u}}$ be an eigenvector of $\overline{\mathbf{a}}(\hat{n})\boldsymbol{g}$. The deformation gradient of the wave has the form

$$(\mathsf{F} \circ \boldsymbol{\phi}^{-1})^i{}_\alpha(\xi) = (\mathsf{F}_0)^i{}_\alpha + \mathfrak{u}^i n_k (\mathsf{F}_0)^k{}_\alpha w(\xi) \ ,$$

where F_0 is the deformation gradient unperturbed material. It follows that the increment of the strain tensor due to the wave is

$$\Delta \mathsf{e}_{ij} = \tfrac{1}{2}\Big(\mathfrak{u}_i(\mathsf{b}_0^{-1})_{jk}\hat{n}^k + \hat{n}^k(\mathsf{b}_0^{-1})_{ki}\mathfrak{u}_j\Big)w(\xi) + \mathcal{O}\left(w^2\right) .$$

About the ambient state, $\mathbf{b}_0^{-1} = \boldsymbol{g}$ and the increment of strain due to the wave is simply $\Delta\mathbf{e} \propto \mathfrak{u}^* \otimes \hat{n}^* + \hat{n}^* \otimes \mathfrak{u}^*$, where $\mathfrak{u}^* = \boldsymbol{g}\mathfrak{u}$ and $\hat{n}^* = \boldsymbol{g}\hat{n}$.

The physical interpretation of the acoustic wave families is based on the eigenvectors. Typically, the eigenvector corresponding to the largest eigenvalue is approximately parallel to the propagation direction, *i.e.*, $\mathfrak{u} \cdot \hat{n} \approx 1$. This represents a longitudinal wave and corresponds to the hydrodynamics wave associated with changes in specific volume. Moreover, the two slower waves are associated with shear strength and their eigenvectors are approximately perpendicular to the direction of propagation, *i.e.*, $\mathfrak{u} \cdot \hat{n} \approx 0$. These represent transverse waves. They require shear stress and hence do not occur for ordinary fluid flow. In terms of the strain tensor, for a longitudinal wave $\Delta\mathbf{e} \propto \hat{n} \otimes \hat{n}$, and for a transverse wave $\hat{n} \cdot \Delta\mathbf{e} \cdot \hat{n} \approx 0$. It is important to note that in contrast to fluid flow, even the longitudinal sound speed may depend on the direction of propagation.

Remark 2.14 For an isotropic material, the sound speeds are independent of the direction of wave propagation. Moreover, the two transverse sound speed have the same magnitude. It is shown in subsection B.2 that the sound speeds are given by

$$\rho c_{\text{long}}^2 = K + \tfrac{4}{3}G$$
$$\rho c_{\text{tran}}^2 = G$$

Since the moduli are positive, the longitudinal sound speed is greater than the transverse sound speed.

For the elastic flow equations to be hyperbolic, the sound speeds must be real. Hence, for any direction $\hat{n}$, the eigenvalues of $\overline{\mathfrak{a}}(\hat{n})\boldsymbol{g}$ must be positive definite. This is equivalent to what is known as **strong ellipticity**,

$$(\vec{n}^* \otimes \vec{m}^*, \overline{\overline{\mathfrak{a}}} : \vec{n}^* \otimes \vec{m}^*) \geq \epsilon \left\|\vec{n}^*\right\|^2 \left\|\vec{m}^*\right\|^2$$

for any $\vec{n}^*, \vec{m}^* \in \mathbb{T}^* \mathcal{S}$ and some $\epsilon > 0$. In fact, ϵ is just the minimum of c^2 over all directions. Strong ellipticity can be expressed as a restricted convexity condition (rank-1 convexity) on the specific energy $\mathcal{E}$, see [11, p. 19]. Details are given in Appendix C.

Remarks:

2.15 We note that for zero stress, the leading order expansion of the specific energy is

$$\mathcal{E} = \tfrac{1}{2}\,\mathbf{E}:\overline{\overline{\mathsf{C}}}:\mathbf{E} + \mathcal{O}\left(\|\mathbf{E}\|^3_{\mathbf{G}^{-1}}\right) .$$

In order to be an energy minimum equilibrium state, $\overline{\overline{\mathsf{C}}}$ must be positive definite, and hence $\overline{\overline{\mathbf{A}}}$ would be positive definite. In general, this is a stronger condition than is needed for the flow equations to be hyperbolic, *i.e.*, hyperbolicity requires only strong ellipticity which is a weaker condition than positivity of the acoustic tensor.

2.16 Uniaxial flow reduces to a one-dimensional problem. For some materials, a state in tension is reached at which a continued increase in strain results in a decrease in stress, *i.e.*, a reversal of the sign of $d(stress)/d(strain)$. For an elastic material, a stress-strain relation of this type implies a loss of hyperbolicity. A non-monotonic variation of stress with strain can result from either thermal softening (decrease in the yield strength with temperature) or a phenomenon known as **dilatancy**. Physically, dilatancy is due to the nucleation and growth of cracks. The phenomenon of crack growth is an unstable process. To describe unstable phenomena, requires degrees of freedom for the state of the material in addition to the total strain tensor (such as plastic strain or volume fraction of cracks) plus rate equations for the evolution of the additional internal degrees of freedom. Consequently, loss of hyperbolicity of the elastic flow equations is associated with a breakdown of the physical assumptions underlying the continuum model.

2.17 Plasticity models have been proposed to describe dilatancy, by appropriately shaping the yield surface in conjunction with a rate independent associated flow rule. These models have had problems with instabilities. The choice of rate independent plasticity is probably the dominant cause of the difficulties. Very likely a rate dependent plastic strain rate would alleviate the ill-posedness associated with the instabilities and lead to plasticity models that could, at least qualitatively, describe dilatancy.

2.18 Plastic flow can be thought of as a non-equilibrium process that relaxes the stress deviator toward its equilibrium value. As is typical with relaxation processes, a non-zero plastic relaxation time can be expected to lower the equilibrium sound speeds. For example, the longitudinal sound speed of an

isotropic material drops from $[(K+\frac{4}{3}G)/\rho]^{1/2}$ in the elastic regime to $(K/\rho)^{1/2}$ in the plastic regime. In addition, since plastic flow is dissipative, traveling waves in the plastic regime can be expected to decay, *i.e.*, rather than an elastic wave $w = w(\hat{n}\cdot\vec{x} - ct)$, a traveling plastic wave would have the form $w = w(\hat{n}\cdot\vec{x} - ct)\exp(-t/\tau)$.

2.7 Shock Jump Conditions

For a shock propagating in the direction $\hat{N}$, it follows from the Lagrangian flow equations (2.9) and (2.10) that the shock jump conditions are given by

$$\begin{aligned} -M\,\Delta(U^i) &= \Delta(\mathsf{P}^{i\alpha})\,N_\alpha \\ -M\,\Delta\Big(\tfrac{1}{2}U_iU^i + \mathcal{E}\Big) &= \Delta(U_i\mathsf{P}^{i\alpha})\,N_\alpha \\ -M\,\Delta(\mathsf{F}^i{}_\alpha) &= \rho_0\,\Delta(U^i)\,N_\alpha \end{aligned} \tag{2.23}$$

where $M = \rho_0 U_s$ is the mass flux through the shock front, and U_s is the shock velocity in the body frame. The jump of a variable U across the shock front is denoted $\Delta(U) = U_1 - U_0$. In addition, the propagation direction is normalized to satisfy $N_\alpha\,N^\alpha = 1$.

Using the relation

$$\Delta(AB) = \bar{A}\Delta(B) + \Delta(A)\bar{B}\ ,$$

where a bar over a variable denotes the average, *i.e.*, $\bar{A} = \frac{1}{2}(A_0 + A_1)$, the jump in the strain is given by

$$\begin{aligned} \Delta(\mathsf{E}_{\alpha\beta}) &= \tfrac{1}{2}\Big[\Delta(\mathsf{F}^i{}_\alpha)\,g_{ij}\,\bar{\mathsf{F}}^j{}_\beta + \bar{\mathsf{F}}^i{}_\alpha\,g_{ij}\,\Delta(\mathsf{F}^j{}_\beta)\Big] \\ -M\,\Delta(\mathsf{E}_{\alpha\beta}) &= \tfrac{1}{2}\,\rho_0\,\Delta(U_i)\,\Big(N_\alpha\bar{\mathsf{F}}^i{}_\beta + \bar{\mathsf{F}}^i{}_\alpha\,N_\beta\Big) \end{aligned} \tag{2.24}$$

Together with a constitutive relation, $\mathbf{P} = \mathbf{F}\,\mathbf{S}(\mathbf{E},\mathcal{E})$, the jump conditions determine a one parameter curve for the shock locus of each wave family. Although the constitutive equation is a function of strain, we note that the deformation gradient is needed to determine the shock locus.

In the previous subsection, we have shown that there are three pair of acoustic wave families corresponding to a quasi-longitudinal wave and two quasi-transverse waves. The quasi-longitudinal wave satisfies $\Delta(\vec{U})\cdot\hat{N} \approx$

$\left|\Delta(\vec{U})\right|$ and is the analog of a gas dynamic shock wave. The quasi-transverse waves satisfy $\Delta(\vec{U})\cdot\hat{N} \ll \left|\Delta(\vec{U})\right|$ and are associated with shear stress.

Physically, the admissible shock waves are restricted to be entropy increasing. Algebraic manipulations to eliminate the velocity leads to the analog of the **Hugoniot equation** for gas dynamic shocks

$$\Delta(\mathcal{E}) = V_0\,\bar{\mathsf{P}}^{i\alpha}\,g_{ij}\,\Delta(\mathsf{F}^{j}{}_{\alpha})\ . \tag{2.25}$$

The Hugoniot equation can be used to show that for weak shocks the entropy change is third order. However, in contrast to the scalar gas dynamic case, the Hugoniot equation is not sufficient by itself to determine the shock locus.

Remark 2.19 Using the relation

$$\bar{\mathsf{P}} = \bar{\mathbf{F}}\bar{\mathbf{S}} + \tfrac{1}{4}\,\Delta(\mathbf{F})\Delta(\mathbf{S})$$

and the symmetry of $\mathbf{S}$, the Hugoniot equation can be expressed as

$$\Delta(\mathcal{E}) = V_0\,\bar{\mathsf{S}}^{\alpha\beta}\Delta(\mathsf{E}_{\alpha\beta}) + \tfrac{1}{4}\,V_0\,\Delta(\mathsf{F}^{i}{}_{\alpha})\,\Delta(\mathsf{S}^{\alpha\beta})\,g_{ij}\,\Delta(\mathsf{F}^{j}{}_{\beta})\ .$$

Consequently, the natural generalization of the gasdynamic Hugoniot equation is not true, *i.e.*, $\Delta(\mathcal{E}) \neq V_0\,\bar{\mathbf{S}}{:}\Delta(\mathbf{E})$.

The shock jump conditions can also be expressed in the spatial frame. From equations (2.5) and (2.13) the jump conditions can be written as

$$\begin{aligned} -M\,\Delta(u^i) &= \Delta(\sigma^{ij})\,n_j \\ -M\,\Delta\Big(\tfrac{1}{2}u_iu^i + \mathcal{E}\Big) &= \Delta(u_i\sigma^{ij})\,n_j \\ -M\Delta(\mathsf{f}^{i}{}_{\alpha}) &= \Delta(\rho\,\mathsf{f}^{j}{}_{\alpha}u^i)\,n_j \end{aligned} \tag{2.26}$$

where $M = (u_s - \hat{n}\cdot\vec{u})\rho$ is the mass flux through the shock front, u_s is the shock velocity in the spatial frame and the propagation direction is normalized to satisfy $n_i\,n^i = 1$. It can be shown using the Piola identity that the Lagrangian and Eulerian form of the jump conditions are equivalent [16].

3 Plastic Strain Rate

Experiments indicate that for small strain the response of many solids is reversible. This is referred to as the elastic regime. In contrast, for large

shear strain, irreversible processes take place which limit the shear stress. The material response that limits the shear stress is referred to as the plastic regime. The plastic strain tensor is the minimal number of degrees of freedom that needs to be added in order to extend elastic flow to the plastic regime in a physically consistent manner. Models with the addition of only a plastic strain tensor can describe the dominant effects of plasticity. But other internal degrees of freedom are need to account for other observed plastic flow phenomenon, such as work hardening.

In this section a form for the plastic strain rate is presented under the assumption that the specific energy of a material can be split into elastic and plastic components

$$\boxed{\mathcal{E} = \mathcal{E}_e(\widehat{\mathbf{E}}_{\boldsymbol{e}}, \eta) + \mathcal{E}_p(\mathbf{E_p})} \,, \tag{3.1}$$

where the choice of elastic strain in terms of the total strain and plastic strain $\widehat{\mathbf{E}}_{\boldsymbol{e}}(\mathbf{E}, \mathbf{E_p})$ is discussed below. We note that the Piola-Kirchhoff stress, $\mathbf{S} = \rho_0 \frac{\partial \mathcal{E}}{\partial \mathbf{E}}$ depends only on the elastic energy while the plastic stress can be written as the sum of two terms $\mathbf{S_p} = \mathbf{S'_p} + \mathbf{S''_p}$, where

$$\mathbf{S'_p} = -\rho_0 \frac{\partial \mathcal{E}_e}{\partial \mathbf{E_p}} \,,$$
$$\mathbf{S''_p} = -\rho_0 \frac{\partial \mathcal{E}_p}{\partial \mathbf{E_p}} \,,$$

associated with the elastic and plastic components of the energy.

For simplicity, the plastic specific energy often is neglected. This is a reasonable approximation for the mechanical properties of stiff material, those for which the component of stress from compression dominates the thermal component of stress. Experiments on metals [25], however, show that the plastic energy is about 10 percent of the external work in the plastic flow regime. Even for stiff materials, when thermal properties are important or for problems in which the material undergoes a large number of cycles, the plastic component of the energy can not be ignored.

Remark 3.1 The specific energy resulting from 'plastic work' maybe due to additional internal degree of freedom, such as those associated with work hardening, and only indirectly with the plastic strain.

Many plasticity models use as the elastic strain $\widehat{\mathbf{E}}_{\boldsymbol{e}} = \frac{1}{2}(\mathbf{C} - \mathbf{C_p})$. Hence, based on super-position of strains the elastic energy is frequently taken to

have the functional form

$$\mathcal{E}_e = \mathcal{E}_e(\mathbf{E} - \mathbf{E_p}, \eta) \ . \tag{3.2}$$

As a consequence of this modeling assumption, the elastic component of the plastic stress tensor and the Piola-Kirchhoff stress tensor are the same $\mathbf{S'_p} = \mathbf{S}$.

Instead, we use $\mathbf{C_p}^{-1}\mathbf{C}$ as a measure for elastic strain. This is motivated by analogy with the energy for an isotropic material. With the composition of maps, $\boldsymbol{\phi} = \boldsymbol{\phi}_e \circ \boldsymbol{\phi}_p$, the natural extension for an elastic-plastic isotropic material is to take the elastic energy to be a function of the invariants of

$$\begin{aligned}\widetilde{\mathcal{G}}^{-1}\widetilde{\mathbf{C}}_\mathbf{e} &= \widetilde{\mathcal{G}}^{-1}\mathbf{F_e}^T g \mathbf{F_e} \\ &= \mathbf{F_p}\Big(\mathbf{C_p}^{-1}\mathbf{C}\Big)\mathbf{F_p}^{-1}\end{aligned}$$

By Lemma A.5 the invariants of $\mathbf{C_p}^{-1}\mathbf{C}$ are the same as those of $\widetilde{\mathcal{G}}^{-1}\widetilde{\mathbf{C}}_\mathbf{e}$. Consequently, we take

$$\boxed{\mathcal{E}_e = \mathcal{E}_e(\mathbf{C_p}^{-1}\mathbf{C}, \eta)} \ . \tag{3.3}$$

Since $\mathbf{C_p}^{-1}\mathbf{C}$ can be expressed in terms of $\mathbf{E}$ and $\mathbf{E_p}$, this form satisfies the requirement of frame indifference. Moreover, though $\mathbf{S}$ and $\mathbf{S'_p}$ are related, they are not equal.

3.1 Yield Condition

We assume that the flow is elastic, $\frac{d}{dt}\mathbf{C_p} = 0$, when $\widehat{\mathsf{Y}}(\mathbf{C}, \mathbf{C_p}) < Y$, where Y is the **yield strength** and $\widehat{\mathsf{Y}}(\mathbf{C}, \mathbf{C_p})$ is a **yield function**. Both the yield strength and the yield function have dimensions of stress. The time derivative of the yield function has two contributions

$$\tfrac{d}{dt}\widehat{\mathsf{Y}} = \tfrac{\partial \widehat{\mathsf{Y}}}{\partial \mathbf{C}} : \tfrac{d\mathbf{C}}{dt} + \tfrac{\partial \widehat{\mathsf{Y}}}{\partial \mathbf{C_p}} : \tfrac{d\mathbf{C_p}}{dt} \ .$$

Plastic flow occurs when the contribution from the total strain rate, $\frac{d}{dt}\mathbf{C}$, raises the value of the yield function to the yield strength. For many applications **rate independent plasticity** models are used. In these models,

the plastic strain rate $\frac{d}{dt}\mathbf{C_p}$ is chosen such that the yield function is never exceeded, *i.e.*,

$$\tfrac{d}{dt}\widehat{\mathsf{Y}} \le 0 \ , \quad \text{if } \widehat{\mathsf{Y}} = Y .$$

This determines the magnitude of $\mathbf{C_p}$, though the direction must be specified by a model.

Remark 3.2 The term "rate independent" refers to the lack of an explicit time constant. For simple problems, such as uniaxial strain in which the total strain increases monotonically, the plastic dissipation depends only on the strain and is independent of strain rate.

As an extension of elastic flow, rate independent plasticity has two problems. From Eqs. (2.14) and (2.15) the total strain rate is $\frac{d}{dt}\mathbf{C} = 2\,\mathbf{F}^T\mathbf{dF}$. Hence the plastic strain rate is no longer equal to a source term, but depends on $\mathsf{d}_{ij} = \frac{1}{2}(u_{i;j} + u_{j;i})$. Consequently, just because the elastic flow equations are hyperbolic, it does not follow that the extended system of PDEs remains hyperbolic. In fact for some choices of the direction of the plastic strain rate and yield function, the rate independent equation have elliptic regions. The initial value problem for these models can be regularized by adding shear layers when the solution runs into an elliptic region. (ref, David Schafer ?) Another problem arises even for rate independent plasticity models in which the extended system of PDEs remains hyperbolic. The equation for plastic strain is not in conservation form. Hence there are not sufficient jump conditions to define strong shock waves. However, "fully dispersed" weak shocks (for which the plastic dissipation provides the required shock entropy) are well defined. Consequently, a rate independent plasticity model only provides solutions for the limited class of initial value problems which do not lead to strong shocks.

Here, we consider rate dependent plasticity. In these models the value of the yield function is allowed to exceed the yield strength. The plastic strain rate serves to relax the yield function back to the yield surface. A rate dependent plasticity model is determined by specifying a plastic strain rate such that three conditions are satisfied:

i. Plastic flow only occurs outside the yield surface, *i.e.*,
$\frac{d}{dt}\mathbf{C_p} = 0$ if $\widehat{\mathsf{Y}}(\mathbf{C}, \mathbf{C_p}) < Y$.

ii. Plastic flow is dissipative, *i.e.*,

$\mathbf{S_p} : \frac{d}{dt}\mathbf{C_p} \geq 0.$

iii. Plastic flow reduces the yield function, *i.e.*,
$\frac{\partial \widehat{Y}}{\partial \mathbf{C_p}} : \frac{d}{dt}\mathbf{C_p} \leq 0.$

The system of PDEs for rate dependent plasticity is hyperbolic whenever the elastic system of PDEs is hyperbolic.

This is because the plastic rate equation is in characteristic form. Since source terms do not affect the flux matrix, the wave speeds of the augmented elastic-plastic system are the same as the original elastic system with added degeneracy for the convective wave speed (which contains the entropy wave family). Hence, the augmented system has real wavespeeds. To remain hyperbolic, a complete set of eigenvectors of the flux matrix are required. Despite the degeneracy in the eigenvalues, the eigenvectors do remain complete. To see this we note that the characteristic form of the PDEs is determined by the left eigenvalues of the flux matrix. Adding rate equations do not affect the characteristic form of the original system and hence the eigenvectors of the acoustic wave families. Furthermore, the eigenvectors of the rate equations depends on the directions associated with the new variables and are linearly independent of the eigenvectors associated with the wave families of the original system. Consequently, the elastic-plastic flow equations are hyperbolic. The same argument applies if additional internal degrees of freedom, along with rate equations for their evolution, are added in order to describe the response of a material more realistically. Isotropic or kinematic work hardening parameters are examples of other internal degrees of freedom that are commonly added.

As a consequence of the plastic strain rate equation, the physically interesting plastic waves are "partly dispersed," *i.e.*, a composite wave consisting of a discontinuous shock followed by a narrow layer in which the yield function relaxes to the yield surface. Unlike fluid dynamics, the end state of a plastic wave depends on the source term for the plastic strain rate and is not fully determined by the Hugoniot jump conditions. For special cases, such as uniaxial strain, the jump conditions plus the yield condition suffice to determine the end state. But in general the jump in the plastic strain across a plastic wave can only be determined by integrating the ODEs for the profile of a traveling wave. This is similar to what occurs for the system of PDEs describing reactive flow with more than one species and multiple

reactions. The change in equilibrium composition for flow through a nozzle, such as a jet engine, depends on the reaction rates relative to the flow rate.

Remark 3.3 Though strong shock waves are well define for rate dependent plasticity, the relaxation zone may be very narrow. Problems can occur in numerical simulations when the cell size is insufficient to resolve the wave profile.

3.2 Associated Flow Rule

An **associated flow rule** relates the plastic strain rate to the yield function. Though the plastic strain can be based on non-associative flow rules (see for example [20]), here we consider only the flow rule obtained from what is referred to as the "maximum dissipation postulate." In the rate independent case, $\mathbf{C}$ is varied over the **yield surface**, $Y = \widehat{\mathsf{Y}}(\mathbf{C}, \mathbf{C_p})$, to find an extremum in the plastic dissipation, Eq. (2.18), for fixed $\mathbf{C_p}$ and $\frac{d}{dt}\mathbf{C_p}$. The extremum occurs when (see [21] and references therein)

$$\frac{\partial \mathbf{S_p}}{\partial \mathbf{C}} : \frac{d}{dt}\mathbf{C_p} = \Upsilon \frac{\partial \widehat{\mathsf{Y}}}{\partial \mathbf{C}} \ , \tag{3.4}$$

where Υ is a Lagrange multiplier which is determined from the constraint that $\mathbf{C}$ lies on the yield surface. For the moment, let us assume that $\frac{\partial \mathbf{S_p}}{\partial \mathbf{C}}$ is everywhere invertible on the space of symmetric rank-two tensors. Then the extremum is unique. Furthermore, by the implicit value theorem we can express the yield function as $\widehat{\mathsf{Y}} = \tilde{\mathsf{Y}}(\mathbf{S_p}(\mathbf{C}, \mathbf{C_p}), \mathbf{C_p})$, and invert Eq. (3.4) to obtain the plastic stress rate

$$\boxed{\frac{d}{dt}\mathbf{C_p} = \Upsilon \frac{\partial \tilde{\mathsf{Y}}}{\partial \mathbf{S_p}}} \ . \tag{3.5}$$

This equation has the interpretation that the plastic strain rate is normal to the yield surface when the yield function is expressed in terms of the plastic stress.

In addition, we assume that for fixed $\mathbf{C_p}$ the interior of the yield surface, $\{\mathbf{S_p} \mid \tilde{\mathsf{Y}}(\mathbf{S_p}, \mathbf{C_p}) \leq Y\}$, is convex and contains the point $\mathbf{S_p} = \mathbf{0}$. From the geometry of the yield surface, it can be shown that the extremum of

plastic dissipation is a maximum and that the maximum is positive. Since the dissipation can be expressed as

$$\mathbf{S_p} : \frac{d}{dt}\mathbf{C_p} = \Upsilon \mathbf{S_p} : \frac{\partial \tilde{Y}}{\partial \mathbf{S_p}} \ ,$$

and $\frac{\partial \tilde{Y}}{\partial \mathbf{S_p}}$ is an outward normal, it follows that $\Upsilon > 0$. In the rate independent case, setting $\frac{d}{dt}\tilde{Y} = 0$ determines the Lagrange multiplier to be

$$\Upsilon = \frac{-\frac{\partial \tilde{Y}}{\partial \mathbf{S_p}} : \frac{\partial \mathbf{S_p}}{\partial \mathbf{C}} : \frac{d}{dt}\mathbf{C}}{\frac{\partial \tilde{Y}}{\partial \mathbf{S_p}} : \frac{\partial \mathbf{S_p}}{\partial \mathbf{C_p}} : \frac{\partial \tilde{Y}}{\partial \mathbf{S_p}} + \frac{\partial \tilde{Y}}{\partial \mathbf{C_p}} : \frac{\partial \tilde{Y}}{\partial \mathbf{S_p}}} \ . \tag{3.6}$$

From the existence of an extremum and $\Upsilon > 0$, it follows that the denominator is non-zero and negative.

Remarks:

3.4 The associated flow rule applies when the yield surface is smooth. For some simple models, such as the maximum shear stress criterion of Tresca, the yield surface has kinks or points at which the normal is discontinuous. Models for crystal plasticity assume the plastic strain is due to slip along preferred crystal planes. This also results in a yield surface with corners. At corners the gradient of the yield surface is ill defined. The plastic strain rate can be defined as a convex linear combination of the normals to the adjacent facets.

3.5 For computational efficiency, algorithms based upon rate independent plasticity frequently substitute the plastic strain rate Eqs. (3.5) and (3.6) directly into an equation for the stress rate with a constant shear modulus

$$\frac{d}{dt}\,\mathsf{dev}\,(\boldsymbol{\sigma}) = 2\,G\,\mathsf{dev}\left(\frac{d}{dt}\mathbf{E} - \frac{d}{dt}\mathbf{E_p}\right) \ .$$

This results in a hypo-elastic model. Though useful for some engineering applications, such a model is neither thermodynamically consistent nor frame indifferent. Simulation results for algorithm of this type should be interpreted with care.

3.6 The compatibility condition for the existence of a mapping can be expressed in terms of the strain tensor rather than the deformation gradient

Eq. (2.11). In general, $\mathbf{E_p}$ does not satisfy the compatibility condition. Consequently, ϕ_p and hence $\mathbf{F_p}$ can not exist. For crystal plasticity, at the molecular scale, one expects ϕ_p to be discontinuous due to dislocations and grain boundaries. On the macroscopic scale the discontinuities are smeared out using some coarse grain averaging procedure to give a continuous plastic strain tensor. The effect of the coarse graining can be thought of as converting the discontinuities to 'source terms' that prevent the compatibility relations from being satisfied. Consequently, $\mathbf{E_p}$ should be thought of as an internal degree of freedom that characterizes some aspects of a material not included in elastic models. The plastic mapping may be used as a heuristic to motivate the structure of the model equations but should not be taken literally and proofs for properties of the model must not rely on the existence of ϕ_p or even $\mathbf{F_p}$.

To generalize to the rate dependent case, we assume that any level set of the yield function satisfies the geometric conditions of a yield surface (*i.e.*, the interior of $\tilde{Y} = Y_1$ for any $Y_1 > Y$ is convex and contains the point $\mathbf{S_p} = 0$), and that the scale factor is a state function, $\Upsilon = \Upsilon(\mathbf{C}, \mathbf{C_p}, \eta) > 0$, to be specified by the plasticity model. We note that Υ has dimensions of inverse time, and in order that there is no plastic flow in the elastic regime we require $\Upsilon = 0$ for $\tilde{Y}(\mathbf{S_p}, \mathbf{C_p}) \leq Y$. The construction of a rate dependent model based on the maximum dissipation postulate guarantees that plasticity is dissipative and that plastic flow relaxes the value of the yield function toward the yield surface.

Remarks:

3.7 The condition that every level set of the yield function satisfy the geometric conditions for a yield surface is a weak assumption. The same condition is needed to account for work hardening.

3.8 Typically, the scale factor Υ is a monotonically increasing function of the distance to the yield surface, *i.e.*, $\tilde{Y} - Y$. Larger values of Υ correspond to a smaller time constant for the relaxation to the yield surface. Rate independent plasticity can be viewed as the limit in which the time constant goes to zero.

3.2.1 Volume Preserving Plastic Flow

Based on the underlying dislocation mechanism for crystal plasticity, many plasticity models take the plastic strain to be volume preserving, *i.e.*, $\mathsf{det}(\mathbf{G}^{-1}\mathbf{C_p}) = 1$. By Lemma A.3, the condition $\frac{d}{dt}\,\mathsf{det}(\mathbf{G}^{-1}\mathbf{C_p}) = 0$ places the constraint on the strain rate that

$$\mathsf{Tr}\left(\mathbf{C_p}^{-1}\tfrac{d}{dt}\mathbf{C_p}\right) = 0\ . \tag{3.7}$$

Hence, if the plastic strain is volume preserving the plastic strain rate is the deviator with respect to $\mathbf{C_p}$ of some tensor. To enforce the condition that plastic strain is volume preserving, it is natural to take the specific energy to be a function of $\mathsf{J}_p^{-2/3}\mathbf{C_p}$, *i.e.*,

$$\mathcal{E} = \mathcal{E}_e(\mathsf{J}_p^{2/3}\mathbf{C_p}^{-1}\mathbf{C}) + \mathcal{E}_p(\mathsf{J}_p^{-2/3}\mathbf{C_p})\ ,$$

where $\mathsf{J}_p^2 = \mathsf{det}(\mathbf{G}^{-1}\mathbf{C_p})$. With this functional form the energy is independent of the plastic volume and it is straight forward to show that the plastic stress is deviatoric, *i.e.*, $\mathsf{dev}_{\mathbf{C_p}^{-1}}(\mathbf{S_p}) = 0$.

The plastic strain rate of Eq. (3.5) is volume preserving when the yield function has the form

$$\tilde{\mathsf{Y}} = \tilde{\mathsf{Y}}(\mathsf{dev}_{\mathbf{C_p}^{-1}}(\mathbf{S_p})\,, \mathbf{C_p})\ . \tag{3.8}$$

However, to verify the plastic strain rate satisfies the required properties of a plasticity model, we need to reexamine the steps in the derivation of Eq. (3.5). In particular, the assumption that $\frac{\partial \mathbf{S_p}}{\partial \mathbf{C}}$ is invertible is not true when $\mathbf{S_p}$ is deviatoric.

With the volume preserving form of the yield function, Eq. (3.8), the extremum condition for the dissipation, Eq. (3.4), can be written as

$$\frac{\partial \mathbf{S_p}}{\partial \mathbf{C}} : \left(\frac{d}{dt}\mathbf{C_p} - \Upsilon \frac{\partial \tilde{\mathsf{Y}}}{\partial \mathbf{S_p}}\Big|_{\mathbf{C_p}}\right) = 0\ .$$

We note that the term in parenthesis is deviatoric. Provided that the null space of $\frac{\partial \mathbf{S_p}}{\partial \mathbf{C}}$ is limited to the deviatoric component, we can conclude that Eq. (3.5) remains valid for the volume preserving plasticity.

Remark 3.9 For porous materials or materials with cracks, the volume preserving assumption of the plastic deformation is not even approximately

valid. Thus, the volume preserving constraint is not a physical law, but merely an approximation that leads to a useful description of many materials, in particular, metals.

4 Illustrative Constitutive Model

A constitutive material model, needed to complete the elastic-plastic flow equations, is composed of three items:

i. A stress-strain relation, which for thermodynamic consistency, is defined by a specific energy function.

ii. A yield function $\tilde{\Upsilon}(\mathbf{S_p}, \mathbf{C_p})$, and a rule for the direction of the plastic strain rate, such as the associated flow rule, Eq. (3.5).

iii. A scalar function $\Upsilon(\mathbf{C}, \mathbf{C_p}, \eta)$ which specifies the rate at which the yield function relaxes toward the yield surface.

This section provides a simple illustrative example of all three components of a constitutive model for an isotropic material.

4.1 Specific Energy

We assume that $\mathcal{E}_p = 0$ and use a variant of Eq. (2.3) for $\mathcal{E}_e$,

$$\mathcal{E}_e = \mathcal{E}_{\text{hydro}}(V, \eta) + \tfrac{1}{2} V_0 \, G \, (I_1 I_3^{-1/3} - 3) \ , \tag{4.1}$$

where G is the shear modulus, and the invariants are $I_1 = \mathsf{J}_p^{2/3} \, \mathsf{Tr} \left(\mathbf{C_p}^{-1} \mathbf{C} \right)$ and $I_3 = \det \left(\mathsf{J}_p^{2/3} \, \mathbf{C_p}^{-1} \mathbf{C} \right) = \mathsf{J}^2$. When the elastic energy depends on the invariants of $\mathsf{J}_p^{2/3} \mathbf{C_p}^{-1} \mathbf{C}$, the plastic stress is related to the elastic stress deviator as follows.

Lemma 4.1. The component of the plastic stress from the elastic energy and the Piola-Kirchhoff stress are related by

$$\mathsf{dev}_{\mathbf{C_p}^{-1}} \left(\mathbf{S'_p} \right) \, \mathbf{C_p} = \mathsf{dev}_{\mathbf{C}^{-1}} \left(\mathbf{S} \right) \, \mathbf{C} \ . \tag{4.2}$$

Proof. Let I_1,I_2, I_3 be the invariants of $\mathsf{J}_p^{2/3}\mathbf{C_p}^{-1}\mathbf{C}$ Applying the chain rule, the stress tensors are given by

$$\begin{aligned} 2\rho_0\,\mathbf{S'_p} &= -\frac{\partial \mathcal{E}_e}{\partial I_1}\cdot\frac{\partial I_1}{\partial \mathbf{C_p}} - \frac{\partial \mathcal{E}_e}{\partial I_2}\cdot\frac{\partial I_2}{\partial \mathbf{C_p}} - \frac{\partial \mathcal{E}_e}{\partial I_3}\cdot\frac{\partial I_3}{\partial \mathbf{C_p}} \\ 2\rho_0\,\mathbf{S} &= \frac{\partial \mathcal{E}_e}{\partial I_1}\cdot\frac{\partial I_1}{\partial \mathbf{C}} + \frac{\partial \mathcal{E}_e}{\partial I_2}\cdot\frac{\partial I_2}{\partial \mathbf{C}} + \frac{\partial \mathcal{E}_e}{\partial I_3}\cdot\frac{\partial I_3}{\partial \mathbf{C}} \end{aligned}$$

From the definition of the invariants, it is straight forward to show that the invariants satisfies

$$\mathsf{dev}_{\mathbf{C_p}^{-1}}\left(\frac{\partial I_j}{\partial \mathbf{C_p}}\right)\mathbf{C_p} = -\,\mathsf{dev}_{\mathbf{C}^{-1}}\left(\frac{\partial I_j}{\partial \mathbf{C}}\right)\mathbf{C}\ .$$

Consequently, the stress tensors satisfy Eq. (4.2). ⊠

The stress stress corresponding for the model, Eq. (4.1), is given by

$$\begin{aligned} \mathbf{S} &= -P(V,\eta)\,\mathsf{J}\,\mathbf{C}^{-1} + G\,(\mathsf{J}_p/\mathsf{J})^{2/3}\,\mathsf{dev}_{\mathbf{C}^{-1}}\left(\mathbf{C_p}^{-1}\right)\ , \\ \boldsymbol{\sigma} &= -P(V,\eta)\,\boldsymbol{g}^{-1} + \frac{G}{\mathsf{J}}\,(\mathsf{J}_p/\mathsf{J})^{2/3}\,\mathsf{dev}_{\boldsymbol{g}^{-1}}\left(\mathbf{b_e}\right)\ , \end{aligned} \tag{4.3}$$

where $P = -\frac{\partial}{\partial V}\mathcal{E}_{\text{hydro}}$ is the hydrostatic pressure, and $\mathbf{b_e} = \mathbf{F}\mathbf{C_p}^{-1}\mathbf{F}^T$. In addition, the plastic stress is given by

$$\begin{aligned} \mathbf{S_p} &= G\,(\mathsf{J}_p/\mathsf{J})^{2/3}\,\mathsf{dev}_{\mathbf{C_p}^{-1}}\left(\mathbf{C_p}^{-1}\mathbf{C}\mathbf{C_p}^{-1}\right) \\ &= G\,(\mathsf{J}_p/\mathsf{J})^{2/3}\,\mathsf{dev}_{\mathbf{I}}\left(\mathbf{C_p}^{-1}\mathbf{C}\right)\mathbf{C_p}^{-1}\ . \end{aligned} \tag{4.4}$$

Remarks:

4.1 It is interesting to note that Eq. (4.3) for the stress can be expressed as

$$\mathbf{S} = -P(V,\eta)\,\mathsf{J}\,\mathbf{C}^{-1} + 2\,G\,(\mathsf{J}_p/\mathsf{J})^{2/3}\,\mathsf{dev}_{\mathbf{C}^{-1}}\left(\mathbf{C_p}^{-1}\mathbf{E_e}\mathbf{C}^{-1}\right)\ .$$

This is equivalent to Eq. (2.4) with $\mathbf{E_e}$ substituted for the strain $\mathbf{E}$ and $\mathsf{J}_p^{-2/3}\mathbf{C_p}$ substituted for the metric $\mathbf{G}$.

4.2 If the parameter G is a constant then the mean pressure corresponds to the hydrostatic pressure and can be expressed as $P = P_{\text{hydro}}(V, e - e_{\text{shear}})$

where the shear energy $e_{\rm shear}$ is a function of only the strain. This is a simple, thermodynamically consistent and computationally efficient way to add strength to a hydrostatic equation of state. Moreover, the material temperature is determined from the hydrostatic equation of state in the usual manner. In practice there is no data with which to define the temperature any better. On the other hand, the shear modulus is expected to decrease as $T \nearrow T_{\rm melt}$.

4.3 A more general functional form for the stress can be obtained in terms of the Helmhotz free energy, $\Psi_e(\mathbf{C_p}^{-1}\mathbf{C}, T) = \mathcal{E}_e(\mathbf{C_p}^{-1}\mathbf{C}, \eta) - T\eta$. Letting the shear modulus be a function of T and V,

$$\Psi_e = \Psi_{\rm hydro}(V,T) + \tfrac{1}{2} V_0\, G(V,T)\,(I_1 I_3^{-1/3} - 3)\ ,$$

and there are contributions to the entropy from both the shear strain and the specific volume. In this case the Cauchy stress is given by

$$\boldsymbol{\sigma} = -\Big\{ P(V,T) + \tfrac{1}{2}\Big[3 - (\mathsf{J}_p/\mathsf{J})^{2/3}\,\mathsf{Tr}(\mathbf{C_p}^{-1}\mathbf{C})\Big] V_0 \frac{\partial}{\partial V} G(V,T) \Big\}\, \boldsymbol{g}^{-1} + (\mathsf{J}_p/\mathsf{J})^{2/3}\,\frac{G(V,T)}{\mathsf{J}}\ \mathsf{dev}_{\boldsymbol{g}^{-1}}(\mathbf{b_e})\ .$$

We note that a consequence of the dependence of G on V is an additional contribution to the pressure. The additional pressure term is proportional to $\Big[3 - (\mathsf{J}_p/\mathsf{J})^{2/3}\,\mathsf{Tr}(\mathbf{C_p}^{-1}\mathbf{C})\Big]$, *i.e.*, the norm of the deviator of the elastic strain. As is shown in a later section, the strain deviator is limited by the yield condition, and the additional pressure term is $\mathcal{O}\left([Y/G]^2\right)$. Typically, Y is 1 percent of G, and the additional pressure term is neglected.

4.2 Von Mises Yield Condition

The simplest yield criterion is known as the **von Mises yield condition**. It defined by the yield function

$$\tilde{\mathsf{Y}}(\mathbf{S_p}, \mathbf{C_p}) = \sqrt{\tfrac{3}{2}}\,\Big\|\mathsf{dev}_{\mathbf{C_p}^{-1}}(\mathbf{S_p})\Big\|_{\mathbf{C_p}}\ . \tag{4.5}$$

Substituting Eqs. (4.2) and (2.2), the yield function in the spatial frame can be written as

$$\tilde{\mathsf{Y}} = \sqrt{\tfrac{3}{2}}\,\mathsf{J}\ \|\mathsf{dev}_{\boldsymbol{g}^{-1}}(\boldsymbol{\sigma})\|_{\boldsymbol{g}}\ . \tag{4.5'}$$

Remark 4.4 The factor of $\sqrt{\frac{3}{2}}$ in the yield function is standard and is chosen to simplify formula involving uniaxial strain. For uniaxial strain with the identity spatial metric, the deviator of the strain tensor has the form $\mathsf{dev}(\mathbf{e}) = \frac{\epsilon_{el}}{3}\,\mathbf{diag}[\ 2,\ -1,\ -1\ ]$, and its norm is $\|\mathsf{dev}(\mathbf{e})\|^2 = \frac{2}{3}\epsilon_{el}^2$. For a simple isotropic material $\mathsf{dev}(\boldsymbol{\sigma}) = 2\,G\,\mathsf{dev}(\mathbf{e})$, and the yield condition reduces to $\epsilon_{el} \le \frac{Y}{2\,G}$.

Plastic flow limits the yield function to be $\tilde{\mathsf{Y}} \lesssim Y$. It follows from the from Eq. (4.5) that the stress deviator is limited by the yield strength. Next we show that plastic flow also limits the deviator of the elastic strain. Substituting Eq. (4.4) for the plastic stress, the yield condition function becomes

$$\tilde{\mathsf{Y}} = \sqrt{\tfrac{3}{2}}\,G\left(\frac{\mathsf{J}_p}{\mathsf{J}}\right)^{2/3}\left\{\mathsf{Tr}\left[\left(\mathsf{dev}_{\mathbf{I}}\left(\mathbf{C_p}^{-1}\mathbf{C}\right)\right)^2\right]\right\}^{1/2} . \tag{4.6}$$

Then the yield condition, $\tilde{\mathsf{Y}} \le Y$, gives the inequality

$$\mathsf{Tr}\left[\left(\mathsf{dev}_{\mathbf{I}}\left(\mathbf{C_p}^{-1}\mathbf{C}\right)\right)^2\right] \le \tfrac{2}{3}\left(\frac{\mathsf{J}}{\mathsf{J}_p}\right)^{4/3}(Y/G)^2 .$$

Hence

$$\boxed{\mathbf{C_p}^{-1}\mathbf{C} = \left(\frac{\mathsf{J}}{\mathsf{J}_p}\right)^{2/3}\mathbf{I}_{\mathbb{T}\mathcal{B}} + \mathcal{O}\left(Y/G\right)} . \tag{4.7}$$

Since we are using $\mathbf{C_p}^{-1}\mathbf{C}$ as a measure of the elastic strain, the deviator of the elastic strain is limited by the yield condition to $\mathcal{O}\left(Y/G\right)$. Typically, Y is about one percent of G. Hence, plastic flow limits the elastic strain deviator to be small.

The gradient of the yield surface is given by

$$\frac{\partial\tilde{\mathsf{Y}}}{\partial\mathbf{S_p}} = \frac{\frac{3}{2}\,\mathbf{C_p}\,\mathsf{dev}_{\mathbf{C_p}^{-1}}\left(\mathbf{S_p}\right)\mathbf{C_p}}{\tilde{\mathsf{Y}}} . \tag{4.8}$$

Then from Eq. (3.5), the plastic strain rate has the form

$$\frac{d}{dt}\mathbf{C_p} = \frac{\frac{3}{2}\,\Upsilon\,\mathbf{C_p}\,\mathsf{dev}_{\mathbf{C_p}^{-1}}\left(\mathbf{S_p}\right)\mathbf{C_p}}{\tilde{\mathsf{Y}}} . \tag{4.9}$$

Using Eq. (4.4) for the plastic stress, the plastic strain rate reduces to

$$\frac{d}{dt}\mathbf{C_p} = \tfrac{3}{2}\,\Upsilon\,\frac{G}{\tilde{\mathsf{Y}}}\left(\frac{\mathsf{J}_p}{\mathsf{J}}\right)^{2/3}\mathbf{C_p}\,\mathsf{dev}_{\mathbf{I}}\left(\mathbf{C_p}^{-1}\mathbf{C}\right) . \tag{4.9'}$$

Remark 4.5 The plastic strain rate equation (4.9) can be expressed as

$$\frac{d}{dt}\mathbf{C_p} \propto \mathbf{F}^T\Big(\boldsymbol{g}\,\mathsf{dev}_{\boldsymbol{g}^{-1}}(\boldsymbol{\sigma})\,\boldsymbol{g}\Big)\mathbf{F}\,(\mathbf{C_p}^{-1}\mathbf{C})^{-1}$$

Aside from the factor $\mathbf{C_p}^{-1}\mathbf{C}$, which to $\mathcal{O}(Y/G)$ is proportional to the identity matrix, this is the **Prandle-Reuss** form for the plastic strain rate.

4.3 Hohenemser-Prager rate

It is natural to take the proportionality factor as a function of the distance to the yield surface. The simplest possibility is the **Hohenemser-Prager rate** [7] (see also, [10, p. 105]) that defines the proportionality factor as

$$\Upsilon = \begin{cases} \frac{1}{\mu}(\tilde{\mathsf{Y}} - Y)\ , & \text{for } \tilde{\mathsf{Y}} > Y \\ 0, & \text{otherwise} \end{cases}$$

where μ is a parameter with dimensions of dynamic viscosity (pressure·time, commonly measured in cgs unit of Poise = micro-bar·s) that sets the scale for the relaxation rate, and Y is the yield strength.

Combined with the von Mises yield, above the yield surface ($\tilde{\mathsf{Y}} > Y$), the plastic strain rate is given by

$$\frac{d}{dt}\mathbf{C_p} = \tfrac{3}{2}\left(\frac{\tilde{\mathsf{Y}} - Y}{\mu\,\tilde{\mathsf{Y}}}\right)\mathbf{C_p}\ \mathsf{dev}_{\mathbf{C_p}^{-1}}(\mathbf{S_p})\ \mathbf{C_p}\ . \tag{4.10}$$

Substituting Eq. (4.4), we obtain

$$\frac{d}{dt}\mathbf{C_p} = \tfrac{3}{2}\left(\frac{\tilde{\mathsf{Y}} - Y}{\mu\,\tilde{\mathsf{Y}}}\right) G\,(\mathsf{J}_p/\mathsf{J})^{2/3}\,\mathbf{C_p}\ \mathsf{dev}_{\mathbf{I}}\left(\mathbf{C_p}^{-1}\mathbf{C}\right)\ . \tag{4.11}$$

It can easily be verified that $\mathsf{Tr}\left(\mathbf{C_p}^{-1}\frac{d}{dt}\mathbf{C_p}\right) = 0$, and hence the plastic strain rate is volume preserving. Moreover, from Eqs. (4.11) and (4.4) the plastic dissipation,

$$\mathsf{S_p} : \frac{d}{dt}\mathbf{C_p} = \tfrac{3}{2}\left(\frac{\tilde{\mathsf{Y}} - Y}{\mu\,\tilde{\mathsf{Y}}}\right) G^2\,(\mathsf{J}_p/\mathsf{J})^{4/3}\left\|\mathsf{dev}_{\mathbf{I}}\left(\mathbf{C_p}^{-1}\mathbf{C}\right)\right\|_{\mathbf{I}}^2$$

is explicitly positive.

For small μ, if the yield function were substantially to exceed the yield surface then the plastic strain rate would be very large and would rapidly increase $\mathbf{C_p}$ in order to decrease the stress and drive the yield function back to the yield surface. However, as the stress approaches the yield surface $\Upsilon \to 0$, *i.e.*, the 'time constant' for relaxation increases and in fact becomes infinite on the yield surface.

4.4 Visco-Plastic Limit

We next show an important consequence of the behavior of the time constant is that in the limit of small μ and slow total strain rate, the von Mises yield strength with the Hohenemser-Prager plastic strain rate reduces to a visco-plastic model [22], *i.e.*, time independent elastic-plasticity plus a viscous component to the shear stress. To obtain this result we need to analyze the behavior of the proportionality constant for the plastic strain rate.

We begin by computing the time derivative of the proportionality constant.

$$\begin{aligned}
\frac{d}{dt}\Upsilon &= \frac{1}{\mu}\frac{d}{dt}\tilde{\mathsf{Y}} = \frac{\tilde{\mathsf{Y}}}{2\,\mu}\frac{d}{dt}\ln\left(\tilde{\mathsf{Y}}^2\right) \\
&= \frac{\tilde{\mathsf{Y}}}{2\,\mu}\left[\frac{d}{dt}\ln \mathsf{Tr}\left[\left(\mathsf{dev}_{\mathbf{I}}\left(\mathbf{C_p}^{-1}\mathbf{C}\right)\right)^2\right] - \frac{d}{dt}\ln(\mathsf{J})^{4/3}\right] \\
&= \frac{\tilde{\mathsf{Y}}}{\mu}\left\{\frac{\mathsf{Tr}\left[\mathsf{dev}_{\mathbf{I}}\left(\mathbf{C_p}^{-1}\mathbf{C}\right)\left(\frac{d}{dt}\mathbf{C_p}^{-1}\right)\mathbf{C}\right]}{\mathsf{Tr}\left[\left(\mathsf{dev}_{\mathbf{I}}\left(\mathbf{C_p}^{-1}\mathbf{C}\right)\right)^2\right]}\right. \\
&\qquad\left. + \frac{\mathsf{Tr}\left[\mathsf{dev}_{\mathbf{I}}\left(\mathbf{C_p}^{-1}\mathbf{C}\right)\mathbf{C_p}^{-1}\frac{d}{dt}\mathbf{C}\right]}{\mathsf{Tr}\left[\left(\mathsf{dev}_{\mathbf{I}}\left(\mathbf{C_p}^{-1}\mathbf{C}\right)\right)^2\right]} - \tfrac{2}{3}\frac{d}{dt}\ln(\mathsf{J})\right\}
\end{aligned} \tag{4.12}$$

By Eq. (4.9')

$$\left(\frac{d}{dt}\mathbf{C_p}^{-1}\right)\mathbf{C} = -\mathbf{C_p}^{-1}\left(\frac{d}{dt}\mathbf{C_p}\right)\mathbf{C_p}^{-1}\mathbf{C}$$
$$= -\tfrac{3}{2}\Upsilon\frac{G}{\tilde{\Upsilon}}(\mathsf{J}_p/\mathsf{J})^{2/3}\,\mathsf{dev}_{\mathbf{I}}\left(\mathbf{C_p}^{-1}\mathbf{C}\right)\mathbf{C_p}^{-1}\mathbf{C}$$

Then from Eq. (4.7), to leading order in Y/G, the first term in curly brackets on the right hand side of Eq. (4.12) is

$$\frac{\mathsf{Tr}\left[\mathsf{dev}_{\mathbf{I}}\left(\mathbf{C_p}^{-1}\mathbf{C}\right)\left(\frac{d}{dt}\mathbf{C_p}^{-1}\right)\mathbf{C}\right]}{\mathsf{Tr}\left[\left(\mathsf{dev}_{\mathbf{I}}\left(\mathbf{C_p}^{-1}\mathbf{C}\right)\right)^2\right]} = -\tfrac{3}{2}\Upsilon\frac{G}{\tilde{\Upsilon}}\times\left[1+\mathcal{O}\left(Y/G\right)\right]$$

From Eqs. (2.14), (4.3) and (4.6) the second term in curly brackets on the right hand side of Eq. (4.12) is

$$\frac{\mathsf{Tr}\left[\mathsf{dev}_{\mathbf{I}}\left(\mathbf{C_p}^{-1}\mathbf{C}\right)\mathbf{C_p}^{-1}\left(\frac{d}{dt}\mathbf{C}\right)\right]}{\mathsf{Tr}\left[\left(\mathsf{dev}_{\mathbf{I}}\left(\mathbf{C_p}^{-1}\mathbf{C}\right)\right)^2\right]} = 3\left(\mathsf{J}_p/\mathsf{J}\right)^{2/3}\frac{G}{\tilde{\Upsilon}^2}\,\mathsf{Tr}\left[\mathbf{F}\mathbf{C_p}^{-1}\mathbf{C}\,\mathsf{dev}_{\mathbf{C}^{-1}}\left(\mathbf{S}\right)\mathbf{F}^T\mathbf{d}\right]$$
$$= 3\,\mathsf{J}\,\frac{G}{\tilde{\Upsilon}^2}\,\mathsf{dev}_{\boldsymbol{g}^{-1}}\left(\boldsymbol{\sigma}\right):\mathbf{d}\times\left[1+\mathcal{O}\left(Y/G\right)\right]$$

From Lemma A.4 the third term in curly brackets on the right hand side of Eq. (4.12) is

$$-\tfrac{2}{3}\frac{d}{dt}\ln\mathsf{J} = -\tfrac{2}{3}\,\vec{\nabla}\cdot\vec{u}\ .$$

Combining the three terms, Eq. (4.12) becomes

$$\frac{d}{dt}\Upsilon + \tfrac{3}{2}\frac{G}{\mu}\Upsilon = \tfrac{3}{2}\frac{G}{\mu}\left[\frac{2\,\mathsf{J}}{\tilde{\Upsilon}}\,\mathsf{dev}_{\boldsymbol{g}}\left(\mathbf{d}\right):\mathsf{dev}_{\boldsymbol{g}^{-1}}\left(\boldsymbol{\sigma}\right)+\mathcal{O}\left(Y/G\right)\right]\ .$$

This form of equation is analyzed in Appendix D. In the limit $\mu\to 0$, $\tilde{\Upsilon} = Y+\mathcal{O}\left(\mu\right)$ and to leading order in Y/G

$$\Upsilon = \frac{2\,\mathsf{J}}{Y}\,\mathsf{dev}_{\boldsymbol{g}}\left(\mathbf{d}\right):\mathsf{dev}_{\boldsymbol{g}^{-1}}\left(\boldsymbol{\sigma}\right)+\mathcal{O}\left(\mu\right)\ . \tag{4.13}$$

Since $\frac{\tilde{\Upsilon}^2-Y^2}{2\,Y} = \mu\,\Upsilon$, from Eq. (4.13) and (4.5') we obtain

$$\tfrac{3}{2}\,\mathsf{J}^2\ \left\|\mathsf{dev}_{\boldsymbol{g}^{-1}}\left(\boldsymbol{\sigma}\right)\right\|_{\boldsymbol{g}}^2 = Y^2+4\,\mu\,\mathsf{J}\,\mathsf{dev}_{\boldsymbol{g}}\left(\mathbf{d}\right):\mathsf{dev}_{\boldsymbol{g}^{-1}}\left(\boldsymbol{\sigma}\right)+\mathcal{O}\left(\mu^2\right)$$

Consequently, in the limit of small μ, the stress can be split into an elastic component and a viscous component

$$\boldsymbol{\sigma} \approx \boldsymbol{\sigma}_{\rm el} + \boldsymbol{\sigma}_{\rm vis} \ .$$

The elastic component $\boldsymbol{\sigma}_{\rm el}$ is given by Eq. (4.3) with the elastic strain such that the elastic stress is restricted to the yield surface, *i.e.*, rate independent plasticity. The viscous component of the stress is given by

$$\boldsymbol{\sigma}_{\rm vis} = \tfrac{4}{3}\,\mu\,\mathsf{J}^{-1}\,\boldsymbol{g}^{-1}\,\mathsf{dev}_{\boldsymbol{g}}\,(\mathbf{d})\;\boldsymbol{g}^{-1} \ .$$

The viscous stress accounts for the leading order effect of plastic flow, namely, the relaxation of the stress deviator to the yield surface.

The portion of the stress-strain work, Eq. (2.17), from the stress exceeding the yield surface, *i.e.*, $\frac{d}{dt}\mathcal{E} - \mathbf{d} : \boldsymbol{\sigma}_{\rm el} = \mathbf{d} : \boldsymbol{\sigma}_{\rm vis}$, is dissipative. The viscous dissipation corresponds to the plastic work from the stress exceeding the yield surface. This is in additon to the plastic dissipation corresponding to rate independent plasticity for which the stress is on the yield surface.

Remark 4.6 From the above derivation, the viscous approximation for plastic flow is **only** valid when the viscous stress is small, *i.e.*, $\|\boldsymbol{\sigma}_{\rm vis}\|_{\boldsymbol{g}^{-1}} \ll Y$.

The visco-plastic constitutive model can be represented by a mechanical system as shown in figure 1. The mechanical system is a composite made up of three types of elements: (i) Spring with a linear stress-strain relation $\boldsymbol{\sigma} = K\boldsymbol{\epsilon}$, or more generally, $\frac{d}{dt}\boldsymbol{\sigma} = K\frac{d}{dt}\boldsymbol{\epsilon}$. (ii) Dashpot with stress-strain relation $\boldsymbol{\sigma} = \mu\frac{d}{dt}\boldsymbol{\epsilon}$. (iii) Slider with stress-strain relation $\frac{d}{dt}\boldsymbol{\epsilon} = 0$ if $\boldsymbol{\sigma} < Y$. More elaborate models allow for a 'history' dependent relaxation to the yield surface. The generalized models are represented by a sequence of springs (G_i) and dashpots (μ_i) elements in parallel. In effect, each spring represents an additional internal degree of freedom. The sequence of springs and dashpots are an approximation to the Laplace transform of the history response function. They allow empirical models to account for the observed frequency dependent viscous response of materials such as polymers. The additional internal degrees of freedom represent continuum variables needed to account for aspects of the the short wavelength structure that are lost in coarse grain or homogenized models of heterogeneous materials.

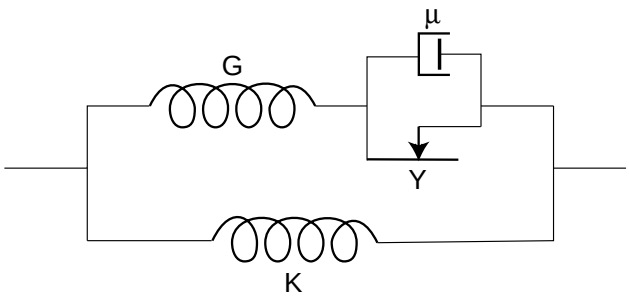

Figure 1: Mechanical representation of visco-plastic constitutive model. The springs K and G represent the response of the volumetric and deviatoric components of the stress, respectively, to the strain. The slider (Y) allows plastic flow above the yield surface, and the dashpot (μ) accounts for the relaxation of the stress to the yield surface.

Remarks:

4.7 Plasticity is the underlying mechanism for viscosity in a solid. This is very different than the viscous mechanisms in liquids and gases. Consequently, the coefficient of viscosity μ for a solid can be very much larger than for a liquid or gas; for metals viscous coefficients are typically in the range of 100 to 1000 Poise, where as the viscous coefficient for liquids and gases is typically measured in centi-poise.

4.8 Typically, the yield strength decreases with temperature. This is referred to as thermal softening, and can result in an instability leading to the formation of shear layers. Morover, the limit $Y \to 0$ corresponds to visco-elastic flow and can be used as a model for liquids. In this case, the material does support shear strain, but only as a transient response. On a time scale set by the ratio of the shear viscosity to the shear modulus, the shear strain relaxes towards zero.

4.9 Viscosity and rate dependent plasticity lead to different shock wave structures. With rate dependent plasticity, split waves occur consisting of an elastic precursor followed by fully dispersed plastic wave. With viscosity the shock can be partly dispersed but would not split.

4.10 For numerical simulations, rate dependent plasticity circumvents the problems with shock waves due to the equations for rate independent plas-

ticity not being fully in conservation form. However, for a strong shock the wave profile can be very narrow and cause problems with resolution. In addition, it should be noted that the small elastic strain approximation is not valid in the profile of a strong shock.

4.11 The rate for crystal plasticity is determined by the motion of dislocations, see for example [8], [9] and references therein. At low deformation rates stress ($\mathbf{d}$ small) the plastic rate is dominated by thermal activation for the movement of a pinned dislocation. This gives rise to the phenomena creep. At high stress rates, in contrast, the plastic strain rate is dominated by the drag on a dislocation as it moves through the crystal lattice. However, there remains questions about the rate at which dislocations are nucleated and grow. In addition, the initial number of dislocations is sensitive to impurities and sample preparation.

4.12 The measured rise time for shock profiles in many metals can be fit with a plastic strain rate in which $\Upsilon \propto (\|\mathsf{dev}_{\boldsymbol{g}^{-1}}(\boldsymbol{\sigma}) - Y\|_{\boldsymbol{g}})^2$, see [24]. In this case, the form in which rate independent approximation accounts for the effect of plasticity would be different than for the Hohenemser-Prager rate model.

4.13 The observed phenomenolgy of plastic flow is quite rich. The basic difficulty with modeling the phenomena stems from the fact that materials are not really homogeneous. As a result, internal variables (in addition to the plastic strain tensor) are needed to characterize the state of the material, along with corresponding rate equation for their dynamics. Many choices are possible for internal variables. Common internal variables range from a simple isotropic work hardening parameter, to a back-stress tensor for kinematic work hardening, to elaborate calibrations such as the mechanical threshold stress (MST) model of Follansbee & Kocks [3]. The difficulty in developing plasticity models lies in the fact that the distribution of inhomogeneities (dislocations, cracks, grain boundaries), unlike the Maxwell distribution in gas dynamics, is not necessarily highly peaked. Consequently, simple mean field theory for coarse grained average quantities is not sufficient. As yet, there is single no theory which can explain all the phenomena, let alone is agreed upon by a majority of researchers.

5 Uniaxial Strain

We chose coordinate systems with identity metrics for the body, plastic and spatial frames; *i.e.*, $\mathsf{G}_{\alpha,\beta} = \delta_{\alpha,\beta}$, $\widetilde{\mathcal{G}}_{AB} = \delta_{AB}$, and $g_{ij} = \delta_{ij}$. Uniaxial strain reduces the flow to a one-dimensional problem by restricting the total deformation gradient to have the form

$$\mathbf{F} = \mathbf{diag}[\ \exp(\epsilon),\ 1,\ 1\ ]\ ,$$

where $\epsilon = \ln(V/V_0)$ is a measure of the total strain, and $\mathbf{diag}[\ d_1,\ d_2,\ d_3\ ]$ denotes a diagonal matrix with diagonal elements d_1, d_2 and d_3. Moreover, $\epsilon = \epsilon(x,t)$ and the velocity $\vec{U} = (u(x,t), 0, 0)$ are assumed to be functions of only one spatial variable. Consequently, the compatibility conditions for the deformation gradient are trivially satisfied.

We further assume that the plastic deformation gradient has the form

$$\mathbf{F_p} = \mathbf{diag}[\ \exp(\tfrac{2}{3}\epsilon_p),\ \exp(-\tfrac{1}{3}\epsilon_p),\ \exp(-\tfrac{1}{3}\epsilon_p)\ ]\ ,$$

where ϵ_p is a measure of the plastic strain. The elastic deformation gradient is then given by

$$\mathbf{F_e} = \exp\Big(\tfrac{1}{3}\epsilon\Big)\,\mathbf{diag}[\ \exp(\tfrac{2}{3}\epsilon_e),\ \exp(-\tfrac{1}{3}\epsilon_e),\ \exp(-\tfrac{1}{3}\epsilon_e)\ ]$$

where $\epsilon_e = \epsilon - \epsilon_p$ is a measure of the elastic strain. We note that $\mathsf{J} = \exp(\epsilon)$ and $\mathsf{J}_p = 1$. This choice reduces the plastic strain tensor to have one independent scalar degrees of freedom, ϵ_p, compared to the six associated with a symmetric rank-two tensor.

Remark 5.1 In general, if the material properties are anisotropic then the elastic and plastic deformation gradients need not remain diagonal. Anisotropic uniaxial flow remains a one-dimensional problem, *i.e.*, functional dependence on only one spatial variable. However, additional degrees of freedom are needed to determine the components of the elastic and plastic strain tensors.

It follows from the form of the deformation gradients that

$$\begin{aligned}\mathbf{C} &= \mathbf{diag}[\ \exp(2\epsilon\ ),\ 1,\ 1\ ]\ ,\\ \mathbf{C_p} &= \exp\Big(-\tfrac{2}{3}\,\epsilon_p\Big)\,\mathbf{diag}[\ \exp(2\epsilon_p),\ 1,\ 1\ ]\ .\end{aligned}$$

Moreover, the elastic strain is characterized by

$$\mathbf{C_p}^{-1}\mathbf{C} = \mathsf{J}^{2/3}\,\mathbf{diag}[\ \exp(\tfrac{4}{3}\epsilon_e),\ \exp(-\tfrac{2}{3}\epsilon_e),\ \exp(-\tfrac{2}{3}\epsilon_e)\ ]\ .$$

Since diagonal matrices commute, in this case the elastic left Cauchy-Green tensor $\mathbf{b_e}$ has the same matrix elements as $\mathbf{C_p}^{-1}\mathbf{C}$ (though they act on different spaces). To leading order, the elastic strain can be expressed as

$$\mathbf{C_p}^{-1}\mathbf{C} = \mathsf{J}^{2/3}\,\mathbf{I}_{\mathbb{T}\mathcal{B}} + \tfrac{2}{3}\,\epsilon_e\,\mathsf{J}^{2/3}\,\mathbf{diag}[\ 2,\ -1,\ -1\ ] + \mathcal{O}\left(\epsilon_e^2\right)\ .$$

Later we will have use of the trace and the deviator of the elastic strain. These are given by

$$\begin{aligned}\mathsf{Tr}\Big(\mathbf{C_p}^{-1}\mathbf{C}\Big) &= \exp(-\tfrac{2}{3}\epsilon_e)\,\Big(\exp(2\epsilon_e)+2\Big)\,\mathsf{J}^{2/3}\\ &= 3\,\mathsf{J}^{2/3} + \mathcal{O}\left(\epsilon_e^2\right)\ ,\end{aligned}$$

$$\begin{aligned}\mathsf{dev}_{\mathbf{I}_{\mathbb{T}\mathcal{B}}}(\mathbf{C_p}^{-1}\mathbf{C}) &= \frac{\exp(2\epsilon_e)-1}{3}\exp(-\tfrac{2}{3}\epsilon_e)\,\mathsf{J}^{2/3}\,\mathbf{diag}[\ 2,\ -1,\ -1\ ]\\ &= \tfrac{2}{3}\,\epsilon_e\,\mathsf{J}^{2/3}\,\mathbf{diag}[\ 2,\ -1,\ -1\ ] + \mathcal{O}\left(\epsilon_e^2\right)\ .\end{aligned}$$

We note that the deviator is proportional to ϵ_e.

The great simplification of uniaxial strain is that diagonal matrices commute, and that the inverse of a diagonal matrix is obtained merely by inverting each diagonal element. We next specialize the illustrative constitutive model of the previous section to the case of uniaxial strain. The three parts of the model, (i) isotropic material stress, (ii) von Mises yield condition, and (iii) Hohenemser-Prager rate for plastic strain, are evaluated in turn.

5.1 Stress

We begin by evaluating the deviatoric term needed for the Piola-Kirchhoff stress

$$\begin{aligned}\mathsf{dev}_{\mathbf{C}^{-1}}\left(\mathbf{C_p}^{-1}\right) &= \mathbf{C_p}^{-1} - \tfrac{1}{3}\,\mathsf{Tr}\Big(\mathbf{C_p}^{-1}\mathbf{C}\Big)\,\mathbf{C}^{-1}\\ &= \mathsf{dev}_{\mathbf{I}_{\mathbb{T}\mathcal{B}}}\left(\mathbf{C_p}^{-1}\mathbf{C}\right)\mathbf{C}^{-1}\\ &= \tfrac{2}{3}\,\epsilon_e\,\mathsf{J}^{2/3}\,\mathbf{diag}[\ 2,\ -1,\ -1\ ]\,\mathbf{C}^{-1} + \mathcal{O}\left(\epsilon_e^2\right)\ .\end{aligned}$$

Therefore the Piola-Kirchhoff stress, Eq. (4.3), is given by

$$\begin{aligned}\mathbf{S} &= \Big[-P(V,\eta)\,\mathsf{J}\,\mathbf{I}_{\mathbb{T}\mathcal{B}} + G\,\mathsf{J}^{-2/3}\,\mathsf{dev}_{\mathbf{I}_{\mathbb{T}\mathcal{B}}}\left(\mathbf{C_p}^{-1}\mathbf{C}\right)\Big]\,\mathbf{C}^{-1} \\ &= \Big[-P(V,\eta)\,\mathsf{J}\,\mathbf{diag}[\,1,\ 1,\ 1\,] + \tfrac{2}{3}\,\epsilon_e\,G\,\mathbf{diag}[\,2,\ -1,\ -1\,]\Big]\,\mathbf{C}^{-1} + \mathcal{O}\left(\epsilon_e^2\right)\,.\end{aligned}$$

and the Cauchy stress is given by

$$\begin{aligned}\boldsymbol{\sigma} &= -P(V,\eta)\,\mathbf{I}_{\mathbb{T}\mathcal{S}} + G\,\mathsf{J}^{-5/3}\,\mathsf{dev}_{\mathbf{I}_{\mathbb{T}\mathcal{S}}}\left(\mathbf{F}\mathbf{C_p}^{-1}\mathbf{F}^T\right) \\ &= -P(V,\eta)\,\mathbf{I}_{\mathbb{T}\mathcal{S}} + G\,\mathsf{J}^{-5/3}\left[\mathbf{F}\mathbf{C_p}^{-1}\mathbf{F}^T - \tfrac{1}{3}\,\mathsf{Tr}(\mathbf{C_p}^{-1}\mathbf{C})\,\mathbf{I}_{\mathbb{T}\mathcal{S}}\right] \\ &= -P(V,\eta)\,\mathbf{I}_{\mathbb{T}\mathcal{S}} + \tfrac{1}{3}\,\frac{G}{\mathsf{J}}\,[\exp(2\epsilon_e) - 1]\exp(-\tfrac{2}{3}\epsilon_e)\,\mathbf{diag}[\,2,\ -1,\ -1\,] \\ &= -P(V,\eta)\,\mathbf{diag}[\,1,\ 1,\ 1\,] + \tfrac{2}{3}\,\epsilon_e\,\frac{G}{\mathsf{J}}\,\mathbf{diag}[\,2,\ -1,\ -1\,] + \mathcal{O}\left(\epsilon_e^2\right)\,.\end{aligned}$$

The plastic stress, Eq. (4.4), is then

$$\begin{aligned}\mathbf{S_p} &= G\,\mathsf{J}^{-2/3}\,\mathsf{dev}_{\mathbf{I}_{\mathbb{T}\mathcal{B}}}\left(\mathbf{C_p}^{-1}\mathbf{C}\right)\,\mathbf{C_p}^{-1} \\ &= \tfrac{2}{3}\,\epsilon_e\,G\,\mathbf{diag}[\,2,\ -1,\ -1\,]\,\mathbf{C_p}^{-1} + \mathcal{O}\left(\epsilon_e^2\right)\,.\end{aligned}$$

The non-hydrostatic shear energy is given by

$$\begin{aligned}\mathcal{E}_{\text{shear}} &= \mathcal{E}_e - \mathcal{E}_{\text{hydro}} \\ &= \tfrac{1}{2}\,V_0\,G\left(I_1\,I_3^{-1/3} - 3\right) \\ &= \tfrac{1}{2}\,V_0\,G\left\{\exp(-\tfrac{2}{3}\epsilon_e)\Big[\exp(2\epsilon_e) + 2\Big] - 3\right\}\,.\end{aligned}$$

To leading order in ϵ_e, the shear energy is given by

$$\mathcal{E}_{\text{shear}} = \tfrac{2}{3}\,V_0\,G\,\epsilon_e^2\,.$$

The same expression is obtained when the shear energy for linear elasticity, $V_0\,G\,\mathsf{Tr}\Big\{\Big[\mathsf{dev}_{\mathbf{I}}\,(\mathbf{E_e})\Big]^2\Big\}$, is specialize to the case of uniaxial strain.

Remark 5.2 For uniaxial strain, the strain tensor, $\mathbf{E} = \mathbf{diag}[\,\frac{\mathsf{J}^2-1}{2},\ 0,\ 0\,]$, has only one non-zero diagonal element. The stress tensor is also diagonal but all three diagonal elements are non-zero. This is in contrast to uniaxial stress in which only one diagonal component of the stress is non-zero, but the strain tensor would have all non-zero diagonal elements.

5.2 Yield Condition

Next we evaluate the von Mises yield function, Eq. (4.5).

$$\begin{aligned}\tilde{\mathsf{Y}}^2 &= \tfrac{3}{2}\,\mathsf{J}^2\,\|\mathsf{dev}_{\mathbf{I}}\,(\boldsymbol{\sigma})\|_{\mathbf{I}}^2 \\ &= \tfrac{3}{2}\,G^2\,\mathsf{J}^{-4/3}\,\left\|\mathbf{F}\mathbf{C}_{\mathbf{p}}{}^{-1}\mathsf{F}^T - \tfrac{1}{3}\,\mathsf{Tr}\left(\mathbf{C}_{\mathbf{p}}{}^{-1}\mathbf{C}\right)\mathbf{I}\right\|_{\mathbf{I}}^2 \\ &= G^2\,[\exp(2\epsilon_e)-1]^2\exp(-\tfrac{4}{3}\epsilon_e) \\ &= 4\,\epsilon_e^2\,G^2 + \mathcal{O}\left(\epsilon_e^3\right)\,.\end{aligned}$$

Hence,

$$\tilde{\mathsf{Y}} = 2\,|\epsilon_e|\,G + \mathcal{O}\left(\epsilon_e^2\right)\,,$$

and on the yield surface $|\epsilon_e| = \frac{Y}{2\,G}$.

5.3 Plastic Strain Rate

The plastic strain rate direction for the flow rule associated with the von Mises yield stress, Eq. (4.8), is

$$\begin{aligned}\frac{\partial\tilde{\mathsf{Y}}}{\partial\mathbf{S}_{\mathbf{p}}} &= \tfrac{3}{2}\,\frac{G}{\tilde{\mathsf{Y}}}\,\mathsf{J}^{-2/3}\,\mathbf{C}_{\mathbf{p}}\,\mathsf{dev}_{\mathbf{I}}\left(\mathbf{C}_{\mathbf{p}}{}^{-1}\mathbf{C}\right) \\ &= \tfrac{1}{2}\,\frac{G}{\tilde{\mathsf{Y}}}\Big[\exp(2\epsilon_e)-1\Big]\,\exp(-\tfrac{2}{3}\epsilon_e)\,\mathbf{C}_{\mathbf{p}}\,\mathbf{diag}[\,2,\,-1,\,-1\,]\,.\end{aligned}$$

This is compatible with the time derivative for the assumed form of $\mathbf{C}_{\mathbf{p}}$

$$\frac{d}{dt}\mathbf{C}_{\mathbf{p}} = \tfrac{2}{3}\left(\tfrac{d}{dt}\epsilon_p\right)\mathbf{C}_{\mathbf{p}}\,\mathbf{diag}[\,2,\,-1,\,-1\,]\,.$$

Therefore, the plastic strain rate reduces to a scalar equation. In the plastic regime, $\tilde{\mathsf{Y}} > Y$,

$$\begin{aligned}\tfrac{d}{dt}\epsilon_p &= \tfrac{3}{4}\,\frac{\tilde{\mathsf{Y}}-Y}{\mu}\,\frac{G}{\tilde{\mathsf{Y}}}\,\Big[\exp(2\epsilon_e)-1\Big]\,\exp(-\tfrac{2}{3}\epsilon_e) \\ &= \tfrac{3}{2}\frac{G\,\mathsf{sgn}(\epsilon_e)}{\mu}\,\Big[|\epsilon_e| - \tfrac{Y}{2\,G}\Big]\,\exp(-\tfrac{Y}{3G}) + \mathcal{O}\left(\Big[|\epsilon_e| - \tfrac{Y}{2\,G}\Big]^2\right)\,,\end{aligned}$$

where $\mathsf{sgn}(\epsilon_e) = 1$ or -1 when $\epsilon_e > 0$ or $\epsilon_e < 0$, respectively.

5.4 One Dimensional Flow Equations

The fully non-linear elastic-plastic flow equations for uniaxial strain with isotropic constitutive relations are summarized below

$$\boxed{\begin{aligned}
\frac{\partial}{\partial t}\Big(\rho\Big) + \frac{\partial}{\partial x}\Big(\rho u\Big) &= 0 \\
\frac{\partial}{\partial t}\Big(\rho u\Big) + \frac{\partial}{\partial x}\Big(\rho u^2 - \sigma^{xx}\Big) &= 0 \\
\frac{\partial}{\partial t}\Big(\rho\, E\Big) + \frac{\partial}{\partial x}\Big(\rho E\, u - \sigma^{xx} u\Big) &= 0 \\
\hline
\frac{\partial}{\partial t}\Big(\rho\, \epsilon_p\Big) + \frac{\partial}{\partial x}\Big(\rho\, u\, \epsilon_p\Big) &= \rho\, \mathcal{R}_p
\end{aligned}} \tag{5.1}$$

where $E = \frac{1}{2}u^2 + e$ is the total specific energy and e is the specific internal energy. This system of equations corresponds to the one-dimensional Euler equations for fluid flow in which the pressure is replaced with the longitudinal component of the stress tensor σ^{xx} plus the addition of a rate equation for the plastic strain variable ϵ_p.

The constitutive relations are given by

$$\boxed{\begin{aligned}
\sigma^{xx} &= -P + \sigma' \\
P &= P_{\text{hydro}}\Big(V, e - \mathcal{E}_{\text{shear}}\Big) \\
\sigma' &= \tfrac{2G}{3\mathsf{J}}\left[\exp(2\epsilon_e) - 1\right]\exp(-\tfrac{2}{3}\epsilon_e) \\
\mathcal{E}_{\text{shear}} &= \tfrac{1}{2}V_0 G\Big\{\exp(-\tfrac{2}{3}\epsilon_e)\Big[\exp(2\epsilon_e) + 2\Big] - 3\Big\}
\end{aligned}} \tag{5.2}$$

where $\mathsf{J} = V/V_0$ and $\epsilon_e = \ln(V/V_0) - \epsilon_p$. This material model corresponds to adding a simple shear strength to a hydrostatic pressure in a thermodynamically consistent manner. To leading order, the shear stress and shear energy are given by

$$\begin{aligned}
\sigma' &= \tfrac{4}{3}\frac{\epsilon_e\, G}{\mathsf{J}} + \mathcal{O}\left(\epsilon_e^2\right) , \\
\mathcal{E}_{\text{shear}} &= \tfrac{2}{3}\, V_0\, G\, \epsilon_e^2 + \mathcal{O}\left(\epsilon_e^3\right) .
\end{aligned}$$

The yield function and rate for the plastic strain variable are given by

$$\boxed{\begin{aligned} \tilde{\mathsf{Y}} &= G\ |\exp(2\epsilon_e) - 1|\ \exp(-\tfrac{2}{3}\epsilon_e) \\ \mathcal{R}_p &= \tfrac{3}{4}\ \frac{(\tilde{\mathsf{Y}} - Y)_+}{\mu}\ \frac{G}{\tilde{\mathsf{Y}}}\ \Big[\exp(2\epsilon_e) - 1\Big]\ \exp(-\tfrac{2}{3}\epsilon_e) \end{aligned}} \tag{5.3}$$

where the subscript '+' denotes the positive part, *i.e.*, $f_+ = f$ for $f > 0$ and 0 otherwise. To leading order the yield function and plastic strain rates are given by

$$\begin{aligned} \tilde{\mathsf{Y}} &= 2\ |\epsilon_e|\ G + \mathcal{O}\left(\epsilon_e^2\right)\ , \\ \mathcal{R}_p &= \tfrac{3}{2}\frac{G\,\mathsf{sgn}(\epsilon_e)}{\mu}\ \Big[|\epsilon_e| - \tfrac{Y}{2G}\Big]_+\ \exp(-\tfrac{Y}{3G}) + \mathcal{O}\left(\Big[|\epsilon_e| - \tfrac{Y}{2G}\Big]^2\right)\ . \end{aligned}$$

Remarks:

5.3 For uniaxial elastic flow, the Hugoniot jump conditions, Eq. (2.26), reduce to the standard shock equations for a fluid with P replaced by $-\sigma^{xx}$. Moreover, the differential thermodynamic relation, Eq. (2.1), reduces to

$$de = \mathsf{S}^{xx}\, d\mathsf{E}_{xx} + T\, d\eta = \sigma^{xx}\, dV + T\, d\eta\ .$$

Again this is the same as for a fluid with P replaced by $-\sigma^{xx}$. Consequently, $\sigma^{xx} = \frac{\partial e}{\partial V}$ and the analogy between uniaxial elastic flow and one-dimensional fluid flow is complete.

5.4 The system of equations for uniaxial elastic-plastic flow has the same form as those for reactive flow. Plasticity corresponds to an endothermic reaction. Hence, the phenomena of a detonation wave does not occur. Instead, the onset of plastic flow has an effect on shock waves similar to a phase transition; *i.e.*, split wave occur consisting of an elastic precursor followed by a plastic wave. However, unlike a phase transition the plastic flow is dissipative and hence irreversible. This shows up in experimental wave profiles in which the split wave is followed by a release wave resulting from a decrease in the driving pressure.

5.5 In the limit of small ϵ_e, shear energy affects the pressure by an amount

$$\Delta P = \tfrac{\Gamma}{V}\,\mathcal{E}_{\text{shear}} = \tfrac{2}{3}\,\Gamma\,\frac{\rho}{\rho_0}\,\epsilon_e^2\,G\ ,$$

where Γ is the Grüneisen coefficient. In the elastic regime, $P_{\text{hydro}} \approx K\epsilon_e$. Typically, $\Gamma \sim 1$ and $G \lesssim K$. Hence, $\Delta P/P \sim \frac{G}{K}\,\epsilon_e = \mathcal{O}(Y/K)$ and consequently the shear energy has a small effect. Frequently, the shear energy is neglected in numerical simulations.

The rate depend plasticity equations are in conservation form. The steady waves of interest are partly dispersed shock waves. They are composed of a discontinuity in which the stress exceeds the yield surface, followed by a relaxation zone in which the stress returns to the yield surface. The discontinuity satisfies the usual Hugoniot jump conditions. Since the plastic strain obeys a rate equation, the jump in the plastic strain variable, ϵ_p, is zero. When the state ahead of the wave is isotropic, the plastic strain at the end state of the dispersed wave is determine by the yield condition. In this special case, one could use rate independent plasticity if the structure of the shock profile is not of interest.

More generally, if the material is precompressed in one direction (say x) and subsequently shocked in a different direct (say y) then the plastic variable behind the wave is determined by the dynamics and not solely by the yield surface. In this case rate independent plasticity is ill-posed. Precompression results in an anisotropic state. For anisotropic constitutive properties, either the stress-strain relation or the yield surface, the rate depend plasticity formulation is needed to resolve the ambiguity in the plastic strain tensor for the end states of wave locus.

For very strong waves, the yield function can exceed the yield strength by a large amount within the very narrow wave profiles. in this regime, the small elastic strain approximation breaks down. the constitutive equations to leading order in ϵ_e, while a valid approximation for small ϵ_e, are not thermodynamically consistent for large ϵ_e. this inconsistency may cause instabilities in the wave profile for strong waves. Though the fully non-linear constitutive relations (5.2) and the plastic strain rates (5.3) appear complicated, they are easily evaluated numerically, and the undesirable side-effects of thermodynamic inconsistencies can readily be avoided.

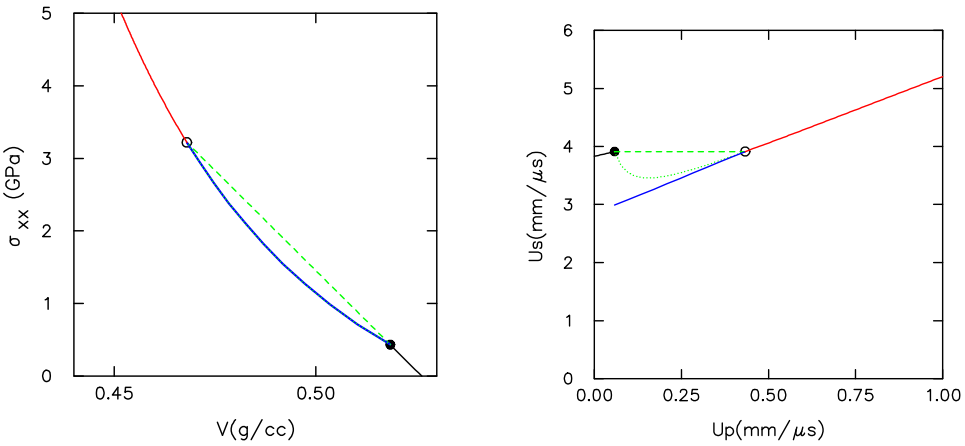

Figure 2: Elastic-plastic Hugoniot locus. Black line corresponds to weak elastic shocks. Green dotted line corresponds to unstable shock waves. Solid circle marks the Hugoniot elastic limit (HEL). Green dashed line is the segment of the Rayleigh line through the HEL to the start of the stable strong shock waves, which is marked by an open circle. Blue line corresponds to the second (plastic) shock of the split waves that replace the unstable shocks. Red line corresponds to strong plastic waves.

6 Wave Structure

The elastic-plastic flow equations have a more complex wave structure than the usual discontinuous shocks that occur in the solution to the Euler equations with a convex equation of state. The transition from elastic to plastic flow has a similar effect as a non-convex equation of state due to a phase transition. In both cases there is a discontinuity in the sound speed at the "phase" boundary that gives rise to split waves. Furthermore, the source terms in the equation for the plastic strain have a similar effect as occurs when the Euler equations are extended to acount for a relaxation phenomena. As a result shock waves in the plastic regime are either fully- or partly-dispersed and not discontinuous.

The uniaxial strain model of the previous section is used to illustrate the wave structures that can occur in the solution to the elastic-plastic flow equations. With parameters in the constitutive relations corresponding to HMX (the explosive cyclo-tetramethelene-tetranitromene but treated here as a non-reactive solid) the principal Hugoniot locus is shown in figure 2

projected in the (V, σ_{xx})-plane and in the (u_p, u_s)-plane.

Next, the profiles for each type of wave, driven by a piston in a numerical simulation, are illustrated. For the calulations the AMRITA environment developed by James Quirk [17, 18] is used in conjunction with an EOS plugin [13] for the constitutive properties. A second order (both space and time) Godunov algorithm in Lagrangian coordinates is used. Moreover, an adaptive mesh refinement solver allows the profiles to be resolved efficiently.

6.1 Weak Purely Elastic Wave

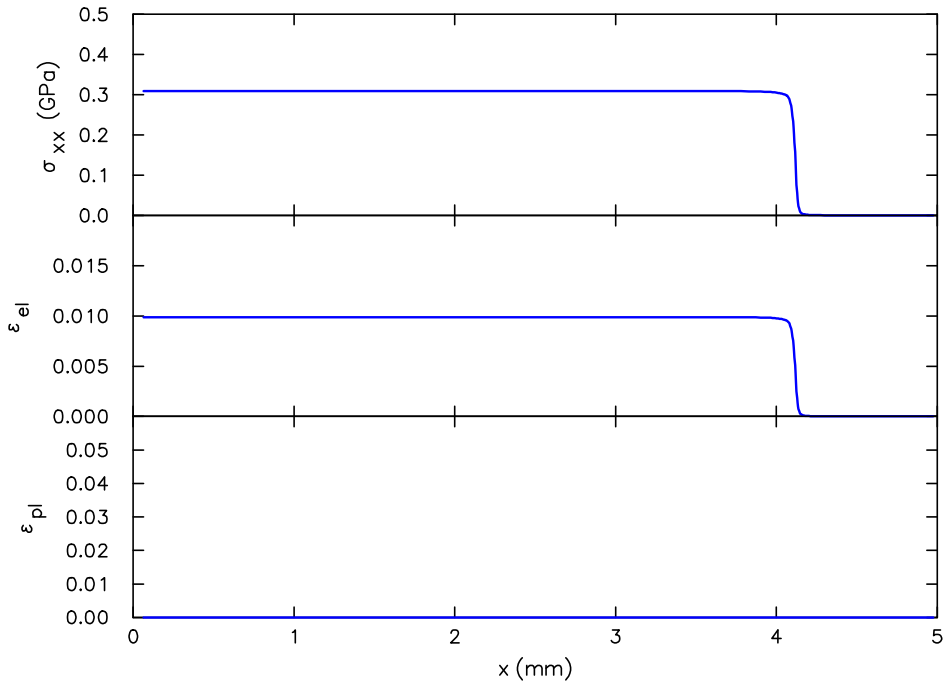

Figure 3: Wave profile for weak elastic wave.

Weak shock waves are in the purely elastic regime, *i.e.*, the plastic strain rate is zero. The shock profile is discontinuous and corresponds to an ordinary fluid dynamic shock wave.

6.2 Split Elastic-Plastic Wave

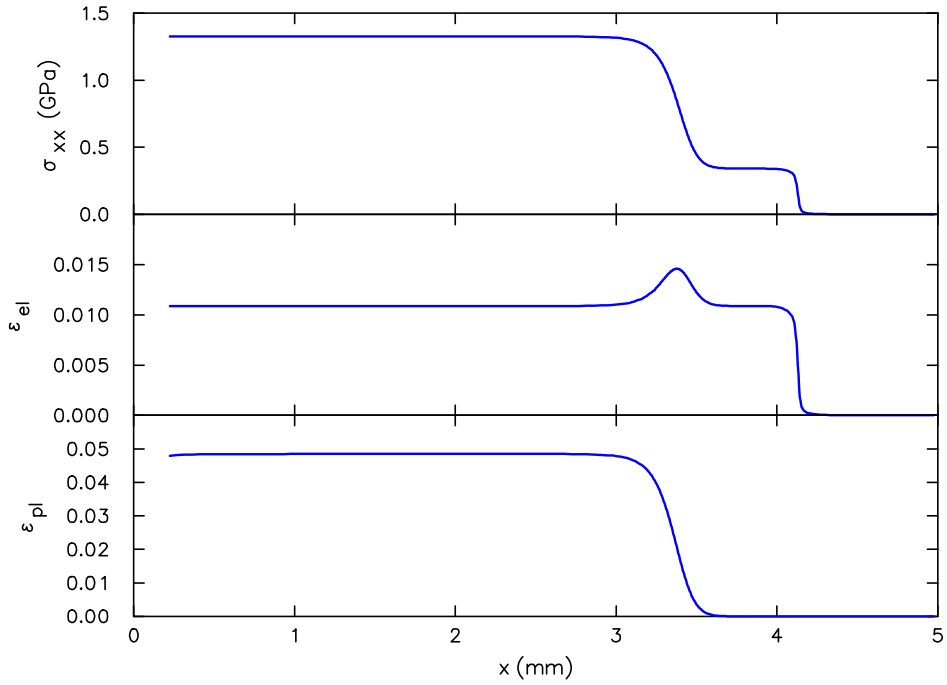

Figure 4: Wave profile for split elastic-plastic wave.

As the wave strength increases above the **Hugoniot elastic limit** shown in figure 2, the shock speed decreases and the shock wave is unstable. It breaks up into a split wave. The lead wave is purely elastic and takes the material upto the yield surface. Plastic flow occurs in the following wave. The limiting of the shear stress above the yield surface results in a discontinuous decrease in the longitudinal sound speed. Consequently, the plastic wave speed is less than the speed of the lead wave, which is at the Hugoniot elastic limit. We show in a subsequent subsection that the plastic wave is fully dispersed. That is to say, the plastic flow provides all of the dissipation required by the Hugoniot jump conditions and the plastic profile is continuous.

6.3 Strong Plastic Wave

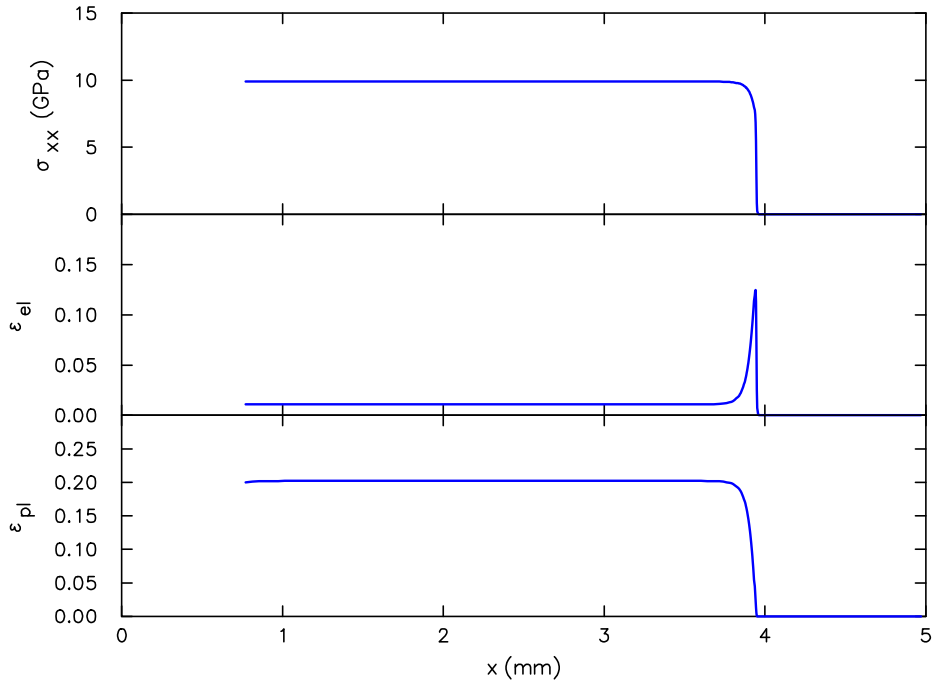

Figure 5: Wave profile for strong plastic wave.

As the wave strength is further increased, the speed of the plastic wave increases until it overtakes the elastic wave. The split waves are then replaced by strong plastic waves. The profile of a strong plastic wave is partly dispersed and consists of a lead shock followed by a continuous relaxation region to the state on the Hugoniot locus. As seen in figure 5, across the lead shock the plastic strain is continuous but the elastic strain is discontinuous. The plastic flow provides only part of the dissipation required by the Hugoniot jump conditions.

6.4 Visco-Elastic Wave

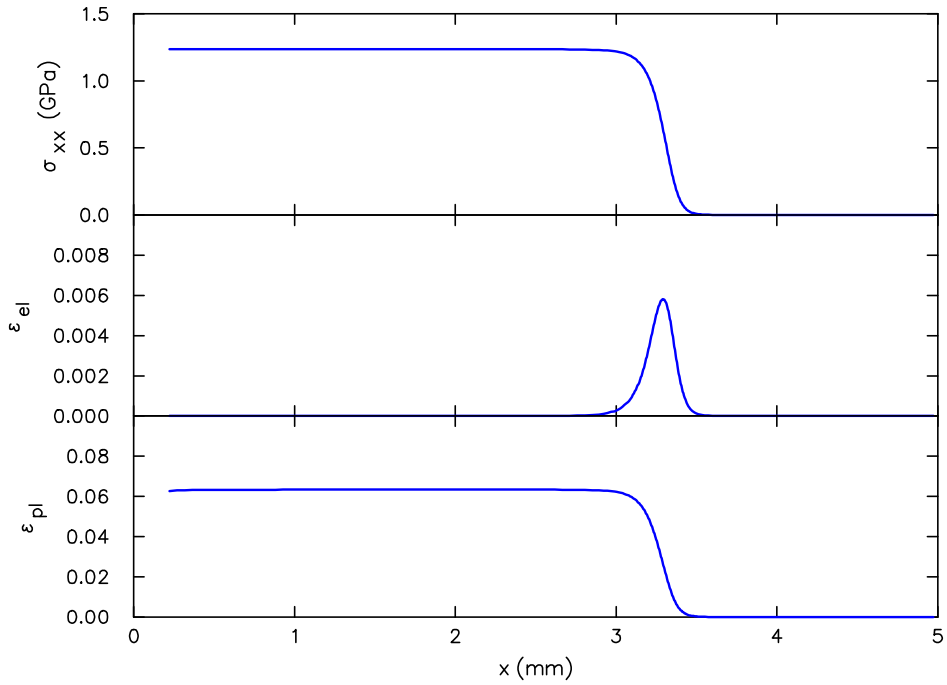

Figure 6: Wave profile for viscous wave, $Y = 0$.

An intesting special case occurs when the yield strength is zero. This corresponds to a visco-elastic material. In this case there are no split waves. Weak waves are fully dispersed as in the plastic wave of a split wave, and strong waves are partly dispersed as in strong plastic waves. The fully dispersed waves have a profile simpilar to what occurs in fluid dynamics when a viscous stress, $Q = \nu\partial_x u$, is added to the pressure. However, there is an important difference for the numerics. The visco-elastic model is hyperbolic and the stable time step is the minimum of the CFL condition and the time constant of the plastic strain rate, *i.e.*, $\Delta t < \min\left(\frac{\Delta x}{c}, \tau\right)$. In contrast a viscous shock profile arises from a parabolic model and the stable time step for an explicit algorithm is $\Delta t < \frac{\rho(\delta x)^2}{\nu}$. As the resolution is increase the viscous time step is proportional to $(\Delta x)^2$, whereas the visco-elastic time step is proportional to Δx. Consequently, it is computational less expensive to resolve shock profiles with a visco-elastic model.

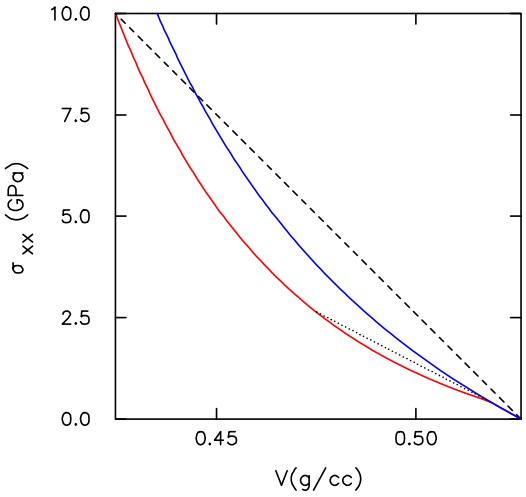

Figure 7: Hugoniot loci in (V, P)-plane. Blue curve is frozen locus, red curve is equilibrium locus. Dotted and dashed black lines are the Rayleigh line for strong plastic wave and second shock of split wave, respectively.

6.5 Partly and Fully Dispersed Waves

The two types of plastic wave profiles, fully- and partly-dispersed, can be understood by examining the frozen and equilibrium Hugoniot loci shown in figure 7. For the frozen locus the plastic strain is held fixed, while for the equilibrium locus the plastic strain is determined by the condition that the stress lies on the yield surface. Also shown in the figure are the Rayleigh lines for weak and strong plastic waves. The **Rayleigh line** is the cord in the (V, σ_{xx})-plane from the initial to final shock states. It follows from the jump conditions that its slope is proportional to the square of the wave speed. Moreover, for a steady traveling wave, the projection of the wave profile in the (V, σ_{xx})-plane lies on the Rayleigh line.

For a weak plastic wave, the Rayleigh line (black dotted line in figure 7) lies between the equilibrium and frozen Hugoniot loci. Consequently, a shock is not possible and the wave profile must be continuous. In contrast, for a strong plastic wave, the Rayleigh line (black dashed line in figure 7) intersects the frozen Hugoniot locus. An analysis of the ODEs for the steady wave profiles shows that the plastic flow doesn't provide enough dissipation at the

initial state for the profile to follow the Rayleigh line. Instead, the profile consists of a shock to the point at which the Rayleigh line intersects the frozen Hugoniot locus followed by a continuous variation along the segment of the Rayleigh line to the final state on the equilibrium Hugoniot locus.

For the visco-elastic model, the elastic segment on which the frozen and equilibrium loci overlap shrinks to zero. A fully dispersed wave profile occurs when the wave speed lies between the equilibrium and frozen sound speeds. A partly dispersed profile occurs for stronger waves with a wave speed greater than the frozen sound speed.

6.6 Entropy Anomalies

An important consequence of the length scale associated with a dispersed wave profile is that an entropy anomaly results from any transient in which a wave profile is formed or changes [12]. The piston driven waves in the examples of the previous subsections serve to illustrate the anomaly when a wave profile is formed. Moreover, the reflection of the wave off the wall at the end of the domain serves to illustrate the anomaly when the wave profile changes.

For the visco-elastic case of the previous subsection the wave profiles of the stress, particle velocity and entropy are shown in figure 8 at a time well after a steady-state shock profile has been reached. Behind the wave front we see that the stress and particle velocity are constant. The entropy anomaly is illustrated by the large increase in entropy near the piston. We note that the extent of the anomalous entropy region is on the same order as the width of the wave profile.

Lagrangian time histories of the stress for a point near the piston and a point overtaken by the steady-state wave are shown in figure 9. Since the piston is impulsively started, the stress rises much more rapidly, near the piston than in the steady-state wave. The rapid rise in stress generates more entropy, and explains the sign of the entropy anomaly shown in the profile of figure 8.

For the Euler equations, this entropy anomaly in numerical solutions would be a "startup" error associated with the artificial shock width of a capturing algorithm. Here the wave profile is determined by the material

model and is fully resolve. The anomaly is in fact part of the solution to the PDEs. It would not shrink in spatial extent with a finer grid.

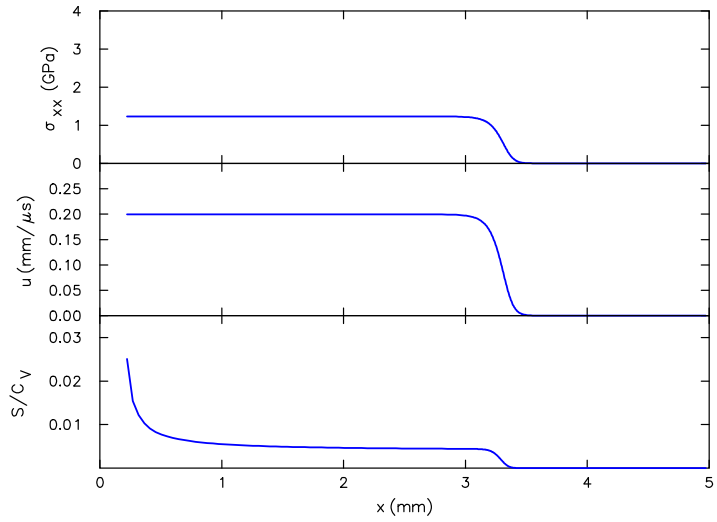

Figure 8: Wave profiles of stress, velocity and entropy for impulsively started piston driven visco-elastic wave.

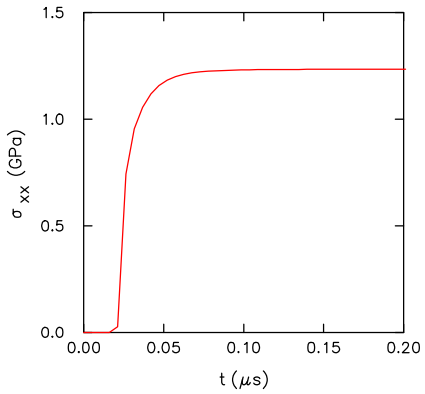

A) x(0) = 0.1 mm

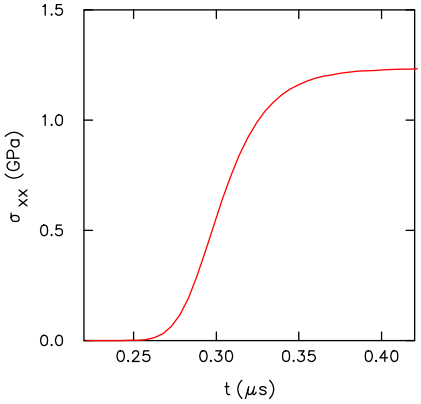

B) x(0) = 1.0 mm

Figure 9: Time history of stress for Lagrangian points showing incident shock for visco-elastic material. A) Transient startup for second cell from piston. B) Steady state shock profile.

The reflection of a wave off a wall is equivalent to the symmetric collision of two waves of the opposite family. Thus, the reflection of a shock serves to illustrate the affect when waves interact. The wave profiles for the visco-elastic case are shown in figure 10 at a time well after the lead shock has reflected off the wall at the end of the computational domain. Behind the reflected wave front, again, the stress and particle velocity are constant. The startup entropy anomaly persists since in that region entropy is merely advected. Now, however, there is an additional entropy anomaly at the wall.

Lagrangian time histories of the stress for a point near the wall and a point overtaken by the steady-state wave are shown in figure 11. Away from the wall, the time history shows a double rise, corresponding to the passage of the incident shock and then the reflected shock. Near the wall, however, the incident and reflected wave profiles overlap. Consequently, the two shocks are not distinguishable and there is no plateau in the stress history. Instead the stress history has an appearance similar to that of a single shock to the final pressure.

The fact that the anomaly is an entropy increase is compatible with a general property of shock waves, namely, the triple shock entropy theorem [4]. The theorem states that the entropy behind a sequence of two shocks is less than the entropy behind a single shock to the same final pressure. The profile near the wall is expected to be more spread out than a single steady shock. Consequently, the entropy behind a single shock should be an upperbound on the entropy anomaly.

A similar entropy anomaly can occur in the numerical solution of the Euler equations. It is exemplified by the Noh problem [14], and often refered to as "excess wall heating." We note that at fixed pressure, the energy increases with entropy. Thus, the excess heating is cause by the entropy anomaly. Excess heating results in a higher temperature. For reactive flows, the excess heating, if sufficiently large, could initiate a detonation wave and thus complete change the solution to the problem.

With a dispersed wave, the entropy anomaly is part of the solution to the PDEs and would not change once the wave profiles are resolved. The anomaly is a numerical error when the width of the wave is artificial, such as occurs in a shock capturing algorithm. The numerical error can be thought of as due to the artificial length scale, and mimics a physical effect when the width of the wave is determined by the material model.

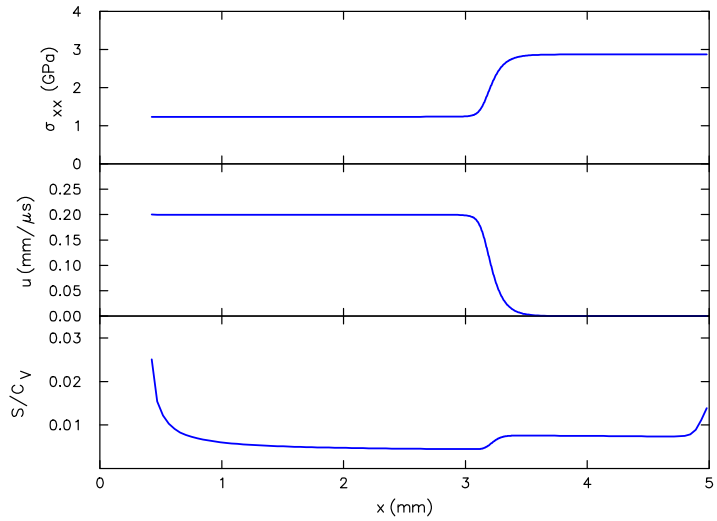

Figure 10: Wave profiles of stress, velocity and entropy for visco-elastic wave after it reflects from wall at $x = 5$.

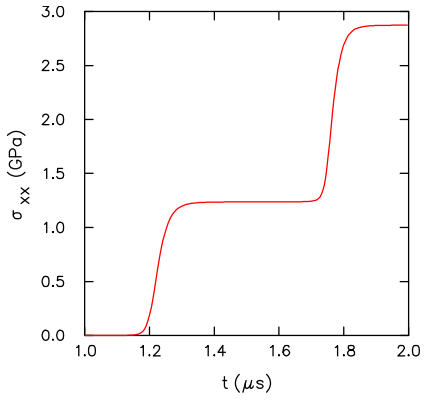

A) x(0) = 4.0 mm

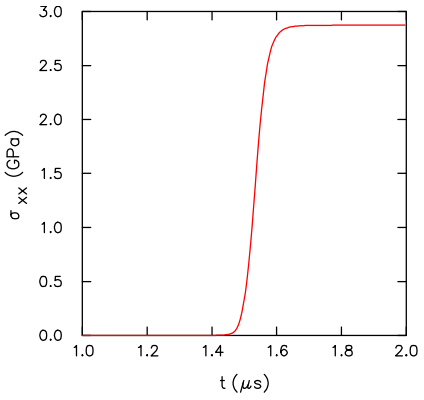

B) x(0) = 4.9 mm

Figure 11: Time history of stress for Lagrangian points showing incident and reflected shock for visco-elastic material. A) Steady state profiles for both incident and reflected shocks. B) Transient next to wall in region where incident and reflected shock profiles overlap.

Appendix A: Useful Lemmas

Lemma A.1. $\frac{\partial}{\partial \mathbf{C}}(\det \mathbf{C}) = (\det \mathbf{C})\mathbf{C}^{-1}$

Lemma A.2. $(\mathbf{Q}\!:\!\frac{\partial}{\partial \mathbf{C}})\mathbf{C}^{-1} = -\mathbf{C}^{-1}\cdot\mathbf{Q}\cdot\mathbf{C}^{-1}$

Lemma A.3. $\frac{d}{dt}\det\mathbf{C} = 0$ iff $\mathsf{Tr}\Big(\mathbf{C}^{-1}\frac{d}{dt}\mathbf{C}\Big) = 0$ iff $\frac{d}{dt}\mathbf{C} = \mathsf{dev}_{\mathbf{C}}(\frac{d}{dt}\mathbf{C})$.

Lemma A.4. $\mathsf{J}^{-1}\frac{d}{dt}\mathsf{J} = \mathsf{Tr}\Big(\boldsymbol{g}^{-1}\mathbf{d}\Big) = \vec{\nabla}\cdot\vec{u}$.

Lemma A.5. The eigenvalues of $\mathbf{Q}\,\mathbf{C}\,\mathbf{Q}^{-1}$ are the same as those of $\mathbf{C}$ for any invertible matrix $\mathbf{Q}$.

Lemma A.6. If $\mathbf{G}$ is a positive symmetric matrix then it can be written in the form $\mathbf{G} = \mathbf{Q}\cdot\mathbf{Q}$ where $\mathbf{Q}$ is positive and symmetric.

Appendix B: Compliance and Stiffness Tensors

The stress $\mathbf{S}$ and strain $\mathbf{E}$ are of symmetric rank-two tensors. They are linearly related by the rank 4 stiffness and compliance tensors, $\overline{\overline{\mathbf{C}}}$ and $\overline{\overline{\mathbf{S}}}$, respectively,

$$\mathbf{S} = \overline{\overline{\mathbf{C}}}\!:\!\mathbf{E} \qquad \text{and} \qquad \mathbf{E} = \overline{\overline{\mathbf{S}}}\!:\!\mathbf{S}\ .$$

i.e., $\mathsf{S}^{\alpha\beta} = \overline{\overline{\mathsf{C}}}^{\alpha\beta,\iota\kappa}\,\mathsf{E}_{\iota\kappa}$ where $\alpha,\beta,\iota,\kappa = 1,2,3$, and similarly $\mathsf{E}_{\alpha\beta} = \overline{\overline{\mathsf{S}}}_{\alpha\beta,\iota\kappa}\,\mathsf{S}^{\iota\kappa}$. By introducing Voigt notation the stress and strain tensors can be treated as vectors, and the stiffness and compliance tensors as matrices. Since the stress and strain tensors can be represented by a symmetric matrix they have six independent entries that can be labeled as follows:

$$\text{Voigt indices} = \begin{pmatrix} 1 & 6 & 5 \\ 6 & 2 & 4 \\ 5 & 4 & 3 \end{pmatrix}\ ,$$

i.e., the mapping from a Voigt index to a tensor index is given by $V(1) = 1,1; V(2) = 2,2; V(3) = 3,3; V(4) = 2,3; V(5) = 3,1; V(6) = 1,2$. The Voigt vector corresponding to the strain tensor is defined as

$$\vec{\mathsf{E}} = (\mathsf{E}_{11}, \mathsf{E}_{22}, \mathsf{E}_{33}, \sqrt{2}\,\mathsf{E}_{23}, \sqrt{2}\,\mathsf{E}_{31}, \sqrt{2}\,\mathsf{E}_{12})^T\ ,$$

and the vector corresponding to the stress tensor is

$$\vec{\mathsf{S}} = (\mathsf{S}_{11}, \mathsf{S}_{22}, \mathsf{S}_{33}, \sqrt{2}\,\mathsf{S}_{23}, \sqrt{2}\,\mathsf{S}_{31}, \sqrt{2}\,\mathsf{S}_{12})^T \ .$$

The $\sqrt{2}$ is introduced in order that $\mathbf{S}\!:\!\mathbf{E} = \vec{\mathsf{S}} \cdot \vec{\mathsf{E}}$.

Remark B.1 The standard convention is

$$\vec{\mathsf{S}}_{\rm std} = (\mathsf{S}_{11}, \mathsf{S}_{22}, \mathsf{S}_{33}, \mathsf{S}_{23}, \mathsf{S}_{31}, \mathsf{S}_{12})^T \ ,$$
$$\vec{\mathsf{E}}_{\rm std} = (\mathsf{E}_{11}, \mathsf{E}_{22}, \mathsf{E}_{33}, 2\,\mathsf{E}_{23}, 2\,\mathsf{E}_{31}, 2\,\mathsf{E}_{12})^T \ .$$

This non-symmetric treatment of stress and strain has side affects on the compliance matrix. It is not suited to the spectral decomposition of the elastic tensor. Also, it affects the coefficients in the formulae for the Reuss average shear modulus.

The stiffness tensor can be expressed as a 6×6 matrix $\widehat{\mathbf{C}}_{a,b} = \overline{\overline{\mathsf{C}}}^{V(a),V(b)}$ where $a, b = 1, 2, 3, 4, 5, 6$. Similarly, for the compliance tensor $\widehat{\mathbf{S}}_{a,b} = \overline{\overline{\mathsf{S}}}_{V(a),V(b)}$. Both $\widehat{\mathbf{C}}$ and $\widehat{\mathbf{S}}$ are symmetric matrices. From the symmetry, we obtain

$$\vec{\mathsf{S}} = \begin{pmatrix} \mathbf{I}_3 & 0 \\ 0 & \sqrt{2}\,\mathbf{I}_3 \end{pmatrix} \widehat{\mathbf{C}} \begin{pmatrix} \mathbf{I}_3 & 0 \\ 0 & \sqrt{2}\,\mathbf{I}_3 \end{pmatrix} \vec{\mathsf{E}} \ ,$$

where $\mathbf{I}_3$ is the 3×3 identity matrix. Similarly,

$$\vec{\mathsf{E}} = \begin{pmatrix} \mathbf{I}_3 & 0 \\ 0 & \sqrt{2}\,\mathbf{I}_3 \end{pmatrix} \widehat{\mathbf{S}} \begin{pmatrix} \mathbf{I}_3 & 0 \\ 0 & \sqrt{2}\,\mathbf{I}_3 \end{pmatrix} \vec{\mathsf{S}} \ .$$

It follows that

$$\widehat{\mathbf{S}} = \begin{pmatrix} \mathbf{I}_3 & 0 \\ 0 & \frac{1}{2}\mathbf{I}_3 \end{pmatrix} \widehat{\mathbf{C}}^{-1} \begin{pmatrix} \mathbf{I}_3 & 0 \\ 0 & \frac{1}{2}\mathbf{I}_3 \end{pmatrix} \ ,$$

whereas the original $4^{\rm th}$ rank tensors satisfy the relation

$$\overline{\overline{\mathbf{S}}}_{\alpha\beta,\iota\kappa} \overline{\overline{\mathbf{C}}}^{\iota\kappa,\mu\nu} = \tfrac{1}{2}\big(\delta_\alpha{}^\mu \delta_\beta{}^\nu + \delta_\alpha{}^\nu \delta_\beta{}^\mu\big) \ .$$

For linear-elasticity, $\overline{\overline{\mathbf{C}}}$ is constant and the energy is given by

$$\mathcal{E} = \tfrac{1}{2}\,\mathbf{E}\!:\!\overline{\overline{\mathbf{C}}}\!:\!\mathbf{E} = \tfrac{1}{2}\,\mathsf{Tr}(\mathbf{S}\mathbf{E}) \ .$$

Alternatively, we could have started by identifying a rank-two tensor S with a 9 dimensional vector $\bar{\mathsf{S}}$

$$\mathsf{S} \to \begin{pmatrix} \bar{\mathsf{S}}_1 & \bar{\mathsf{S}}_6 & \bar{\mathsf{S}}_5 \\ \bar{\mathsf{S}}_9 & \bar{\mathsf{S}}_2 & \bar{\mathsf{S}}_4 \\ \bar{\mathsf{S}}_8 & \bar{\mathsf{S}}_7 & \bar{\mathsf{S}}_3 \end{pmatrix} \ .$$

Then symmetric rank-two tensors are mapped into Voigt vectors by the 6×9 transformation matrix

$$\mathsf{U} = \begin{pmatrix} \mathbf{I}_3 & 0 & 0 \\ 0 & \frac{1}{\sqrt{2}}\mathbf{I}_3 & \frac{1}{\sqrt{2}}\mathbf{I}_3 \end{pmatrix} \ .$$

The transformation has the following properties $\mathsf{U}\mathsf{U}^T = \mathbf{I}_6$ and $\mathsf{U}^T\mathsf{U} = \mathsf{sym}(\mathbf{I}_9)$. Consequently, the map is an isometry from symmetric rank-two tensors to vectors of rank 6, while the antisymmetric rank-two tensor are in the kernel (null space) of U.

We note that $\vec{\mathsf{S}} = \mathsf{U}\bar{\mathsf{S}}$. Furthermore,

$$\bar{\mathsf{S}} = \mathsf{U}^T\hat{\hat{\mathbf{C}}}\mathsf{U}\bar{\mathsf{E}} \ ,$$

where the effective 6×6 stiffness matrix is given by

$$\hat{\hat{\mathbf{C}}} = \begin{pmatrix} \mathbf{I}_3 & 0 \\ 0 & \sqrt{2}\,\mathbf{I}_3 \end{pmatrix} \hat{\mathbf{C}} \begin{pmatrix} \mathbf{I}_3 & 0 \\ 0 & \sqrt{2}\,\mathbf{I}_3 \end{pmatrix} \ .$$

Let the 6×6 Hermitian matrix $\hat{\hat{\mathbf{C}}}$ have the spectral decomposition

$$\hat{\hat{\mathbf{C}}} = \sum_{i=1}^{6} \lambda_i \vec{e}_i \otimes \vec{e}_i \ .$$

Then the spectral decomposition of the rank 4 stiffness tensor, see for example [26], is given by

$$\bar{\bar{\mathbf{C}}} = \sum_{i=1}^{6} \lambda_i \bar{\boldsymbol{e}}_i \otimes \bar{\boldsymbol{e}}_i \ ,$$

where $\bar{\boldsymbol{e}}_i = \mathsf{U}^T\vec{e}_i$ is the symmetric rank-two tensor corresponding to the Voigt vector $\vec{e}_i$.

About the ambient equilibrium state, $\mathbf{E} = 0$ and $\mathbf{S} = 0$, the spectral decomposition of the stiffness tensor gives the leading order term in the expansion of the stress-strain relation

$$\mathbf{S} = \sum_{i=1}^{6} \lambda_i (\mathbf{E} : \bar{\boldsymbol{e}}_i) \bar{\boldsymbol{e}}_i \ ,$$

and the specific energy

$$\mathcal{E} = \mathcal{E}_0 + \frac{1}{2} V_0 \sum_{i=1}^{6} \lambda_i (\mathbf{E} : \bar{\boldsymbol{e}}_i)^2 \ .$$

At a stable equilibrium point, the energy must be a minimum. Hence, the λ_i are all positive. From linear algebra, a necessary and sufficient coefficient for a Hermitian matrix, $\hat{\hat{\mathbf{C}}}$, to be positive is that the determinants of all the principle minors are positive. This places constraints on the coefficients of the stiffness tensor at a stable equilibrium state.

Remark B.2 A stiffness tensor with low symmetry, for example corresponding to a monoclinic crystal, does not necessarily have $\mathbf{I}_3$ as an eigenfunction of $\overline{\overline{\mathbf{C}}}$. In this case, the standard decomposition of the specific energy as the sum of volumetric and deviatoric components, $\mathcal{E}(\mathbf{E}) = \mathcal{E}_1(V) + \mathcal{E}_2(\mathsf{dev}\,\mathbf{E})$, is not possible.

The spectral decomposition also provides bounds on the acoustic wave speeds. For propagation in the direction $\hat{n}$, the wave speed c for the ambient equilibrium state satisfies the condition that ρc^2 is an eigenvalue of the 3×3 Hermitian matrix $\hat{n} \cdot \overline{\overline{\mathbf{C}}} \cdot \hat{n}$. (In general, the matrix in Eq. (C.1) needs to be considered.) By the Rayleigh-Ritz principle the maximum sound speed is given by

$$\begin{aligned}
\rho c_{\max}^2 &= \max_{\hat{m}} \Big[\hat{m} \otimes \hat{n} : \overline{\overline{\mathbf{C}}} : \hat{m} \otimes \hat{n} \Big] \\
&\leq \max_{\hat{m}} \Big[|| \,\mathsf{sym}(\hat{m} \otimes \hat{n})||^2 \Big] \cdot \max_{\hat{m}} \left[\frac{\mathsf{sym}(\hat{m} \otimes \hat{n}) : \overline{\overline{\mathbf{C}}} : \mathsf{sym}(\hat{m} \otimes \hat{n})}{|| \,\mathsf{sym}(\hat{m} \otimes \hat{n})||^2} \right] \\
&\leq \max_{\vec{e}} \left[\frac{(\vec{e}, \hat{\hat{\mathbf{C}}} \vec{e})}{||\vec{e}||^2} \right] \\
&\leq \lambda_{\max} \ ,
\end{aligned}$$

where $\mathsf{sym}(\hat{m}\otimes\hat{n}) = \frac{1}{2}\Big(\hat{m}\otimes\hat{n} + \hat{n}\otimes\hat{m}\Big)$ and we have used the fact that

$$||\,\mathsf{sym}(\hat{m}\otimes\hat{n})||^2 = \tfrac{1}{2}\Big[1 + (\hat{m}\cdot\hat{n})^2\Big] \leq 1 \ .$$

Similarly, the minimum sound speed is given by

$$\begin{aligned}
\rho c^2_{\min} &= \min_{\hat{m}}\Big[\hat{m}\otimes\hat{n} : \overline{\overline{\mathbf{C}}} : \hat{m}\otimes\hat{n}\Big] \\
&\geq \min_{\hat{m}}\Big[||\,\mathsf{sym}(\hat{m}\otimes\hat{n})||^2\Big]\cdot\min_{\hat{m}}\left[\frac{\mathsf{sym}(\hat{m}\otimes\hat{n}) : \overline{\overline{\mathbf{C}}} : \mathsf{sym}(\hat{m}\otimes\hat{n})}{||\,\mathsf{sym}(\hat{m}\otimes\hat{n})||^2}\right] \\
&\geq \tfrac{1}{2}\min_{\vec{e}}\left[\frac{(\vec{e},\hat{\hat{\mathbf{C}}}\vec{e})}{||\vec{e}||^2}\right] \\
&\geq \tfrac{1}{2}\lambda_{\min} \ ,
\end{aligned}$$

where we have used the fact that

$$||\,\mathsf{sym}(\hat{m}\otimes\hat{n})||^2 = \tfrac{1}{2}\Big[1 + (\hat{m}\cdot\hat{n})^2\Big] \geq \tfrac{1}{2} \ .$$

Therefore, independent of the direction of propagation, the sound speeds are bounded by

$$\tfrac{1}{2}\lambda_{\min} \leq \rho c^2 \leq \lambda_{\max} \ .$$

For an isotropic material, the lower bound is sharp for $3K > 2G$ (Poisson ratio $\nu > 0$) and for $3K = 2G$ ($\nu = 0$) both bounds are sharp.

B.1 Isotropic Material

The specific energy of a linearly elastic isotropic material is given by

$$\begin{aligned}
\rho_0\mathcal{E} &= \frac{1}{2}\lambda(\mathsf{Tr}\ \mathbf{E})^2 + G||\mathbf{E}||^2 \\
&= \frac{1}{2}K(\mathsf{Tr}\ \mathbf{E})^2 + G||\,\mathsf{dev}\,\mathbf{E}||^2 \ ,
\end{aligned}$$

where $\lambda = K - \frac{2}{3}G$ is the Lamé coefficient, K is the bulk modulus and G is the shear modulus.

Then the stress-strain relations have the simple form (which is a special case of the spectral decomposition with eigenvalue $3\,K$ and fivefold degenerate eigenvalue $2\,G$)

$$\begin{aligned}\mathbf{S} &= K(\mathsf{Tr}\ \mathbf{E})\mathbf{I}_3 + 2G\,\mathsf{dev}\,\mathbf{E}\\ \mathbf{E} &= \frac{1}{9K}(\mathsf{Tr}\,\mathbf{S})\mathbf{I}_3 + \frac{1}{2G}\,\mathsf{dev}\,\mathbf{S}\ .\end{aligned}$$

The stiffness and compliance tensors are given by

$$\begin{aligned}\overline{\overline{\mathsf{C}}}^{\alpha\beta,\iota\kappa} &= \lambda\delta^{\alpha\beta}\delta^{\iota\kappa} + G(\delta^{\alpha\iota}\delta^{\beta\kappa} + \delta^{\alpha\kappa}\delta^{\beta\iota})\ ,\\ \overline{\overline{\mathsf{S}}}_{\alpha\beta,\iota\kappa} &= \Big(\frac{1}{9K} - \frac{1}{6G}\Big)\delta_{\alpha\beta}\delta_{\iota\kappa} + \frac{1}{4G}(\delta^{\alpha\iota}\delta^{\beta\kappa} + \delta^{\alpha\kappa}\delta^{\beta\iota})\ .\end{aligned} \tag{B.1}$$

Here for simplicity we have assumed that the metric is the identity matrix, *i.e.*, $\mathsf{G}_{\alpha\beta} = \delta_{\alpha\beta}$. The corresponding Voigt matrices have the form

$$\widehat{\mathbf{C}} = \begin{pmatrix} C_u & 0\\ 0 & C_\ell\end{pmatrix} \qquad \text{and} \qquad \widehat{\mathbf{S}} = \begin{pmatrix} S_u & 0\\ 0 & S_\ell\end{pmatrix}\ ,$$

where the u block represents the indices 1, 2, 3 and the ℓ block represents the indices 4, 5, 6. The components of the stiffness matrix are given by

$$C_u = \begin{pmatrix} K+\frac{4}{3}G & K-\frac{2}{3}G & K-\frac{2}{3}G\\ K-\frac{2}{3}G & K+\frac{4}{3}G & K-\frac{2}{3}G\\ K-\frac{2}{3}G & K-\frac{2}{3}G & K+\frac{4}{3}G\end{pmatrix} \qquad \text{and} \qquad C_\ell = G\,\mathbf{I}_3\ ,$$

and the components of the compliance matrix are given by

$$S_u = \begin{pmatrix} \frac{1}{9K}+\frac{1}{3G} & \frac{1}{9K}-\frac{1}{6G} & \frac{1}{9K}-\frac{1}{6G}\\ \frac{1}{9K}-\frac{1}{6G} & \frac{1}{9K}+\frac{1}{3G} & \frac{1}{9K}-\frac{1}{6G}\\ \frac{1}{9K}-\frac{1}{6G} & \frac{1}{9K}-\frac{1}{6G} & \frac{1}{9K}+\frac{1}{3G}\end{pmatrix} \qquad \text{and} \qquad S_\ell = \frac{1}{4G}\,\mathbf{I}_3\ .$$

B.2 Isotropic Sound

Let $\hat{N}$ be the direction of propagation for an acoustic wave. From the isotropic stiffness tensor Eq. (B.1), we obtain

$$\overline{\mathsf{C}}^{\beta\iota} = N_\alpha\overline{\overline{\mathsf{C}}}^{\alpha\beta\iota\kappa}N_\kappa = G\delta^{\beta\iota} + (\lambda+G)N^\beta N^\iota\ .$$

In the ambient equilibrium state the acoustic wave speeds, ρc^2, and the direction of the displacement vectors are the eigenvalues and eigenfunctions of $\overline{\mathsf{C}}$. It is easy to verify that $\hat{N}$ is an eigenvector with eigenvalue $\lambda + 2\,G = K + \frac{4}{3}G$. This corresponds to a longitudinal sound wave. Furthermore, any $\hat{T}$ orthogonal to $\hat{N}$ is an eigenvector with eigenvalue G. These correspond to transverse shear waves.

As expected for an isotropic material, the wave speeds are independent of the direction of propagation. Moreover, in the plane orthogonal to the propagation direction, there is no preferred direction for the transverse wave. Consequently, the eigenvalue for a shear wave is doubly degenerate. We also note that the longitudinal sound speed is greater than the transverse shear wave speed.

B.3 Isotropic Averages

A coarse grain average of a polycrystalline material results in an isotropic response when the crystals are randomly oriented. Two approximations are instructive. Assuming a uniform strain leads to the Voigt average [28] and represents an upper bound [6], while assuming uniform stress leads to the Reuss average [19] and represents a lower bound [6].

The Voigt average corresponds to averaging the stiffness tensor over all orientations

$$\langle \overline{\overline{\mathsf{C}}}^{\alpha\beta,\iota\kappa} \rangle_V = \int \frac{d\omega}{4\pi} R^{\alpha}{}_{\alpha'} R^{\beta}{}_{\beta'} \overline{\overline{\mathsf{C}}}^{\alpha'\beta',\iota'\kappa'} (R^T)_{\iota'}{}^{\iota} (R^T)_{\kappa'}{}^{\kappa} \ ,$$

where R is the rotation matrix corresponding to the solid angle ω. Since the measure is invariant under the rotation group (Haar measure on a compact group), the average projects out the isotropic representation:

$$\langle \overline{\overline{\mathbf{C}}} \rangle = \left(\frac{\overline{\overline{\mathbf{C}}} : \overline{\overline{\mathbf{C}}}^K}{\left\| \overline{\overline{\mathbf{C}}}^K \right\|^2} \right) \overline{\overline{\mathbf{C}}}^K + \left(\frac{\overline{\overline{\mathbf{C}}} : \overline{\overline{\mathbf{C}}}^G}{\left\| \overline{\overline{\mathbf{C}}}^G \right\|^2} \right) \overline{\overline{\mathbf{C}}}^G \ ,$$

where

$$(\overline{\overline{\mathsf{C}}}^{K})^{\alpha\beta,\iota\kappa} = \delta^{\alpha\beta}\delta^{\iota\kappa}$$
$$(\overline{\overline{\mathsf{C}}}^{G})^{\alpha\beta,\iota\kappa} = -\frac{2}{3}\delta^{\alpha\beta}\delta^{\iota\kappa} + \delta^{\alpha\iota}\delta^{\beta\kappa} + \delta^{\alpha\kappa}\delta^{\beta\iota} \ .$$

It follows that the Voigt average of the bulk and shear moduli are given by

$$K_V = \tfrac{1}{9}\Big[\widehat{\mathbf{C}}_{11} + \widehat{\mathbf{C}}_{22} + \widehat{\mathbf{C}}_{33} + 2\Big(\widehat{\mathbf{C}}_{12} + \widehat{\mathbf{C}}_{23} + \widehat{\mathbf{C}}_{31}\Big)\Big]$$
$$G_V = \tfrac{1}{15}\Big[\widehat{\mathbf{C}}_{11} + \widehat{\mathbf{C}}_{22} + \widehat{\mathbf{C}}_{33} - \Big(\widehat{\mathbf{C}}_{12} + \widehat{\mathbf{C}}_{23} + \widehat{\mathbf{C}}_{31}\Big) + 3\Big(\widehat{\mathbf{C}}_{44} + \widehat{\mathbf{C}}_{55} + \widehat{\mathbf{C}}_{66}\Big)\Big] \ .$$

The Voigt average bulk modulus K_V also corresponds to the hydrostatic modulus, $\frac{1}{9}\,\mathsf{Tr}(\overline{\overline{\mathbf{C}}}{:}\mathbf{I}_3)$, *i.e.*, $\mathbf{E} \propto \mathbf{I}_3$.

Similarly the Reuss average corresponds to averaging the compliance tensor over all orientations. The average compressibilities are given by

$$\frac{1}{K_R} = \Big[\widehat{\mathbf{S}}_{11} + \widehat{\mathbf{S}}_{22} + \widehat{\mathbf{S}}_{33} + 2\Big(\widehat{\mathbf{S}}_{12} + \widehat{\mathbf{S}}_{23} + \widehat{\mathbf{S}}_{31}\Big)\Big]$$
$$\frac{1}{G_R} = \tfrac{4}{15}\Big[\widehat{\mathbf{S}}_{11} + \widehat{\mathbf{S}}_{22} + \widehat{\mathbf{S}}_{33} - \Big(\widehat{\mathbf{S}}_{12} + \widehat{\mathbf{S}}_{23} + \widehat{\mathbf{S}}_{31}\Big) + 3\Big(\widehat{\mathbf{S}}_{44} + \widehat{\mathbf{S}}_{55} + \widehat{\mathbf{S}}_{66}\Big)\Big] \ .$$

Remarks:

B.3 Typically, the Reuss average is written in terms of $\widehat{\mathbf{C}}^{-1}$ rather than $\widehat{\mathbf{S}}$. With this notation the last 3 terms in the formula for G_R are multiplied by a factor of $\frac{3}{4}$ instead of 3.

B.4 The sound speeds computed from the Voigt and Reuss averages, $\rho c^2_{\text{long}} = K + \frac{4}{3}G$ and $\rho c^2_{\text{trans}} = G$, are upper and lower bounds for average material but not necessarily on the sound speed for a given propagation direction. The spectral decomposition provides bounds on the latter.

Appendix C: Convexity of Specific Energy

The PDEs for elastic flow are hyperbolic if and only if the acoustic wave speeds are real. From Eq. (2.20) this is equivalent to the matrix

$$\overline{\mathsf{A}}(\hat{N})^{i}{}_{j} = \mathsf{F}^{i}{}_{\alpha'} N_\alpha \overline{\overline{\mathsf{C}}}^{\alpha'\alpha\beta'\beta} N_\beta (\mathsf{F}^T)_{\beta'}{}^{j'} g_{j'j} + (N_\alpha \mathsf{S}^{\alpha\beta} N_\beta)\, \delta^{i}{}_{j}$$

having positive eigenvalues for all $\hat{N}$. Here we formulate the hyperbolicity condition in terms of a requirement on the specific energy $\mathcal{E}(\mathbf{E}, \eta)$.

By Lemma A.5 the condition for real sound speeds is equivalent to the matrix

$$(\mathsf{F}^{-1})^{\alpha''}{}_{i}\overline{\mathsf{A}}(\hat{N})^{i}{}_{j}\mathsf{F}^{j}{}_{\beta''} = N_{\alpha}\overline{\overline{\mathsf{C}}}^{\alpha''\alpha\beta'\beta}N_{\beta}\mathsf{C}_{\beta'\beta''} + (N_{\alpha}\mathsf{S}^{\alpha\beta}N_{\beta})\,\delta^{\alpha''}{}_{\beta''} \tag{C.1}$$

having positive eigenvalues. From the definitions of the stress tensor $\mathbf{S}$ and the stiffness tensor $\overline{\overline{\mathbf{C}}}$, the hyperbolicity condition can be expressed as the condition on $\mathcal{E}$ that the matrix

$$\Big(\hat{N}\frac{\partial^2\mathcal{E}}{\partial\mathbf{C}\partial\mathbf{C}}\hat{N}\Big)\,\mathbf{C} + \tfrac{1}{2}\Big(\hat{N}\frac{\partial\mathcal{E}}{\partial\mathbf{C}}\hat{N}\Big)\mathbf{I}_{\mathbb{T}_{\vec{X}}\mathcal{B}} \tag{C.2}$$

has positive eigenvalues for all $\hat{N}$. Alternatively, elastic flow is hyperbolic if and only if

$$(\vec{N}\otimes\vec{M}):\frac{\partial^2\mathcal{E}}{\partial\mathbf{C}\partial\mathbf{C}}:(\vec{N}\otimes\vec{M}) > -\tfrac{1}{2}\Big(\vec{N}\cdot\frac{\partial\mathcal{E}}{\partial\mathbf{C}}\cdot\vec{N}\Big)\left\|\vec{M}\right\|_{\mathbf{C}}^2 \tag{C.3}$$

for all $\vec{M}, \vec{N} \in \mathbb{T}_{\vec{X}}\mathcal{B}$ where $\mathbf{C}$ is the metric used for inner products. It is natural to use $\mathbf{C}$ as the metric in the body frame since it is the sound speeds in the spatial frame that are physical, see Remark 2.13.

When the stress $\mathbf{S} = 2\rho_0\frac{\partial\mathcal{E}}{\partial\mathbf{C}}$ vanishes, this is equivalent to rank-1 convexity. Namely, $\mathcal{E}\big(\mathbf{E} + t\,[\vec{N}\otimes\vec{M} + \vec{M}\otimes\vec{N}]\big)$ is a convex function of t. It is the analog of the hyperbolicity condition for fluid dynamics, that is, $(\rho c)^2 = \frac{\partial^2\mathcal{E}}{\partial V^2} > 0$ if and only if $\mathcal{E}(V,\eta)$ is a convex function of V. We note that stress is negative in compression and causes the hyperbolicity condition to be stronger than rank-1 convexity.

A slightly stronger condition than rank-1 convexity is

$$(\vec{N}\otimes\vec{M}):\frac{\partial^2\mathcal{E}}{\partial\mathbf{C}\partial\mathbf{C}}:(\vec{N}\otimes\vec{M}) \geq \epsilon\,\|N\|_{\mathbf{C}}\,\|M\|_{\mathbf{C}}\ , \tag{C.4}$$

where $\epsilon > 0$ and again $\mathbf{C}$ is used for the metric. When $\frac{\partial^2\mathcal{E}}{\partial\mathbf{C}\partial\mathbf{C}}$ is replaced by the acoustic tensor $\overline{\overline{\mathbf{A}}}$ this is the condition of strong ellipticity. Then ϵ can be identified with the minimum of c^2 over all directions and polarizations. Consequently, for Eq. (C.4), ϵ is the minimum over all directions $\hat{N}$ of $\frac{1}{4}(c^2 - V_0\mathsf{S}_n)$ where $\mathsf{S}_n = \hat{N}\cdot\mathbf{S}\cdot\hat{N}$ is the normal stress. Strong ellipticity is a condition needed for existence of solutions in elasto-statics, for example, see [11]. It is also sufficient for hyperbolicity.

Appendix D: Small Viscosity Limit

The rate equation has the form

$$\frac{d}{dt}\Upsilon + \frac{A}{\mu}\Upsilon = \frac{B(t)}{\mu} \ .$$

This can be written as

$$\frac{d}{dt}\Big(\exp\big(\tfrac{At}{\mu}\big)\,\Upsilon\Big) = \frac{B(t)}{\mu}\exp\big(\tfrac{At}{\mu}\big) \ .$$

The solution is given by

$$\Upsilon(t) = \int_0^t \frac{dt'}{\mu}\,B(t')\exp\big(\tfrac{A(t'-t)}{\mu}\big) \ .$$

In the limit of small μ, the exponential is highly peaked. If $B(t)$ varies slowly on the time scale μ/A, *i.e.*,

$$\frac{\mu}{A}\frac{d}{dt}B \ll B \ ,$$

then to leading B can be taken out of the integral, yielding

$$\begin{aligned}\Upsilon(t) &\approx B(t)\int_0^t \frac{dt'}{\mu}\,\exp\big(\tfrac{A(t'-t)}{\mu}\big) \\ &\approx B(t)\int_{-\infty}^0 \frac{dt'}{\mu}\,\exp\big(\tfrac{At'}{\mu}\big) = \frac{B(t)}{A}\end{aligned}$$

Consequently, in the limit of small viscosity

$$\boxed{\Upsilon(t) = \frac{B(t)}{A}} + \mathcal{O}\left(\mu\right) \ .$$

Appendix E: Lie Derivative

To illustrate the concept of a Lie derivative we begin by considering the particle acceleration, which formally is defined by

$$\vec{a} = \frac{d}{dt}\vec{u} = \left(\frac{\partial}{\partial t}\vec{U}\right)\circ\boldsymbol{\phi}^{-1} \ .$$

The difficulty is that the standard definition of the derivative,

$$\frac{\partial}{\partial t}\vec{U} = \lim_{\Delta t \to 0} \frac{\vec{U}(\vec{X}, t+\Delta t) - \vec{U}(\vec{X}, t)}{\Delta t} \ ,$$

is not well defined because $\vec{U}(\vec{X}, t+\Delta t) \in \mathbb{T}_{\boldsymbol{\phi}(\vec{X},t+\Delta t)}\mathcal{S}$ and $\vec{U}(\vec{X}, t) \in \mathbb{T}_{\boldsymbol{\phi}(\vec{X},t)}\mathcal{S}$. Though the tangent spaces $\mathbb{T}_{\vec{X}}\mathcal{S}$ are finite dimensional, and hence isomorphic, the isomorphism is not unique.

In this case, we can use the pull-back and push-forward maps of the flow $\boldsymbol{\phi}$ to provide the needed isomorphism between the tangent spaces.

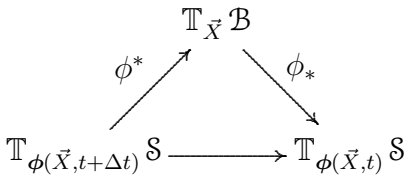

Then the time derivative, defined as,

$$\frac{\partial}{\partial t}\vec{U} = \lim_{\Delta t \to 0} \frac{\phi_*(\vec{X}, t)\phi^*(\vec{X}, t+\Delta t)\vec{U}(\vec{X}, t+\Delta t) - \vec{U}(\vec{X}, t)}{\Delta t} \ ,$$

is well defined. On a flat space, metric $g_{ij} = \delta_{ij}$, this gives the standard definition for the convective derivative, $\frac{d}{dt} = \frac{\partial}{\partial t} + \vec{u} \cdot \nabla$.

This idea can be generalized to be independent of the reference frame $\mathcal{B}$. First, for a vector field $\vec{u}(\vec{x}) \in \mathbb{T}_{\vec{x}}\mathcal{S}$ we define a flow, $\boldsymbol{\psi}_{\vec{u}}$, by the differential equation

$$\frac{\partial}{\partial t}\boldsymbol{\psi}_{\vec{u}}(\vec{x}, t) = \vec{u} \circ \boldsymbol{\psi}_{\vec{u}}(\vec{x}, t)$$

with the initial condition $\boldsymbol{\psi}_{\vec{u}}(\vec{x}, 0) = \vec{x}$. Then the push-forward $\boldsymbol{\psi}_*$ maps the tangent space at $\vec{x}$ onto the tangent space at $\boldsymbol{\psi}(\vec{x}, t)$, and the pull-back $\boldsymbol{\psi}^*$ maps the tangent space at $\boldsymbol{\psi}(\vec{x}, t)$ onto the tangent space at $\vec{x}$. The **Lie derivative** of a tensor field, see *e.g.*, [11, §1.6], such as the Eulerian strain, is given by

$$\mathbf{L}_{\vec{u}}\,\mathbf{e} = (\boldsymbol{\psi}_{\vec{u}})_*(\vec{x}, t)\frac{d}{dt}\Big[(\boldsymbol{\psi}_{\vec{u}})^*\mathbf{e}(\vec{x}, t)\Big] \ .$$

In effect, one transforms into a common vector space in order to take the derivative and then transforms back to the desired space.

The Lie derivative allows evolution equations to be defined in a mannar such that frame indifference is satisfied, see [11, Box 6.1, p. 99]. In particular, we have defined the plastic strain rate in the Lagrangian frame. It can then be transformed into the Eulerian frame. The theory is physically the same when viewed in any inertial frame.

Acknowledgement

The author wishes to thank his colleauge Bradley Plohr. Discussion with him on elastic-plastic flow have greatly contributed to the authors understanding and is the basis for these notes.

References

[1] J. K. Dienes, *On the analysis of rotation and stress rate in deforming bodies*, Acta Mechanica **32** (1979), 217–232. 16, 25

[2] T. C. Doyle and J. L. Ericksen, *Nonlinear elasticity*, Advances in Mechanics IV, Academic Press, 1956. 12

[3] P. S. Follansbee and U. F. Kocks, *A constitutive description of the deformation of copper based on the use of the mechanical threshold stress as an internal state variable*, Acta Metall. **36** (1988), 81–93. 50

[4] L. F. Henderson and R. Menikoff, *Triple shock entropy theorem and its consequences*, J Fluid Mech **366** (1998), 179–210. 66

[5] W. Herrmann, *Elastic-plastic constitutive relastions at large strain*, Shock Compression of Condensed Matter – 1991 (S. C. Schmidt, R. D. Dick, J. W. Forbes, and D. G. Tasker, eds.), Elsevier Science Publishers, 1992, pp. 379–382. 25

[6] R. Hill, *The elastic behaviour of a crystalline aggregate*, Proc. Roy. Soc. London **A65** (1952), 349–354. 74

[7] K. Hohenemser and W. Prager, *Beitragzur mechanik desbildsamen verhaltensvonflubstahl (Contribution to the mechanics of the malleable behavior of cast iron)*, Z. Angew. Math. Mech. **12** (1932), 1–14. 45

[8] J. N. Johnson, *Micromechanical considerations in shock compression of solids*, High-Pressure Shock Compression of Solids (J. R. Asay and M. Shahinpoor, eds.), Springer-Verlag, 1993. 50

[9] J. N. Johnson and D. L. Tonks, *Dynamic plasticity in transition from thermal activation to viscous drag*, Shock Compression of Condensed Matter – 1991 (S. C. Schmidt, R. D. Dick, J. W. Forbes, and D. G. Tasker, eds.), Elsevier Science Publishers, 1992, pp. 371–378. 50

[10] J. Lubliner, *Plasticity theory*, Macmillan Publishing, 1990. 45

[11] J. E. Marsden and T. J. R. Hughes, *Mathematical foundations of elasticity*, Printice-Hall, 1983. 3, 6, 25, 29, 76, 78, 79

[12] R. Menikoff, *Errors when shock waves interact due to numerical shock width*, SIAM J Sci Comp **15** (1994), 1227–1242. 64

[13] R. Menikoff and J. J. Quirk, *Versatile user-friendly EOS package*, Tech. Report LA-UR-01-6222, Los Alamos National Laboratory, 2001, `http://t14web.lanl.gov/Staff/rsm/preprints.html#EOSpackage`. 59

[14] W. F. Noh, *Errors for calculations of strong shocks using artificial viscosity and an artificial heat flux*, J Comp Phys **72** (1987), 78–120. 66

[15] B. J. Plohr and D. H. Sharp, *A conservative Eulerian formulation of the equations for elastic flow*, Advances in Applied Mathematics **9** (1988), 481–499. 2

[16] ———, *A conservative formulation for plasticity*, Advances in Applied Mathematics **13** (1992), 462–493. 21, 32

[17] J. J. Quirk, *Amrita - a computational facility for cfd modelling*, p. ?, von Karmen Institute, 1998, `http://www.galcit.caltech.edu/~jjq/vki/vki:cfd29::jjq_l1.ps.gz`. 59

[18] ———, *AMR_sol: Design principles and practice*, p. ?, von Karmen Institute, 1998, `http://www.galcit.caltech.edu/~jjq/vki/vki:cfd29::jjq_l2.ps.gz`. 59

[19] A. Reuss, *Berechnung der fliebgrenze von mischkristallen auf grund der plastizitätsbedingung für einkristalle (Calculation of the plastic flow boundary of mixed crystals based on the plasticity condition for single crystals)*, Z. Angew. Math. Mech. **9** (1929), 49–58. 74

[20] M. Scheidler and T. W. Wright, *A continuum framework for finite viscoplasticity*, International Journal of Plasticity **17** (2001), 1033–1085. 37

[21] J. C. Simo, *A framework for finitstrain elastoplasticity based on maximum plastic dissipation and the multiplicative decomposition: Part I continuum formulation*, Computer Methods in Applied Mechanics and Engineering **66** (1988), 199–219. 37

[22] J. C. Simo and T. J. R. Hughes, *Computational inelasticity*, Springer-Verlag, 1998. 2, 14, 46

[23] J. C. Simo and K. S. Pister, *Remark on rate constitutive equations for finite deformation problems: Computational implications*, Computer Methods in Applied Mechanics and Engineering **46** (1984), 201–215. 16, 25

[24] J. W. Swegle and D. E. Grady, *Shock viscosity and the prediction of shock wave rise times*, J. Appl. Phys. **58** (1985), 692–701. 50

[25] G. I. Taylor and H. Quinney, *The latent energy remaining in a metal after cold working*, Proc. Roy. Soc. London **A143** (1933), 307–326. 33

[26] P. S. Theocaris and D. P. Sokolis, *Spectral decomposition of the linear elastic tensor for monoclinic symmetry*, Acta Cryst. **A55** (1909), 635–647. 70

[27] J. Trangenstein and P. Colella, *A higher-order Godunov method for modeling finite deformation in elastic-plastic solids*, Comm. Pure Appl. Math **44** (1991), 41–100. 22

[28] W. Voigt, *Lehrbuch der krystall physik (Textbook on crystal physics)*, Teubner, Leipzig, 1928. 74

Index